' You see things; and you say,

"Why?"

But I dream things that never were; and I say,

"Why not?" '

George Bernard Shaw

Noble Laureate for Literature, 1925

'At a U.S. Senate hearing in 1970, an elderly senator from Louisiana asked (Glenn) Seaborg sarcastically, "What do you know about plutonium?" With admirable restraint, Seaborg gave a "vague but reassuring answer."

He was the discoverer of plutonium.'

Excerpt from 'The Impossible takes Longer.' by David Pratt

'The Dude abides.'

Jeffrey "The Dude" Lebowski

in The Big Lebowski

University of Alberta

The Effects of Mixing, Reaction Rate and Stoichiometry on Yield for Mixing Sensitive Reactions

by

Syed Imran Ali Shah

A thesis submitted to the Faculty of Graduate Studies and Research
in partial fulfillment of the requirements for the degree of

Master of Science

Department of Chemical & Materials Engineering and
Department of Mechanical Engineering

Spring 2010
Edmonton, Alberta

Examining Committee

Dr. Suzanne Kresta, Chemical & Materials Engineering

Dr. Larry Kostiuk, Mechanical Engineering

Dr. Greg Dechaine, Chemical & Materials Engineering

To my parents, my brother & my sister.

Oh, and Life, the Universe & Everything too…

Abstract

Competitive-Consecutive and Competitive-Parallel reactions are both mixing sensitive reactions; the yield of desired product from these reactions depends on how fast the reactants are brought together. Recent experimental results have suggested that the mixing effect may depend strongly on the stoichiometry of the reactions. To investigate this, a 1-D, non-dimensional, reaction-diffusion model at the micro-mixing scale has been developed. Assuming constant mass concentration and diffusivities, systems of PDE's have been derived on a mass fraction basis for both types of reactions. A single general Damköhler number and specific dimensionless reaction rate ratios were derived for both reaction schemes. The resulting dimensionless equations were simulated to investigate the effects of mixing, reaction rate ratio and stoichiometry of the reactions. It was found that decreasing the striation thickness and the dimensionless rate ratio maximizes yield for both types of reactions and that the stoichiometry has a considerable effect on yield. All three variables were found to interact strongly. Phase plots showing the interactions between the three variables were developed.

Acknowledgements

My deepest regards and gratitude go to my supervisor, Dr. Suzanne Kresta, for her guidance, support, patience and understanding throughout my program. Her willingness to make time and listen to whatever I had to say about dragons, education, mixing, turbulence and life (amongst the countless other topics and hours of fun conversation we've enjoyed!) meant everything to me. She is an admirable, engaging person who sincerely cares and I have been very fortunate to have worked with her.

I would also like to express sincerest thanks to my co-supervisor, Dr. Larry Kostiuk, whose remarkable insight and point of view were invaluable to this project. His perspective on things never seized to amaze me and he's one of the coolest guys I know.

I also have to thank Dr. Thomas Martin, who introduced me to Mixing by convincing me to take his course. If it weren't for his enthusiasm I probably would never have known about the subject that has captured my interest and imagination ever since.

I'd like to thank my friends and colleagues in the Mixing group: İnci, Shad, Alena (and Matej!), Márcio, Oscar and Patrick, for making my time in the group so very enjoyable and for being kind enough to let me enjoy their company. They are all interesting, wonderful people who really made the office a fun place to be.

My friends Kartik, Collins, Hector, Vivek, Bikki, Jk and Obs are also deserving of my gratitude. Spending time with them was most memorable and it made completing this program much easier than it otherwise would have been.

I'd also like to thank the staff at the Cross Cancer Institute, the University Metabolic Centre and especially Dr. Christopher Smith at the University Health Centre for helping me to get healthy again, a minor factor that was somewhat instrumental in the completion of this thesis.

I am also very appreciative of the funding from various sources that miraculously managed to find its way into my hands at the end of every month. I used it to eat, and eating was useful.

And last, but by far not the least, I would like to thank my parents and my family for their unwavering love and support. I am where I am today because of them and without their love I would truly be lost.

Table of Contents

		Pg.
1	**Introduction & Literature Review**	1
1.1	Mixing as it pertains to Chemical Reactions	1
1.2	Mixing Sensitive Reactions	3
1.3	Scaling Mixing and Reactions: The Damköhler Number	4
1.4	Review of the Mixing literature	5
1.5	Review of the Non-Linear Reaction Dynamics	7
1.6	Qualitative Descriptors of the effects of Mixing and Reaction Rates.	13
1.7	Objectives and proposed contributions	15
1.8	Thesis Outline	16
2	**Model to Study the Effect of Mixing, Reaction Rates and Stoichiometry on Yield for Mixing Sensitive Reactions**	18
2.1	Chapter Overview	18
2.2	Model Description and Governing Equations	18
2.2.1	Competitive-Consecutive (C-C) Reaction Scheme	21
2.2.2	Competitive-Parallel (C-P) Reaction Scheme	25
2.3	Numerical Solution of Equations	28
2.4	Results and Discussion	29
2.4.1	Competitive-Consecutive (C-C) Reaction	29
2.4.2	Competitive-Parallel (C-P) Reaction	31
2.4.3	Yield of desired product *P*	32
2.4.4	Effect of reaction rate ratio on yield of *P*	33
2.4.5	Effect of mixing on yield of *P*	33
2.5	Conclusions	34
2.6	Tables for Chapter 2	36
2.7	Figures for Chapter 2	39
3	**Design Protocols for Mixing Sensitive Reactions**	45
3.1	Chapter Overview	45
3.2	Measures for Design	45
3.3	Numerical Details	47
3.4	Results and Discussion	49
3.4.1	Competitive-Consecutive (C-C) Reaction	50

3.4.1.1 Effect of Damköhler number (*Da*) 50
3.4.1.2 Effect of non-dimensional reaction rate ratio (k_2/k_1) 51
3.4.1.3 Effect of Stoichiometry 52
3.4.1.4 Summary of the effects on C-C reaction schemes 53

3.4.2 Competitive-Parallel (C-P) Reaction 53
3.4.1.1 Effect of Damköhler number (*Da*) 54
3.4.1.2 Effect of non-dimensional reaction rate ratio (k_2/k_1) 54
3.4.1.3 Effect of Stoichiometry 55
3.4.1.4 Summary of the effects on C-P reaction schemes 57
3.4.3 Phase Plots of variables for C-C and C-P reaction schemes for the purpose of design 58

3.5 Conclusions 60
3.6 Tables for Chapter 3 62
3.7 Figures for Chapter 3 64

4 Conclusions and Future work 77
4.1 Conclusions 77
4.2 Future work 79

5 References 81

A Appendix A: Figures and tables of COMSOL Data 85
A.1 Summary 85
A.2 Competitive-Consecutive Reaction Scheme 86
A.2.1 Plots and data of Y_P versus Damköhler number with curves of the stoichiometry cases for different non-dimensional reaction rate ratios. 86
A.2.2 Plots and data of Y_P versus Damköhler number with curves of non-dimensional reaction rate ratios for individual stoichiometry cases. 92
A.2.3 Plots and data of Y_P versus non-dimensional reaction rate ratio with curves of the stoichiometry cases for different Damköhler numbers. 100
A.2.4 Plots and data of Y_P versus non-dimensional reaction rate ratio with curves of Damköhler numbers for individual stoichiometry cases. 106

A.3 Competitive-Parallel Reaction Scheme 114
A.3.1 Plots and data of Y_P versus Damköhler number with curves of the stoichiometry cases for different non-dimensional reaction rate ratios. 114

A.3.2 Plots and data of Y_P versus Damköhler number with curves of non-dimensional reaction rate ratios for individual stoichiometry cases. 120
A.3.3 Plots and data of Y_P versus non-dimensional reaction rate ratio with curves of the stoichiometry cases for different Damköhler numbers. 124
A.3.4 Plots and data of Y_P versus non-dimensional reaction rate ratio with curves of Damköhler numbers for individual stoichiometry cases. 130

List of Figures

		Pg.
1-1	A lamellar structure generated by the blinking vortex flow. A circular blob is stretched and folded, generating thin striations that are modelled as a parallel array of lamellar, alternately of species *A* and *B* (the 'bar-code') – taken from Clifford et al. (2000).	11
2-1	Geometry for proposed mixing model at t=0.	39
2-2	Spatial and temporal evolution of mass fractions for C-C Cases:	40
	(a) 1, (k_2/k_1=10^{-5}, Da=1)	40
	(b) 2, (k_2/k_1=10^{-5}, Da=10000)	40
	(c) 3, (k_2/k_1=1, Da=1)	41
	(d) 4, (k_2/k_1=1, Da=10000)	41
2-3	Spatial and temporal evolution of mass fractions for C-P Cases:	42
	(a) 1, (k_2/k_1=10^{-5}, Da=1)	42
	(b) 2, (k_2/k_1=10^{-5}, Da=10000)	42
	(c) 3, (k_2/k_1=1, Da=1)	43
	(d) 4, (k_2/k_1=1, Da=10000)	43
2-4	Yield of *P* versus time for the C-C cases	44
2-5	Yield of *P* versus time for the C-P cases	44
3-1	Initial conditions for (a) C-C and (b) C-P reaction scheme simulations.	64
3-2	Plots of Yield of *P* vs. Da for decreasing k_2/k_1 ratios for the C-C cases.	65
	(a) k_2/k_1 = 1	65

(b) k_2/k_1 = 0.1 65
(c) k_2/k_1 = 0.01 65
(d) k_2/k_1 = 0.001 66
(e) k_2/k_1 = 0.0001 66
(f) k_2/k_1 = 0.00001 66

3-3 Plots of Yield of *P* vs. k_2/k_1 for two sample C-C stoichiometries. The curves represent the different *Da*. Curves for *Da*=0.01 lie exactly under the curves for *Da*=1. 67

(a) C-C Stoichiometry Case 1: $A + B \overset{k_1'}{\rightarrow} \mathrm{P}\,;\, P + B \overset{k_2'}{\rightarrow} S$ 67
(b) C-C Stoichiometry Case 7: $A + B \overset{k_1'}{\rightarrow} \mathrm{P}\,;\, 2P + 2B \overset{k_2'}{\rightarrow} S$ 67

3-4 Plots of Yield of *P* vs. k_2/k_1 for various *Da* at $Da \cdot t^*$=500 for C-C cases. 68

(a) *Da* = 1 68
(b) *Da* = 100 68
(c) *Da* = 10000 68

3-5 Plot of Yield of *P* vs.k_2/k_1 for *Da*=10000 at $Da \cdot t^*$=50000 for C-C cases. 69

3-6 Plots of Yield of *P* vs. *Da* for decreasing k_2/k_1 ratios for the C-P cases. 70

(a) k_2/k_1 = 1 70
(b) k_2/k_1 = 0.1 70
(c) k_2/k_1 = 0.01 70
(d) k_2/k_1 = 0.001 71
(e) k_2/k_1 = 0.0001 71
(f) k_2/k_1 = 0.00001 71

3-7 Plots of Yield of *P* vs. k_2/k_1 for two sample C-P stoichiometries. The curves represent the different *Da*. Curves for *Da*=0.01 lie exactly under the curves for *Da*=1. 72

(a) C-P Stoichiometry Case 2: $A + B \overset{k_1'}{\rightarrow} \mathrm{P}\,;\, C + B \overset{k_2'}{\rightarrow} S$ 72

(b) C-P Stoichiometry Case 3: $A + 2B \overset{k_1'}{\rightarrow} \mathrm{P}\,;\, \mathrm{C} + B \overset{k_2'}{\rightarrow} S$ 72

3-8 Plots of Yield of *P* vs. k_2/k_1 for various *Da* at $Da \cdot t^*$=500 for C-P cases. 73

(a) *Da* = 1 73
(b) *Da* = 100 73
(c) *Da* = 10000 73

3-9 Plot of Yield of *P* vs.k_2/k_1 for *Da*=10000 at $Da \cdot t^*$=50000 for C-P cases. 74

3-10 Design spaces for Yield of *P* for *Da* and k_2/k_1 at $Da \cdot t^*$=500 for C-C cases. 75

(a) Y_P is at least 0.85 (85%) 75
(b) Y_P is at least 0.95 (95%) 75
(c) Y_P is at least 0.99 (99%) 75

3-11 Design spaces for Yield of *P* for *Da* and k_2/k_1 at $Da \cdot t^*$=500 for C-P cases. 76

(a) Y_P is at least 0.85 (85%) 76
(b) Y_P is at least 0.95 (95%) 76
(c) Y_P is at least 0.99 (99%) 76

List of Tables

		Pg.
1-1	Classic Mixing Sensitive Reaction Schemes	3
2-1	General Mixing Sensitive Reaction Schemes	36
2-2	General initial conditions for C-C and C-P reaction schemes @ t^*=0.	36
2-3	Stoichiometric initial conditions based on w_{B_0} for C-C and C-P reaction schemes.	37
2-4	Numerical values for simulated C-C test cases. Stoichiometric coefficients $\alpha, \beta, \gamma, \epsilon$ were set to 1, representing the reaction: $A + B \overset{k_1'}{\rightarrow} P$, $P + B \overset{k_2'}{\rightarrow} S$ and initial mass fraction of species *B* was always 1 ($w_{B_0} = 1$).	37
2-5	Numerical values for simulated C-P test cases. Stoichiometric coefficients γ, ϵ were set to 1, representing the reaction: $A + B \overset{k_1'}{\rightarrow} P$, $C + B \overset{k_2'}{\rightarrow} S$ and initial mass fraction of species *B* was always 0.5 ($w_{B_0} = 0.5$).	38
3-1	Stoichiometries of reaction schemes and the corresponding non-dimensional reaction rate ratio for the eight different C-C reactions. *Da* was always $Da = k_1' \left(\frac{\rho_T}{M}\right) \frac{L_B^2}{D_B}$.	62
3-2	Stoichiometries of reaction schemes and the corresponding non-dimensional reaction rate ratio and Damköhler number for the four different C-P reactions.	63

Nomenclature

c	Molar Concentration in Cox et al. (1998), [kmol/m^3]
c_{B_0}	Initial concentration of limiting reagent in Cox et al. (1998), [kmol/m^3]
Da	Damköhler Number, [-]
Da_{II}	Damköhler Number in Cox et al. (1998), [-]
D	Diffusivity, [m^2/s]
I'	Non-dimensional concentration of species *I* in Cox et al. (1998), [-]
k_1	Rate constant 1 in Cox et al. (1998), [m^3/kmol s]
k_2	Rate constant 2 in Cox et al. (1998), [m^3/kmol s]
k_1'	Rate constant 1, [m^3/kmol s]
k_2'	Rate constant 2, [varies]
$\frac{k_2}{k_1}$	Non-dimensional reaction rate ratio, [-]
L	Striation thickness, [m]
M	Molecular weight, [kg/kmol]
R	Reaction term [kg/m^{3}s]
t	Time, [s]
t^*	Non-dimensional time, [-]
T	Non-dimensional time in Cox et al. (1998), [-]
w	Mass fraction, [-]
W	Striation Thickness in Cox et al. (1998), [m]
x	Distance, [m]
x^*	Non-dimensional distance, [-]
X	Non-dimensional distance in Cox et al. (1998), [-]
Y_P	Yield of desired Product *P*, [-]

Greek Letters

$\alpha, \beta, \gamma, \epsilon$	Stoichiometric Coefficients, [-]
ε	Reaction rate ratio in Cox et al. (1998), [-]
ε_D	Local dissipation of Turbulent Kinetic Energy per mass, [m^2/s^3]

ρ	Mass Concentration, [kg/m^3]
ν	Kinematic viscosity [m^2/s]
τ_M	Mixing time, [s]
τ_R	Reaction time, [s]

Subscripts

A	Species *A* (reactant)
B	Species *B* (reactant)
C	Species *C* (reactant)
i	Species *A*, *B*, *C*, *I*, *P* or *S*
I	Species *I* (inert)
I'	Any species *I'* in Cox et al. (1998)
0	Initial value
P	Species *P* (product)
S	Species *S* (by-product)
T	Total
Y, Z	Species Mixtures

1

Introduction & Literature Review

1.1 MIXING AS IT PERTAINS TO CHEMICAL REACTIONS

Mixing and reactions are intrinsically related – reactions involving multiple reactants cannot occur without the reactants being contacted intimately at a molecular level. Reactants however are added at macroscopic scales and are initially segregated. For the reaction to occur, the pure reactants need to be brought together, which is usually at a macroscopic scale, and homogenized down to the molecular scale, so that the molecules can collide and collision probabilities governing the production of new chemicals take over. This process requires a reduction of scale and differences in concentration to occur. This process of reduction of the scale of this segregation and the differences in concentration is, in essence, the very definition of mixing as it pertains to chemical reactions.

Chemical reactions are only one of many processes which require careful consideration of mixing. *The Handbook of Industrial Mixing: Science and Practice* (Paul et al., 2004), describes mixing as a "reduction in inhomogeneity to achieve a desired process result". Usually the quantity being homogenized is a scalar such as concentration, temperature or phase. Some common chemical engineering processes that are dependent on mixing include liquid-liquid blending, solids suspension in liquids, distillation, heat transfer in liquid reactors and the topic of this thesis, chemical reactions. For the particular case of reactions, it would be the concentrations of the reactants which would be mixed and the desired process result would be to maximize the yield of desired product.

Any reaction involving two or more reactants is completely dependent on mixing to even take place. If a reaction is slow the mixing can be completed before the reaction begins, so effectively the mixture is perfectly mixed, i.e. the concentration of reactants is almost uniform within the mixture. In these cases the traditional approach for determining yield outlined by Levenspiel (1972) works very well. However, in the case of faster reactions, it is often possible for the reaction to occur on the same or smaller time scale than that of the mixing. This means that when the reaction occurs, which takes place on a molecular scale, it is subject to a heterogeneous distribution of local concentrations and hence occurs at varying rates. In a reaction where only one product can occur, the rate of mixing can slow down the local reaction rates and hence slow down the entire reaction leading to a longer residence time within a reactor. While the rate of the reaction is the only thing affected in a reaction with just one possible product, in a situation where there are multiple competing reactions it is also possible for a product distribution to arise, and the mixing can greatly affect the outcome of products from a given reaction. An everyday example of such a reaction situation is combustion in internal combustion engines, e.g. cars and other automobiles, where the rate at which air is mixed with the fuel within the piston cylinders affects not only the efficiency but also the products that are exhausted to the atmosphere, most of which is carbon dioxide and water but some of which are harmful by products such as carbon monoxide and NO_x compounds. When the combustion is inefficient, possibly due to improper mixing of fuel and oxidant, engine knock occurs and more of the harmful by products can be produced.

A part of the chemical industry deals with the production of chemicals from reactions. Industrial chemical reacting flows are usually carried out on a very large scale. This makes them rather complex processes which depend on the properties of the reactants, the fluid mechanics of the flows and the micro scale diffusive behaviour of the reactants and the reaction process. The mixing requirements for reactions which are particularly sensitive to the mixing condition in such large scale production facilities can often be incorrectly predicted since the process is so very complicated, so it is necessary to provide better methods of prediction for these mixing sensitive reactions.

1.2 MIXING SENSITIVE REACTIONS

There is a class of reactions where the progress of the reaction depends heavily on how fast the reactants are brought together. These reactions usually consist of two or more competitive reactions either occurring in parallel, where two or more reactions involving the same reactants take place at the same time, or in consecutive sequence, where the desired product of one of the reactions participates in another undesired reaction with the original reactants. Both types of reaction schemes can involve considerable production of unwanted by-product despite the desired reaction being as much as a million times faster than the undesired reaction. Typical representations of the above mentioned reactions schemes are given in Table 1:

Table 1. Classic Mixing Sensitive Reaction Schemes

$\boldsymbol{Competitive\ Consecutive}$ $(\boldsymbol{C-C})$	$\boldsymbol{Competitive\ Parallel}$ $(\boldsymbol{C-P})$
$A + B \overset{k_1'}{\rightarrow} P$	$A + B \overset{k_1'}{\rightarrow} P$
$P + B \overset{k_2'}{\rightarrow} S$	$C + B \overset{k_2'}{\rightarrow} S$

For both cases $k_1' >> k_2'$, *P* is the desired product and *S* is the undesired by-product. Therefore, for a perfectly homogeneous mixture of reactants present in a stoichiometric ratio of one (*A*:*B* = 1:1), the yield of by-product *S* should be very small for both cases. However, several previous investigations (Baldyga and Bourne, 1999, Patterson *et al.*, 2004) have shown that the yield of by-product can indeed be quite significant: an effect which has been attributed to imperfect mixing. The mixing of reactants can be an integral part of the reaction process because for these reactions where multiple products are possible the mixing not only affects the reaction rate but also the product distribution within the system. The effects of mixing and reaction rate ratio have been studied extensively for the base stoichiometry shown above (for example Baldyga and Bourne, 1999, Cox et al., 1998, Clifford et al., 1998a, Cox, 2004, Patterson et al., 2004).

The primary aim of this thesis is to study the effect of having a different overall reaction stoichiometry on the yield of desired product and the possible diffusive mass transfer limitations that may be associated with this difference.

1.3 SCALING MIXING AND REACTIONS: THE DAMKÖHLER NUMBER

As described in the previous sections, there is a considerable effect of mixing on a reaction involving two or more components. Scaling of such effects can be done using dimensionless numbers, such as the Reynolds number which scales inertial forces to viscous forces within a fluid to determine the level of turbulence in it. The Damköhler number is the dimensionless number used to scale the rate of mixing to the rate of reaction for any given mixing sensitive reaction. It is named after Gerhard von Damköhler, a German combustion engineer who pioneered the use of turbulence to enhance the mixing of fuel with air within the engines of World War II airplanes in order to make the fuel and engines more efficient. There are several forms of the Damköhler number, but the one which we are most interested in is the Mixing Damkohler number (*Da*) which is given by (Patterson *et al.*, 2004):

$$Da = \frac{\tau_M}{\tau_R} \tag{1.1}$$

where τ_M is the characteristic mixing time and τ_R is the characteristic reaction time. As with the Reynolds number, which is flexible in the use of a characteristic velocity and length scale, the Mixing Damköhler number is amenable to a variety of expressions when it comes to the characteristic mixing time and, in the case of multiple competing reactions, the characteristic reaction time as well. This can be attributed to the nature of turbulent mixing which is a process that spans several length and time scales, all the way from the macro tank scale to the micro diffusion scale. This very nature has made τ_M a term which is difficult to nail down, especially in the case of reacting flows for which almost all the scales have some significance. Also, though this variability may make the Damköhler number more versatile to adapt to different conditions, not unlike the Reynolds number which has enjoyed much success in being adapted to various

different flow conditions and geometries, it leaves the question of which characteristic mixing and reaction times are most suitable for the case of mixing sensitive reactions. The academic and industrial mixing communities have proposed several definitions of τ_M, τ_R and *Da* with respect to the reacting flow problem, and some of those efforts have been summarized in the following sections.

1.4 REVIEW OF THE MIXING LITERATURE

Investigations of yield from homogeneous reactions have been investigated by chemical engineers for quite some time, Danckwerts (1953, 1958) being an early example of such work. Levenspiel (1972) provides analytical solutions for the yield for any reaction provided it is perfectly well mixed. Academics and industrialists alike have been interested in this, as evidenced by the plethora of publications and works in the literature. *Chapter 13* of the *Handbook of Industrial Mixing: Science and Practice* (2004) is an excellent review of the literature from the point of view of the mixing community. *Turbulent Mixing and Chemical Reactions* by Baldyga and Bourne (1999) is also an excellent source of theoretical information on the area.

Since perfect mixing for mixing sensitive reactions is almost impossible to realise in practice, there have been several forays into investigating the effect of imperfect mixing on the final yield of desired product given (for example Patterson et al., 2004, Baldyga and Bourne, 1992, 1999, Bhattacharya, 2005).

In the chemical industry, reactions are normally carried out in semi-batch stirred tanks. This is usually a very complex process involving fluid mechanics, reaction kinetics and mass transfer at the micro-scale. The reactants are added at the macro-scale, which is usually the scale of the inlet pipe or tank, and the reaction takes place at the molecular scale. In between there is the so called meso-mixing scale, which is regarded as the scale reduction step of the mixing process. The mixing of miscible reactants is dependant mostly on the fluid mechanics and diffusive mass transfer of the reactants. Mixing and turbulence are very closely related and the rate of mixing is greatly influenced by the turbulence intensity within the tank, which can vary by orders of magnitude in different

regions of the tank. The maximum intensity is usually at the impeller, and the minimum is mostly in the bulk of the tank. Therefore, for most mixing sensitive reactions the reactants are injected at the impeller.

Mixing performance within a tank can be characterised by using certain mixing sensitive reactions (Baldyga and Bourne, 1992, 1999, Baldyga et al., 1996, Paul et al., 2004, Bhattacharya, 2005). These reactions are normally two stage reactions and usually take the form of a competitive-consecutive or consecutive-parallel reaction. There are a number of industrially relevant reactions which take this form, and for which maximizing the yield of the desired product is critical to the success of the process. It is therefore of great interest to industry to be able to predict the yield for these mixing sensitive reactions.

There have been several approaches to modelling and predicting the yield for reacting flows. There is one set of literature that focuses on the fluid mechanics. This is the full Computational Fluid Dynamics (CFD) approach where the entire tank is modelled with reaction a complex geometry, which is normally very computationally expensive and time consuming. There have been several attempts to introduce new models such as PDF models by Rodney Fox and others (Fox, 1998, 2003, Van Vliet et al., 2001), to speed up the simulation process and achieve results that match experiments.

At the other end of the spectrum, the focus is a simple geometry. Though these are a lot simpler to work with and write the equations for, the simplicity comes at the expense of a full representation of the physics and fluid mechanics. These are the Lagrangian micro-mixing models by Baldyga, Bourne and others (Baldyga and Pohorecki, 1995, Baldyga and Bourne, 1999, Villermaux and Falk, 1994). They have focused on keeping the geometry simple while trying to replicate experimental results. The models' greatest advantage is that they are very inexpensive computationally and, in some cases, have analytical solutions. The micro-mixing models have evolved from being simple alternating striations of reactants to the Engulfment model by Baldyga and Bourne (1999) which takes into account turbulence and is widely regarded as the best micro-mixing model currently available. The scales of these models are usually at or below the

Kolmogorov scale of turbulent eddies, therefore they are assumed to be independent of the large scale fluid mechanics. The Generalized Mixing Model proposed by Villermaux and Falk (1994) is a similar model extended to take into account meso-mixing effects as well.

There have also been attempts to integrate these two sets of models so as to capture the best of both worlds, the fluid mechanics from the CFD models and the diffusion effects and simplicity of the micro-mixing models. An example of this is given by Fox (1998), who combined Villermaux and Falk's (1994) Generalized Mixing Model and CFD for turbulent mixing simulations. Muzzio and Liu (1996) took a similar approach of integrating a micro-mixing model and CFD for laminar mixing.

Although there is a multitude of models of varying complexity, the one thing they all lack is any effect of stoichiometry. They are either one stage infinitely fast reactions or C-C and C-P reactions with a single stoichiometry. While the solution of the yield for a general stoichiometry when the mixing is perfect has been known for a long time (Levenspiel, 1972), the effects of imperfect mixing for reactions of varying stoichiometries have not been investigated.

The reacting flow problem for multiple competing reactions has also caught the eye of physicists and mathematicians since it presents interesting non-linear behaviour. A summary of these efforts is given in the next section.

1.5 REVIEW OF THE NON-LINEAR REACTION DYNAMICS

The C-C reaction provides an interesting non-linear problem that has been extensively investigated by physicists and chaos mathematicians like Cox, Clifford and others (Clifford, 1999, Clifford and Cox, 1999, Clifford et al., 1998a, 1998b, 1999, 2000, Cox et al., 1998, Cox, 2004). The wealth of literature on C-C reactions has gone relatively unnoticed by the chemical engineering mixing community. The C-P reaction scheme has been of less interest to the mathematics and physics communities and there is a smaller body of work attached to it (Taitelbaum et al., 1996, Sinder, 2002, Sinder et al., 2003,

Hecht and Taitelbaum, 2006). A summary of the investigation of C-C and C-P reaction schemes by physicists and mathematicians is given in the following paragraphs.

Mixing sensitive reactions exhibit interesting behaviours at reactant interfaces. There are several studies investigating these behaviours for reactions. Cornell & Droz (1997) is an example of such a study, where the behaviour of the reaction front for the general single step reaction $mA + nB \rightarrow Products$ was investigated. Cox, Clifford and Roberts (1998) and later Cox and Finn (2001) investigated the reaction interface for the classic C-C reaction extensively. They provided figures and analytical expressions for the profiles of each reaction species at the reaction interface using a model which consisted of 1D alternating reactant striations of varying thickness. The striations had uniform initial concentrations for which they wrote mole balance Partial Differential Equations (PDE's) for each of the species participating in the reaction.

In the long time investigations, Cox et al (1998) first started with stationary and segregated stripes of alternating reactants, i.e. Zebra Stripes, with uniform initial concentrations of reactants across the striations. They performed a mole balance and derived the equations in molar concentrations. The non-dimensionalization was done using the rate constant and concentrations and the striation thickness was avoided. The equations for non-dimensionalization were as follows:

$$T = t \cdot \left(k_1 c_{B_0}\right), \qquad X = x \cdot \left(\frac{k_1 c_{B_0}}{D}\right)^{\frac{1}{2}}, \qquad I' = \frac{c_{I'}}{c_{B_0}} \tag{1.2}$$

where (t,x, $c_{I'}$) and (T,X,I') are dimensional and dimensionless time, space and concentration for species I' respectively. k_1 is the rate constant for the desired reaction, c_{Bo} is the initial concentration of the limiting reagent and D is the diffusivity, which was assumed to be equal for all four species (A, B, R, S) involved. Their R is equivalent to our P. Their choice for these non-dimensionalizing equations was because they intended to use striations of unequal thickness within the same domain which made using the striation thickness as a non-dimensionalizing parameter difficult since it wouldn't be constant. However, since they looked at only one type of stoichiometry, the rate

expressions were a constant for them and therefore were the obvious choice for non-dimensionalization.

Initially they looked at a model which had a single striation thickness of initially segregated reactants (Cox et al., 1998). They investigated the effects of initial scale of segregation, i.e. striation thicknesses, and the reaction rate ratio for the classic competitive consecutive reaction scheme. The found that decreasing the scale of segregation, i.e. striation thickness, and the reaction rate ratio (k_2/k_1) was favourable. The formulations of the Damköhler number and reaction rate ratio that they found were as follows:

$$Da_{II} = \frac{k_1 c W^2}{D} \; and \; \varepsilon = \frac{k_2}{k_1} \tag{1.3}$$

where W represents the initial striation thickness of the reactants, k_1 is the reaction rate of the desired reaction, c is the molar concentration, D is the diffusivity and ε is the reaction rate ratio. Using this model they investigated the yield from zebra stripes of equal thicknesses (Clifford et al., 1998a). They confirmed that decreasing the scale of segregation can have a significant favourable effect on the yield of desired product. They also included a parameter to allow for non-stoichiometric initial concentrations of reactants and investigated the effects of having more A than B., less A than B and a stoichiometric mixture quite extensively. They also found that if initial ratio of reactants (A:B) is less than 1, the yield will go to zero and only if the initial ratio is above 1 can there be a significant yield of desired product.

Clifford (1999) and Clifford and Cox (1999) took the constant striation thickness model further by assuming a more realistic Gaussian distribution of concentration of reactants within the striations. They compared the full Partial Differential Equations (PDE's) of the Gaussian model with the uniform concentration model and an Ordinary Differential Equation (ODE) model. The uniform concentration model was found to over predict the yield and the ODE model agreed quite well with the full PDE solution results. This was somewhat of a departure from the rest of the literature on the subject, but provides an interesting perspective on the problem.

The next step Clifford, Cox and Roberts took was to introduce multiple initial striation thicknesses into the model, the so called "Bar Code" model (Clifford et al., 1999, 2000) as can be seen at the bottom of Figure 1-1. The motivation for this model was that it was a closer representation of what striations look like in a chaotic mixing situation since there is a wide distribution of striation thicknesses in the real system. They used the same reaction equations developed for the periodic equal initial striation thickness models (Clifford et al., 1998a). They investigated several combinations of 'thick' and 'thin' striations by varying the total number and the arrangement of the striations and found that grouping similar sized striations together maximized yield of the desired product. More importantly, they discovered that using an average striation thickness for the system always over predicted yield. Including a larger number of striations in the model brought the value of yield obtained when assuming an average striation thickness closer to that obtained from direct simulation of the distribution of striations.

Clifford et al. then did a similar investigation of the effect on yield of desired product as done for the equal striation thickness effects (Clifford et al., 1999). They investigated the effect of arrangement of striations of alternating reactants (*A* and *B*) with varying thicknesses on the yield. The arrangements were chosen such that the widths of the alternating reactants were positively correlated, negatively correlated or placed randomly. Because of the large computational requirements, they applied the Gaussian Method developed by Clifford which was mentioned earlier (Clifford, 1999). They found that a positive correlation between the *widths* of the striations, i.e. striations of similar widths grouped together, provided the most yield of desired product for intermediate times but that there is a crossover at large times where in fact the random arrangement provides the largest final yield of desired product. The negatively correlated case, i.e. alternating 'thick' and 'thin' striations, provided the worst yield. They then go on to test their lamellar model on a real system generated by a blinking vortex flow with a blob of B placed in a sea of A (shown in Figure 1-1). They obtained the initial striation distribution using a transect across a chaotically mixed structure, to which they then applied their Gaussian Method to solve for the yield. The yield from the real striation distribution was compared to the yield from the same system rearranged to be positively correlated with respect to width and negatively correlated with respect to

width. It was found that the real and positively correlated systems provided much higher yields than the negatively correlated system and agree with each other to within 7%. This can be expected since in real systems the stretching rates caused by mixing will be similar in certain regions, hence causing striations to be roughly the same width in roughly the same region, which should give a positively correlated arrangement of striations.

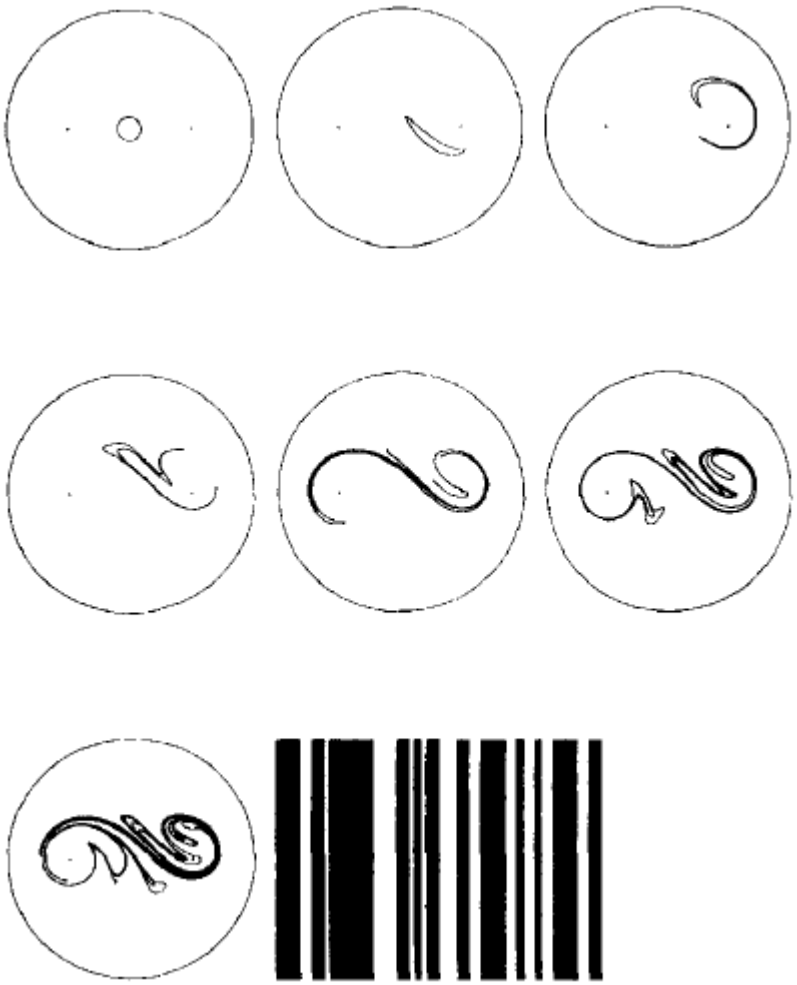

Figure 1-1. A lamellar structure generated by the blinking vortex flow. A circular blob is stretched and folded, generating thin striations that are modelled as a parallel array of lamellar, alternately of species *A* and *B* (the 'bar-code') – taken from Clifford et al. (2000).

The next step in Clifford, Cox and Roberts' quest for simulation of reality was to include a stretching parameter to take the reaction-diffusion model to a reaction-diffusion-advection model (Clifford et al., 1998b). This was to account for the stretching that is normally encountered by striations when mixing is occurring. Although this would normally require 2D simulations, they applied a co-ordinate transformation to the equations such that the 1D striations would be stretched at a constant rate, the Lyapunov exponent. They simulated a 2D sine flow along with their 1D lamellar stretching model and compared the results with the 2D results of Muzzio and Liu (1996). They found that their 1D lamellar stretching model had close agreement with respect to product quality with the 2D simulations at a significantly lower computational cost. However, they also admitted that this agreement was for a less than realistic flow field.

There have also been attempts to get at the yield for full chaotic mixing fields (Cox, 2004, Muzzio and Liu, 1996). Interestingly enough, the work by Muzzio and Liu came before all the aforementioned work, but was done at a very large computational cost. Most of the work by Cox et al. seems to have concentrated on trying to replicate the results of this full chaotic field with a 1D model which would be considerably less expensive computationally. Cox also summarized these efforts, the 1D modeling, 2D modeling and reduced models, including various chaotic mixing models, such as the Baker Map model for simulating stretching and folding (Cox, 2004). He found that the yield of desired product in a C-C reaction is underestimated by a 1D lamellar model that ignores the effects of fluid mixing but overestimated by the two other lamellar models (continuous stretching and discrete stretching and folding (Baker Map)) that include the fluid mixing.

All this work was done for only the C-C reaction scheme and for the one classic stoichiometry. The C-P reaction scheme has a considerably smaller body of work attached to it as compared to the C-C reaction scheme, with the majority of work concentrating on the reaction front behaviour (Taitelbaum et al., 1996, Sinder, 2002, Sinder et al., 2003, Hecht and Taitelbaum, 2006). Previous investigations of the C-P scheme also suffer from the same issue as the C-C: only one stoichiometry has been considered.

The Damköhler number for the classic C-C reaction has been suggested by Cox et al. (1998), but there is no such suggestion for a C-C reaction scheme with a general stoichiometry. There is a similar lack of definition for the C-P reaction scheme. Though the reaction rate ratio remains dimensionless for the classic versions of the C-C and C-P reaction schemes, this is not the case for reactions which have different stoichiometries and hence rate expressions. This means that any ratio of reaction rates would have dimensions, which makes it difficult to compare reactions with different stoichiometries. Definition of a non-dimensional reaction rate ratio would be required.

1.6 QUALITATIVE DESCRIPTORS OF MIXING AND REACTION RATE RATIO

Before proceeding, it is important for the reader to have a good qualitative feel of what is meant by good or poor mixing and favourable or unfavourable reaction rate ratios with respect to chemical reactions since this terminology will consistently be referred to in the proceeding chapters, with the intention of eventual assignment of quantitative definitions to the qualitative descriptions. But until that is done, a thorough qualitative description is necessary.

What is meant by well mixed and poorly mixed when talking about chemical reactions? For this we need to define the limits of perfectly well mixed and perfectly segregated mixtures from the point of view of reactions involving two or more miscible reagents, present either in pure form or individually diluted with a miscible inert before being mixed.

The limit of perfectly well mixed from the point of view of reactions is an instant perfectly homogeneous concentration field such that the yield of desired product will be a maximum. This also corresponds to the perfectly micro-mixed mixing condition. This has been described in Levenspiel (1972) and is usually the basis used for design of reactors in chemical engineering and it is what is taught throughout the chemical engineering curriculum. Our definition of good mixing from the standpoint of reactions would be an initial state of segregation that approaches this perfectly well mixed condition and hence approaches the maximum yield of desired product possible.

At the other end of the spectrum is the perfectly segregated situation or complete segregation of reactants in concentration without diffusion and with a minimum surface area of contact between reactants. In this case, since there is no diffusion, the reaction can occur only at the interface and then comes to a complete halt, so the yield of desired product is minimized. In the absence of diffusion, the only way to increase the yield would be to increase the surface area of contact between reactants, in which case the extent of the reaction is completely dependent on the scale of segregation. The situation is vastly improved with the introduction of diffusion because then the reactants away from the interfaces are granted access to one another. Diffusion is the final agent of mixing at the smallest scales of segregation and it is this phenomenon which allows for intimate contact between reactants that are not immediately at the interface.

With diffusion present, the perfectly segregated case would be one that would have segregated reactants with a minimum surface area of contact which will take infinitely long to obtain a sizeable yield of desired product. Our definition of poor mixing would be the approach to this limit such that the yield of desired product is minimized.

When the scale of segregation is varied by adjusting the initial striation thickness of the reactants, the limit of perfectly mixed is the case where striation thickness goes to zero, and the limit of perfectly segregated occurs when the striation thicknesses are infinitely thick with just one interface. In the well mixed case the striation thickness approaches zero and in poorly mixed case the striation thicknesses approach infinity. Therefore, as the initial striation thickness decreases the mixing condition improves and as the striations get thicker the mixing condition worsens.

Since a Damköhler number (*Da*) will be used to quantify mixing, where the only variable is the striation thickness and the diffusivity is constant, we could also say that as *Da* approaches zero the mixture is approaching perfectly well mixed, and as *Da* approaches infinity the mixture approaches perfectly segregated with diffusion. The perfectly segregated case with no diffusion occurs if the diffusion coefficients of the reactants approach zero.

How do we define favourable and unfavourable reaction rate ratios?

According to perfectly well mixed reaction kinetics (Levenspiel, 1972, Fogler, 1999), the faster the desired reaction is compared to the undesired reaction, the larger the final yield of desired product will be. Since our objective is to maximize the yield of desired product, a very small k_2/k_1 would be favourable and a very large k_2/k_1 would be highly undesirable. The limits for the non-dimensional reaction rate ratio k_2/k_1would therefore be the most desirable when $k_2/k_1 = 0$, which means that the second undesirable reaction doesn't take place at all regardless of the concentrations of reactants present, and k_2/k_1 approaches infinity when the undesired by-product is formed instantaneously. Therefore a favourable reaction rate ratio would be one that approaches $k_2/k_1 = 0$ and an unfavourable reaction rate ratio would be one that approaches $k_2/k_1 = \infty$. The actual ranges of the ratio will eventually be determined from the simulations described later in this work.

1.7 OBJECTIVES AND PROPOSED CONTRIBUTIONS

The objectives of this work are:

1) Develop a model which has a general Damköhler number for any mixing sensitive reaction with a variable stoichiometry.
2) Investigate the effects of stoichiometry, mixing and relative reaction rates on the final yield of desired product for mixing sensitive reactions of both types: C-C and C-P.
3) Investigate the transient behaviour of these different reactions at the reaction interface for short and long times.
4) And finally, to develop a set of figures or charts to facilitate design of reactors for two competing reactions which are mixing sensitive.

The ultimate goal of this work is to give a so called "leg up" to the chemical engineering practitioner who is designing a reactor for a previously un-investigated mixing sensitive reaction. Prediction of the yield for mixing sensitive reactions has been particularly

difficult, as documented in *Chapter 13* of the *Handbook of Industrial Mixing*, owing mostly to a lack of information about the reaction schemes, reaction rate ratios, mixing requirements etc. The work on mixing sensitive reactions that has been documented in the *Handbook* is for specific known reactions, so the results are not directly transferable to a new reaction, and any general treatment has been restricted to specific stoichiometries, all with coefficients of one. Designs involving more complex reactions often rely on experience and trial and error, or extensive pilot scale testing.

From the more theoretical point of view, there has been quite a bit of debate on the formulation of the Damköhler number for two stage reactions: does one use the rate of the first reaction, the second reaction, or the reaction for which the information is available? What is the appropriate mixing time? Once a standard Damköhler number can be determined it will be possible to develop a framework around which charts or figures predicting yield for mixing sensitive reactions can be produced, thus making it easier for the practicing chemical engineer to deal with complex reaction systems involving multiple interacting parameters. Even if the model does not serve to predict the yield exactly, it will at least serve to provide a framework for the analysis of new reaction schemes. In the end, the hope is that this work will assist the practising chemical engineer in understanding the design requirements of reactors for mixing sensitive reactions by clarifying the dominant variables and the interactions between them.

1.8 THESIS OUTLINE

This thesis, written in a paper-based format, consists of four chapters in addition to the Introduction. **Chapter 2,** Paper 1, contains the derivation of the model proposed to take into account the three effects of mixing, reaction rate ratio and stoichiometry of the reaction and some preliminary results. In **Chapter 3**, Paper 2, a detailed investigation of these three effects is presented along with an evaluation and discussion of the results. **Chapter 4** summarizes this thesis and provides recommendations for possible further extensions of the work presented. The cited literature is listed in **Chapter 5**. **Appendix A**

includes all the figures and data of the results obtained from COMSOL for this investigation.

Since this thesis has been written in a paper-based format, there is some overlap between the chapters. The introductory chapter is a compilation of the introduction sections of the two papers in Chapters 2 and 3, and, in order to avoid repetition, the introduction sections of the papers have been replaced with chapter overviews. The conclusions of the chapters have been left since they are instrumental in emphasizing the important points in the individual chapters. The final conclusions chapter is a summation of the conclusions with future contributions added.

2

Model to Study the Effects of Mixing, Reaction Rates and Stoichiometry on Yield for Mixing Sensitive Reactions

2.1 CHAPTER OVERVIEW

This chapter presents the derivation of a model capable of investigating the effects of initial mixing condition, reaction rate ratio and stoichiometry for mixing sensitive reactions of two types: the Competitive-Consecutive (C-C) reaction and Competitive-Parallel (C-P) reaction. **Section 2.2** contains the theory and derivation of the model for the two mixing sensitive reaction schemes. **Section 2.3** includes the numerical solution of the equations, and **Section 2.4** contains some preliminary results and discussion of those results. **Section 2.5** summarizes and concludes the chapter. **Sections 2.6** and **2.7** are the tables and figures for this chapter respectively.

2.2 MODEL DESCRIPTION AND GOVERNING EQUATIONS

The model that has been developed is based on an idealized one-dimensional geometry of initially alternating layers of reactants at the micro-mixing scale with a cross section as shown in Figure 2-1(a). Figure 2-1(b) depicts an isolated segment of the overall structure in the vicinity of x=0, which is placed at the interface between the generic reactant mixtures Y and Z, thereby creating a domain of interest bounded by the symmetric of zero-flux boundaries at the mid-planes of these layers. In this formulation the mixtures Y and Z are allowed to take on different species compositions depending

on the reaction scheme being considered and the imposed stoichiometry. Figure 2-1(c) shows the geometry for the specific case of pure striations of *A* and *B*.

A system of non-dimensional reactive-diffusive Partial Differential Equations (PDE's) based on a mass balance has been developed for each of the species in the reaction system. It is assumed that the fluid in the system remains homogeneous in phase and is at a constant temperature, as well as being quiescent. Given these assumptions, the general unsteady 1D species mass balance reaction-diffusion equation is given by:

$$\frac{\partial(\rho_i)}{\partial t} = D_i \frac{\partial^2(\rho_i)}{\partial x^2} + R_i \tag{2.1}$$

where ρ_i is the individual species mass concentration, D_i is the individual species diffusivity with respect to the mixture, and R_i represents the reaction source/sink terms. x and t are the space and time coordinates respectively. The model assumes that the initial striation thicknesses of the reactant mixtures are equal, L_Z , as shown in Figure 1b with $L_Y = L_Z$. One of the objectives of this model is to allow for the investigation of initial mixing conditions, varied using the initial striation thicknesses. Using the initial striation thickness, space (x) and time (t) can be made non-dimensional by:

$$x^* = \frac{x}{L_Z} = \frac{x}{L_B} \qquad\qquad t^* = \frac{t\,D_Z}{L_Z^2} = \frac{t\,D_B}{L_B^2} \tag{2.2}$$

The choice of D_Z and L_Z for non-dimensionalization was made because later on in this work the composition for the *Z* layer is to be restricted to a mixture containing only an inert *I* and/or the limiting reagent *B*, which is always assumed to be the limiting reagent of the reaction regardless of the scheme, effectively making $D_Z = D_B$ and $L_Z = L_B$, as shown in Equation (2.2). It was preferred to use the properties of the limiting reagent for non-dimensionalization because it is the main species of interest that is initially present within the system. Species mass concentrations (ρ_i) were converted to mass fractions (w_i) using:

$$\rho_T = \sum \rho_i \qquad\qquad w_i = \frac{\rho_i}{\rho_T} \tag{2.3}$$

Using Equations (2.2)-(2.3) to modify Equation (2.1), the non-dimensional general species equation for the unsteady 1-D, stationary, reactive-diffusive system is given by:

$$\frac{\partial(w_i)}{\partial t^*} = \frac{D_i}{D_B}\frac{\partial^2(w_i)}{\partial x^{*2}} + \frac{L_B^2}{\rho_T D_B}R_i \tag{2.4}$$

The assumption of all the species having the same diffusivities was also applied, hence making the coefficient of the elliptical term in Equation (2.4) unity and giving:

$$\frac{\partial(w_i)}{\partial t^*} = \frac{\partial^2(w_i)}{\partial x^{*2}} + \frac{L_B^2}{\rho_T D_B}R_i \tag{2.5}$$

Equation (2.5) represents the reaction-diffusion equation for some arbitrary reaction, represented by the source/sink term R_i. The particulars of this term define themselves once a reaction scheme is specified. For the purposes of this paper, the reaction scheme will be specified as either a generalized Competitive-Consecutive (C-C) or Competitive-Parallel (C-P) reaction between the two layers. For these purposes, layer *Z* was assumed to be composed of a homogeneous mixture of limiting reagent, *B*, and an inert, *I*, while layer *Y* was composed of either a single reactant, *A*, or two reactants, *A* and *C*, again with an inert species mixed into this layer. Table 2-1 shows the generalized reaction schemes for the two types of mixing sensitive reactions that will be investigated. In order to focus the investigation on the different reaction schemes, the effect of species diffusivity was not investigated in this work.

A and *B* represent the initial reactants for the C-C scheme. *A*, *B* and *C* represent the initial reactants for the C-P scheme. *P* is the desired product and *S* the undesired product for both reaction schemes. An inert, *I*, is also present, but it does not participate in the reaction. $k_1^{'}$, $k_2^{'}$ represent the rate constants for the desired and undesired reactions respectively and $\alpha, \beta, \gamma, \epsilon$ are the stoichiometric coefficients.

If it is assumed that the reactions are elementary, expressions for R_i can be written a priori as molar rate expressions. In order to be used in Equation (2.5), these molar-based expressions are converted to mass fraction rate expressions by multiplication of the corresponding molecular masses of each species. To keep the focus on the effects of

stoichiometry, It was further assumed that the molecular mass of *A*, *B* and *C* were identical (*M*). As an example, the source term for species *A* for both C-C and C-P is given by:

$$R_A\left[\frac{mass}{m^3 s}\right] = -k_1^{'}[A][B]^{\epsilon} M_A = -k_1^{'}\frac{\rho_A}{M_A}\left(\frac{\rho_B}{M_B}\right)^{\epsilon} M_A = -k_1^{'}\frac{\rho_T^{1+\epsilon}}{M_B^{\epsilon}} w_A w_B^{\epsilon} \qquad (2.6)$$

These mass fraction rate expressions are then placed in Equation (2.5). The molecular masses of *P* and *S* depend on the stoichiometry and are derived using the Law of Mass Action. For example, the molecular mass of *P* for the C-P scheme would be:

$$M_P = M_A + \epsilon M_B = (1+\epsilon)M \qquad (2.7)$$

Expressions for the source and sink terms for all participating species can be written as shown for species *A* in Equation (2.6). It should be noted that this source/sink term contains all the information for the reaction scheme of interest. The R_i terms for the other species are significantly different for the C-C and C-P reaction schemes, hence the systems of partial differential equations (PDE's) are developed separately in the following sub-sections.

2.2.1 Competitive-Consecutive (C-C) Reaction Scheme

The C-C reaction scheme is the reaction scheme in which the desired product (*P*), once formed, participates in an undesired reaction with one of the original reactants (in this case, *B*). The species that participate in the reaction are *A*, *B* and *P*. The desired product is *P* and the undesired by-product is *S*. The general stoichiometry for this type of reaction scheme was given in Table 1. The source and sink term expressions for *A*, *B*, *P*, *S* and inert *I* for the C-C reaction scheme are developed by a procedure similar to that shown in Equation (2.6). Once these expressions are substituted in Equation (2.5) and simplified, the following system of equations is obtained:

A: $$\frac{\partial(w_A)}{\partial t^*} = \frac{\partial^2(w_A)}{\partial x^{*2}} - \left[k_1^{'}\left(\frac{\rho_T}{M}\right)^{\epsilon}\frac{L_B^2}{D_B} w_A w_B^{\epsilon}\right] \qquad (2.8)$$

B:
$$\frac{\partial(w_B)}{\partial t^*} = \frac{\partial^2(w_B)}{\partial x^{*2}} - \epsilon\left[k_1^{'}\left(\frac{\rho_T}{M}\right)^{\epsilon}\frac{L_B^2}{D_B}w_A w_B^{\epsilon}\right] - \frac{\alpha\gamma}{\beta}\left[\frac{\alpha^{\beta-1}\beta}{(1+\epsilon)^{\beta}}k_2^{'}\left(\frac{\rho_T}{M}\right)^{\beta+\gamma-1}\frac{L_B^2}{D_B}w_P^{\beta}w_B^{\gamma}\right] \tag{2.9}$$

P:
$$\frac{\partial(w_P)}{\partial t^*} = \frac{\partial^2(w_P)}{\partial x^{*2}} + (1+\epsilon)\left[\begin{matrix} k_1^{'}\left(\frac{\rho_T}{M}\right)^{\epsilon}\frac{L_B^2}{D_B}w_A w_B^{\epsilon} \\ -\frac{\alpha^{\beta-1}\beta}{(1+\epsilon)^{\beta}}k_2^{'}\left(\frac{\rho_T}{M}\right)^{\beta+\gamma-1}\frac{L_B^2}{D_B}w_P^{\beta}w_B^{\gamma}\end{matrix}\right] \tag{2.10}$$

S:
$$\frac{\partial(w_S)}{\partial t^*} = \frac{\partial^2(w_S)}{\partial x^{*2}} + \left(1+\epsilon+\frac{\alpha\gamma}{\beta}\right)\left[\frac{\alpha^{\beta-1}\beta}{(1+\epsilon)^{\beta}}k_2^{'}\left(\frac{\rho_T}{M}\right)^{\beta+\gamma-1}\frac{L_B^2}{D_B}w_P^{\beta}w_B^{\gamma}\right] \tag{2.11}$$

I:
$$\frac{\partial(w_I)}{\partial t^*} = \frac{\partial^2(w_I)}{\partial x^{*2}} \tag{2.12}$$

In order to compare the effect of the relative rates of the desired and undesired reactions while allowing for different reaction stoichiometries, it is necessary to provide a non-dimensional expression for the reaction rate ratio of the desired and undesired reactions. Using the ratio of k'_2/k'_1 is insufficient since this ratio would have different dimensions for each reaction stoichiometry, making comparison difficult. An ideal non-dimensional ratio should give relative rates of the desired reaction to the undesired reaction while retaining a physical meaning that can be intuitively understood. This can be accomplished by comparing the mass conversion rates associated with the first and second reactions. For the C-C scheme this was done by comparing the mass rate of consumption of desired product *P* in the second reaction to the mass rate of production of *P* in the first reaction as shown:

$$\frac{k_2}{k_1} = \frac{mass\ rate\ of\ consumption\ of\ P\ by\ undesired\ reaction}{mass\ rate\ of\ production\ of\ P\ by\ desired\ reaction} \tag{2.13}$$

The objective is to make this ratio as small as possible to maximize the amount of P produced. By using mass rate expressions to replace the statements in Equation (2.13) and then simplifying the resulting expression, non-dimensional reaction rate ratio for the general C-C reaction scheme becomes:

$$\frac{k_2}{k_1} = \left[\frac{\beta}{\alpha}\left(\frac{\alpha}{1+\epsilon}\right)^{\beta}\left(\frac{\rho_T}{M}\right)^{\beta+\gamma-\epsilon-1}\right]\frac{k_2^{'}}{k_1^{'}} \tag{2.14}$$

This physically meaningful k_2/k_1 captures both an effect of stoichiometry as well as the effect of the reaction rate constants of the two reactions, as well as having the benefit of significantly simplifying Equations (2.8)-(2.12) to give:

A:
$$\frac{\partial(w_A)}{\partial t^*} = \frac{\partial^2(w_A)}{\partial x^{*2}} - \left[\left(k_1^{'}\left(\frac{\rho_T}{M}\right)^{\epsilon}\frac{L_B^2}{D_B}\right)w_A w_B^{\epsilon}\right] \tag{2.15}$$

B:
$$\frac{\partial(w_B)}{\partial t^*} = \frac{\partial^2(w_B)}{\partial x^{*2}} - \left[\left(k_1^{'}\left(\frac{\rho_T}{M}\right)^{\epsilon}\frac{L_B^2}{D_B}\right)w_A w_B^{\epsilon}\right] - \frac{\alpha\gamma}{\beta}\left[\left(k_1^{'}\left(\frac{\rho_T}{M}\right)^{\epsilon}\frac{L_B^2}{D_B}\right)\frac{k_2}{k_1}w_P^{\beta}w_B^{\gamma}\right] \tag{2.16}$$

P:
$$\frac{\partial(w_P)}{\partial t^*} = \frac{\partial^2(w_P)}{\partial x^{*2}} + (1+\epsilon)\left[\begin{array}{c}\left(k_1^{'}\left(\frac{\rho_T}{M}\right)^{\epsilon}\frac{L_B^2}{D_B}\right)w_A w_B^{\epsilon} \\ -\left(k_1^{'}\left(\frac{\rho_T}{M}\right)^{\epsilon}\frac{L_B^2}{D_B}\right)\frac{k_2}{k_1}w_P^{\beta}w_B^{\gamma}\end{array}\right] \tag{2.17}$$

S:
$$\frac{\partial(w_S)}{\partial t^*} = \frac{\partial^2(w_S)}{\partial x^{*2}} + \left(1+\epsilon+\frac{\alpha\gamma}{\beta}\right)\left[\left(k_1^{'}\left(\frac{\rho_T}{M}\right)^{\epsilon}\frac{L_B^2}{D_B}\right)\frac{k_2}{k_1}w_P^{\beta}w_B^{\gamma}\right] \tag{2.18}$$

I:
$$\frac{\partial(w_I)}{\partial t^*} = \frac{\partial^2(w_I)}{\partial x^{*2}} + [0] \tag{2.19}$$

Examination of equations (2.15)-(2.19) shows there is an expression common to all four of the equations involving reactions, which takes the form of a Damköhler number (*Da*) given by:

$$Da = k_1^{'}\left(\frac{\rho_T}{M}\right)^{\epsilon}\frac{L_B^2}{D_B} = \frac{k_1^{'}\left(\frac{\rho_T}{M}\right)^{\epsilon}}{\left(\frac{D_B}{L_B^2}\right)} = \frac{rate\ of\ desired\ fast\ \ reaction}{rate\ of diffusion/micromixing} \qquad (2.20)$$

$$= (rate\ of\ desired\ fast\ reaction) * (diffusion/micromixing\ time\ )$$

This *Da* depends on the rate constant of the desired reaction and the initial striation thickness of the reactants. It scales the rate of diffusion at the smallest scale of mixing with the desired reaction rate. The effect of the second reaction rate is included through the rate ratio, k_2/k_1. Looking at Equation (2.20), a small Damköhler number indicates that diffusion in the smallest striation is fast compared to the desired/fast reaction and a large Damköhler number indicates that diffusion is slow compared to the fast reaction. A small *Da* is expected to give a high yield.

Cox et al.'s (1998) formulations of Damköhler number and dimensionless reaction rate ratio for the classic C-C reaction scheme are obtained from our general forms of the Damköhler number (Equation (2.20)) and dimensionless reaction rate ratio (Equation 2.14)) when α, β, γ and ϵ equal 1, which gives the classic C-C reaction scheme. A factor of 0.5 appears in the k_2/k_1 ratio because we used a mass balance in the derivation of the equations and Cox et al. used a mole balance.

Substituting Equation (2.20) into Equations (2.15)-(2.19) gives the final set of equations:

A: $$\frac{\partial(w_A)}{\partial t^*} = \frac{\partial^2(w_A)}{\partial x^{*2}} - [(Da)w_A w_B^{\epsilon}] \qquad (2.21)$$

B: $$\frac{\partial(w_B)}{\partial t^*} = \frac{\partial^2(w_B)}{\partial x^{*2}} - [(Da)w_A w_B^{\epsilon}] - \frac{\alpha\gamma}{\beta}\left[(Da)\frac{k_2}{k_1}w_P^{\beta}w_B^{\gamma}\right] \qquad (2.22)$$

P: $$\frac{\partial(w_P)}{\partial t^*} = \frac{\partial^2(w_P)}{\partial x^{*2}} + (1+\epsilon)\left[(Da)w_A w_B^{\epsilon} - (Da)\frac{k_2}{k_1}w_P^{\beta} w_B^{\gamma}\right] \quad (2.23)$$

S: $$\frac{\partial(w_S)}{\partial t^*} = \frac{\partial^2(w_S)}{\partial x^{*2}} + \left(1+\epsilon+\frac{\alpha\gamma}{\beta}\right)\left[(Da)\frac{k_2}{k_1}w_P^{\beta} w_B^{\gamma}\right] \quad (2.24)$$

I: $$\frac{\partial(w_I)}{\partial t^*} = \frac{\partial^2(w_I)}{\partial x^{*2}} + [0] \quad (2.25)$$

Using Equations (2.21)-(2.25), the effect of reaction rates and striation thickness on C-C reactions can be investigated using the non-dimensional reaction rate ratio (k_2/k_1) and the Damköhler number (*Da*).

2.2.2 Competitive-Parallel (C-P) Reaction Scheme

A C-P reaction scheme is a reaction scheme in which one of the original reactants (in this case, *B*) participates in two reactions simultaneously. One reaction gives a desired product (*P*) and the second reaction gives an undesired by-product (*S*). The species that participate in the reactions are *A*, *B* and *C*. The products are *P*, the desired product, and *S*, the undesired product. The general stoichiometry for this type of reaction is shown in Table 2-1. The source and sink term expressions for *A*, *B*, C, *P*, *S* and inert *I* for the C-P reaction scheme were developed following same procedure as shown for the C-C reaction scheme above and then replaced in Equation (2.5) to get a set of PDE's for the C-P reaction scheme.

As with the C-C reaction scheme, variable stoichiometry requires the introduction of a physically meaningful, non-dimensional reaction rate ratio for the C-P scheme. Since the C-P reaction scheme has only one reagent (*B*) which participates in both reactions, the non-dimensional reaction rate ratio for the C-P scheme becomes:

$$\frac{k_2}{k_1} = \frac{mass\ rate\ of\ consumption\ of\ B\ by\ undesired\ reaction}{mass\ rate\ of\ consumption\ of\ B\ by\ desired\ reaction} \quad (2.26)$$

which, on substitution of rate expressions, can be written as:

$$\frac{k_2}{k_1} = \left[\frac{\gamma}{\epsilon}\left(\frac{\rho_T}{M}\right)^{\gamma-\epsilon}\right]\frac{k_2^{'}}{k_1^{'}} \tag{2.27}$$

As with the k_2/k_1 ratio defined for the C-C reaction scheme, minimization of this ratio would yield the maximum desirable product (*P*). This k_2/k_1 also includes the effects of stoichiometry and reaction rate constants for the two reactions. Substitution of Equation (2.27) into the C-P PDE's and simplifying gives:

A: $$\frac{\partial(w_A)}{\partial t^*} = \frac{\partial^2(w_A)}{\partial x^{*2}} - \left[\left(k_1^{'}\left(\frac{\rho_T}{M}\right)^{\epsilon}\frac{L_B^2}{D_B}\right)w_A w_B^{\epsilon}\right] \tag{2.28}$$

B: $$\frac{\partial(w_B)}{\partial t^*} = \frac{\partial^2(w_B)}{\partial x^{*2}} - \epsilon\left[\left(k_1^{'}\left(\frac{\rho_T}{M}\right)^{\epsilon}\frac{L_B^2}{D_B}\right)w_A w_B^{\epsilon}\right] - \epsilon\left[\left(k_1^{'}\left(\frac{\rho_T}{M}\right)^{\epsilon}\frac{L_B^2}{D_B}\right)\frac{k_2}{k_1}w_c w_B^{\gamma}\right] \tag{2.29}$$

C: $$\frac{\partial(w_C)}{\partial t^*} = \frac{\partial^2(w_C)}{\partial x^{*2}} - \frac{\epsilon}{\gamma}\left[\left(k_1^{'}\left(\frac{\rho_T}{M}\right)^{\epsilon}\frac{L_B^2}{D_B}\right)\frac{k_2}{k_1}w_c w_B^{\gamma}\right] \tag{2.30}$$

P: $$\frac{\partial(w_P)}{\partial t^*} = \frac{\partial^2(w_P)}{\partial x^{*2}} + (1+\epsilon)\left[\left(k_1^{'}\left(\frac{\rho_T}{M}\right)^{\epsilon}\frac{L_B^2}{D_B}\right)w_A w_B^{\epsilon}\right] \tag{2.31}$$

S: $$\frac{\partial(w_S)}{\partial t^*} = \frac{\partial^2(w_S)}{\partial x^{*2}} + \left(\epsilon+\frac{\epsilon}{\gamma}\right)\left[\left(k_1^{'}\left(\frac{\rho_T}{M}\right)^{\epsilon}\frac{L_B^2}{D_B}\right)\frac{k_2}{k_1}w_c w_B^{\gamma}\right] \tag{2.32}$$

I: $$\frac{\partial(w_I)}{\partial t^*} = \frac{\partial^2(w_I)}{\partial x^{*2}} + [0] \tag{2.33}$$

The same Damköhler number that appeared in the C-C reaction equations shows up in the C-P equations. This allows us to use one general Damkohler number for both types of mixing sensitive reaction schemes. Both compare the fastest rate of reaction to the

smallest mixing time scales in the system. This allows us to use a general non-dimensional number to describe mixing for both types of mixing sensitive reaction.

Finally, substituting Equation (2.20) into Equations (2.28)-(2.33) gives the C-P equations for numerical simulations:

A: $$\frac{\partial(w_A)}{\partial t^*} = \frac{\partial^2(w_A)}{\partial x^{*2}} - [(Da) w_A w_B^{\epsilon}] \tag{2.34}$$

B: $$\frac{\partial(w_B)}{\partial t^*} = \frac{\partial^2(w_B)}{\partial x^{*2}} - \epsilon\,[(Da) w_A w_B^{\epsilon}] - \epsilon\left[(Da)\frac{k_2}{k_1} w_c w_B^{\gamma}\right] \tag{2.35}$$

C: $$\frac{\partial(w_C)}{\partial t^*} = \frac{\partial^2(w_C)}{\partial x^{*2}} - \frac{\epsilon}{\gamma}\left[(Da)\frac{k_2}{k_1} w_c w_B^{\gamma}\right] \tag{2.36}$$

P: $$\frac{\partial(w_P)}{\partial t^*} = \frac{\partial^2(w_P)}{\partial x^{*2}} + (1+\epsilon)[(Da) w_A w_B^{\epsilon}] \tag{2.37}$$

S: $$\frac{\partial(w_S)}{\partial t^*} = \frac{\partial^2(w_S)}{\partial x^{*2}} + \left(\epsilon + \frac{\epsilon}{\gamma}\right)\left[(Da)\frac{k_2}{k_1} w_c w_B^{\gamma}\right] \tag{2.38}$$

I: $$\frac{\partial(w_I)}{\partial t^*} = \frac{\partial^2(w_I)}{\partial x^{*2}} \tag{2.39}$$

This formulation for both C-C and C-P schemes allows the use of one Damköhler number to describe the mixing relative to the desired reaction rate. It also provides a physically meaningful non-dimensional reaction rate ratio to describe the relative rates of reaction. While there is no explicit expression for the effect of stoichiometry, both of the non-dimensional measures include stoichiometric coefficients, showing that both the mixing and the relative reaction rates are affected by the stoichiometry of the reaction scheme.

2.3 NUMERICAL SOLUTION OF EQUATIONS

The two systems of equations for the C-C (Equations (2.21)-(2.25)) and the C-P (Equations (2.34)-(2.39)) reaction schemes were solved using COMSOL Multi-physics 3.4, a commercial Finite Element PDE solver. The 1-D transient convection and diffusion mass transport model was used with the mass fractions for each species specified as independent variables. Elements were specified as Lagrange-quadratic. A 1-D geometry line of unit length equally split into two domains ($-\frac{1}{2} \leq x^* < 0$ and $0 \leq x^* \leq \frac{1}{2}$) and a mesh of 2048 equally spaced elements was generated. Boundary Conditions (BC's) for all cases were specified as:

$$\frac{\partial(w_i)}{\partial x^*} = 0 \; at \; x^* = -\frac{1}{2} \; and \; x^* = \frac{1}{2} \; for \; all \; t^* \; and \; i = A, B, C, P, S \; and \; I \quad (2.40)$$

The general initial conditions for the two reactions schemes are shown in Table 2-2. The initial conditions were chosen to replicate the segregated striation condition of the model.

A final constraint imposed on the simulations is that the reactants need to be present in stoichiometric quantities. Using this constraint it is possible to express the initial mass fractions as a function of the initial mass fraction of the limiting reagent *B* $\left(w_{B_0}\right)$, as shown in Table 2-3. For the C-C case, the only reactants present initially are *A* and *B*. Therefore, the alternating striations in mass fraction would be unity for *A* and unity for *B*. For the C-P cases, however, there are three initial reactants present. In this model, it is assumed that reactants *A* and *C* are well mixed and present in the *Y* striation and that the limiting reagent *B* is in the *Z* striation. The inert species *I* was allowed to be present in both *Y* and *Z* striations as required and assumed to be well mixed with the other reactants. Another condition specified for the C-P case is that the ratios of *A*, *B* and *C* are such that either *A* or *C* could consume all of the available *B*, so *B* is always the limiting reagent.

Simulations for both reaction schemes were run until the equivalent of t^*=500 in the case of *Da* =1. Since the simulations are solved in time, the dimensionless times to which the simulations were run were scaled according to the Damköhler number.

Therefore, t^*=500 for Da=1 is equal to t^*=50000 for Da=0.01 and t^*=0.05 for Da=10000, i.e. the values of $Da \cdot t^*$ are equal for all the cases. In fact, $Da \cdot t^*$ is actually equivalent to a non-dimensional reaction time where $Da \cdot t^* = t/\tau_R$. Therefore, running the simulations to $Da \cdot t^*$ =500 is the same as the simulations being run for 500 reaction times. All these dimensionless times are in fact equal in *real* time. For most of the cases it was seen that all of the limiting reagent *B* is consumed by t^*=500 or equivalent.

The solutions COMSOL returned were profiles of mass fraction for the various species over the non-dimensional space x^* for each non-dimensional time step t^*.

2.4 RESULTS AND DISCUSSION

2.4.1 Competitive-Consecutive (C-C) Reaction

In order to use the model for the C-C reaction, numerical values were assigned to the variables in the model, as shown in Table 2-4. The stoichiometric coefficients were all set to 1 in order to match the classic reaction scheme used by Cox and others (Muzzio and Liu, 1996, Clifford et al., 1998a ,1998b, 1999, 2000, Clifford, 1999, Clifford and Cox, 1999, S. M. Cox 2004,). This allows comparison of results for the effect of striation thickness and reaction rates. The initial conditions were chosen such that only pure *A* and *B* are present in the system.

Looking at the C-C cases in Table 2-4, the values of k_2/k_1 and Da for Case 1 are favourable conditions for high yield of *P*, i.e. $k_2/k_1 \ll 1$ and $Da = 1$. For Case 4, the yield of *P* should be small, i.e. $k_2/k_1 = 1$and $Da \gg 1$. The two cases are meant to represent the two extremes of very favorable reaction rate ratio and perfect mixing and very unfavorable kinetics and mixing conditions. Cases 2 and 3 have good k_2/k_1 with bad mixing and bad k_2/k_1 with good mixing. The solutions COMSOL returns are the profiles of mass fraction for the various species over the non-dimensional space x^* for each time step t^*. Figure 2-2 shows the spatial and temporal evolution of species over a single non-dimensional striation. Before discussing the profiles in detail, it is important to note a couple of points about the profiles. A vertical line represents a sharp interface. A curved line represents a gradient in the concentration. Finally, a horizontal line represents uniform concentration across the space.

Looking at Figures 2-2(a) and 2-2(c), one can see that all of the species are uniformly distributed for all time steps greater than t^*=0. This is not the case for Figures 2-2(b) and 2-2(d). This can be attributed to the smaller striation thicknesses i.e. the lower Damköhler number, for Cases 1 and 3. As the striations are thinner for those cases, the species can diffuse across completely in a shorter amount of time than for Cases 2 and 4 where the striations are 100 times thicker. The thicker striations allow for spatial in-homogeneity of the species. The thinner striation thicknesses allow for differences only in temporal distribution of species and not spatial distribution. The thicker striations cause differences in both temporal and spatial distributions. Figures 2-2(b) and 2-2(d) also exhibit an interface between reactants whereas 2-2(a) and 2-2(c) do not.

Despite the fact that there is complete mixing for both Cases 1 and 3, there is a very large difference in the yield of *P* for the two cases. For Case 1, which has both good mixing and a favourable reaction rate ratio, the majority of the mass present is that of *P*, the desired product (Fig 2-2(a)(iii)). For Case 3, however, the mass fraction of the undesired product is always higher than that of the desired product (Fig 2-2(c)(iii)). There is a significant drop of mass fraction of *P* from 0.99 to 0.25, showing the dramatic effect of reaction rate ratio for the same mixing conditions.

Looking at Figures 2-2(b)(iii) and 2-2(d)(iii), the same reversal of *P* and *S* is observed. The reaction rate ratio has a profound effect on the yield of desired product that is independent of mixing. When the reaction rate ratio is good, the undesired reaction doesn't participate. All of the product *P* forms at the interface of *A* and *B*, making the profile of mass fraction of *P* symmetric about the mid-plane, x^*=0, as shown in Figures 2-2(b)(ii) and 2-2(b)(iii). When the undesirable by-product reaction occurs at a comparable rate to that of the desired reaction, a significant asymmetry in the profiles of mass fraction for all species is visible (Figures 2-2(d)(ii) and 2-2(d)(iii)). This can be attributed to the fact that the second reaction occurs only on the right hand side of x^*=0 where *P* is in contact with *B*. This causes *P* to be used up only when it is exposed to *B* with *S* forming only on one side.

The key results are as follows: First, a small striation thickness allows for uniform concentrations of species, i.e. perfect mixing, across the striations whereas larger

striations can cause spatial inhomogeneities in species mass fraction. Second, the reaction rate ratio is an independent factor which can significantly alter the yield of desired product regardless of the mixing condition. This effect is predictable in the sense that if the ratio is good the yield is good and if the ratio is poor the yield is poor. Finally, for the larger striation thicknesses, a good reaction ratio causes symmetric concentration profiles of desired product *P*, while a bad ratio causes the product profiles to skew towards the *A* side of the striation. Perfect mixing simplifies the reaction analysis and shortens the reaction time. Having favourable kinetics improves the yield significantly.

Changing the stoichiometry was found to not affect the profiles for the good reaction rate ratio cases (k_2/k_1=10^{-5}) for both good and bad mixing conditions (1< *Da* <10000). The profiles of all the species were identical to those presented above. The profiles for the bad reaction rate ratio (k_2/k_1=1) and good mixing (*Da*=1) look the same as before, but the amounts of *P* and *S* produced change. The case of both bad rate ratio (k_2/k_1=1) and poor mixing (*Da*=10000) always resulted in a larger amount of *S* produced than *P*, and all the profiles were skewed towards *B*. The amount of *S* and *P* produced vary with stoichiometry and the profiles are skewed more or less depending on the stoichiometry. The effect of stoichiometry is captured by calculating the amount of product formed or the yield of *P*. This is done in the following sections and in Chapter 3.

2.4.2 Competitive-Parallel (C-P) Reaction

Table 2-5 shows the variable settings for the C-P simulations. The four cases are identical to the ones used for the C-C simulations. The stoichiometry chosen is the classic C-P reaction scheme. The initial conditions were chosen such that $w_{B_0} = 0.5$; the initial amounts of *A*, *C* and *I* present in the system were calculated using the formulae in Table 2-3. The solutions COMSOL returns are the profiles of mass fraction for the various species over the non-dimensional space *x** for each time step *t**. Figure 2-3 shows the spatial and temporal evolution of species including the inert.

The C-P case profiles show many of the same characteristics as the C-C cases. Cases 1 and 3, with the thinner initial striations, once again show spatial homogeneity for all the

species across the entire striation thickness, where as Cases 2 and 4 show spatial variations in mass fraction for all the species across the striations. The yields of *P* and *S* flip when the reaction ratio is varied from favourable (k_2/k_1 =10^{-5}) to unfavourable (k_2/k_1 =1). Cases 1 and 2 have a high yield of *P*; Cases 3 and 4 have an equal yield of *P* and *S*. The cases with the large striation thicknesses (*Da*=10000) show symmetry in product mass fraction profiles about *x**=0 when the second reaction is insignificant (k_2/k_1 =10^{-5}) and significant asymmetry when it is actively participating in the reaction (k_2/k_1 =1). The main difference between the C-C and C-P reactions is that once the product *P* is formed in the C-P reaction, it does not get consumed by a side reaction. Therefore, in terms of measuring the yield of *P*, the C-P reaction scheme is a lot less mixing sensitive than the C-C reaction scheme. For the C-C reaction, the longer that *P* sits in contact with *B*, the higher the chance that the yield of *P* will decrease.

Changing the stoichiometry for the C-P reactions resulted in some non-linear profile changes. While the profiles for the well mixed cases remained uniform across the striation the magnitudes of desired and undesired product produced varied. The profiles for the poorly mixed cases look different from the profiles presented here owing partly to the different initial conditions required when the stoichiometry was changed and also because of the stoichiometries themselves. As with the C-C cases, calculating the product formed or yield of *P* captured all of these changes, as further discussed in Chapter 3.

2.4.3 Yield of desired product *P*

It is easy to assess how much product has formed for the cases with uniform distribution of species across the striation but it is a lot more difficult to assess yield for the non-uniform profiles of mass fraction. In order to simplify this, the profiles of *P* were integrated to obtain the total mass of *P* present in the system at an instant in time using:

$$Y_P = \frac{mass\ of\ species\ P\ at\ t^*}{max\ mass\ of\ P\ obtainable} = \frac{\int_{-0.5}^{0.5} w_P dx^*(t^*)}{0.5 w_{B_o}\left(1+\frac{1}{\epsilon}\right)} \tag{2.41}$$

Following Y_P over time gives the progression of yield over time. Figure 2-4 shows the yield of *P* over time as the reaction progresses for the four C-C cases, and Figure 2-5 shows the same results for the four C-P cases. Plotting $Da \cdot t^*$on the x-axis allows all four curves to be displayed on the same figure. These figures confirm the conclusions drawn above that good mixing and a good reaction rate ratio will maximize the yield of desired product (Case 1 in both Figures 2-4 and 2-5), and poor mixing with an unfavourable reaction rate ratio minimizes the yield of desired product (Case 4 for both Figures 2-4 and 2-5). This also confirms the notion that minimization of the Damköhler number and reaction rate ratio is desirable. Clifford et al. (1998a) also got results for their stoichiometric ratio cases that qualitatively agree with our figures for the classic stoichiometry. We can only compare them qualitatively because our non-dimensionalization parameters are different from theirs.

2.4.4 Effect of reaction rate ratio on yield of *P*.

Figures 2-4 and 2-5 show that the reaction rate ratio will affect how much product is formed regardless of the mixing condition. This is evident in the comparison of Cases 1 and 3, which are both well mixed, and Cases 2 and 4, which are both poorly mixed, in both Figures 2-4 and 2-5, which shows that the favourable reaction rate ratio always provides a higher final yield of *P*. It is impossible to get a good yield of desired product if the reaction rate ratio is unfavourable, regardless of the mixing condition (Cases 3 and 4 in both Figures 2-4 and 2-5). Clifford et al. (1998a) also came to the same conclusion for the effect of reaction rate ratio in their investigations. They too found that a smaller reaction rate ratio is favourable for maximizing the yield of desired product.

2.4.5 Effect of mixing on yield of *P*.

There is a significant effect of mixing on Y_P evident in Figures 2-4 and 2-5. When the reaction rate ratio is favourable, having good mixing can cause a substantial increase in yield of desired product, as seen by comparing Cases 1 and 2 in both the figures (Y_P=0.5 to 1 for C-C and Y_P=0.5 to 1 for C-P) . If the reaction rate ratio is unfavourable, a similar favourable effect of mixing is seen by comparing Cases 3 and 4, though it is not as

profound as when the reaction rate ratio is good (Y_P=0.03 to 0.24 for C-C and Y_P=0.33 to 0.5 for C-P). This seems to point toward the effect of mixing being limited by the reaction rate ratio, i.e. the reaction rate ratio will determine the final yield and good mixing helps one to realise that asymptotic value of yield. In the case of the C-C reaction scheme, poor mixing will severely affect the yield of desired product in a negative way. This conclusion is also true for the C-P scheme. It is also interesting to note that for the well mixed cases (Cases 1 and 3) the final yield of P is attained much quicker than when the mixing is poor (Cases 2 and 4). This suggests that the mixing limits the pace of the reaction as well, and in the case of the C-C, due to the nature of the reaction, this has a significant effect on the final yield of *P*. Cox and others in their investigations came to a similar qualitative conclusion on the effect of mixing on the yield for a two stage Competitive-Consecutive reaction (Cox et al., 1998, Clifford et al., 1998a). They too found that minimizing the Damkohler number leads to an increase the yield of desired product.

2.5 CONCLUSIONS

A model was developed to investigate the effects of stoichiometry, mixing and reaction rate ratio for Competitive-Consecutive and Competitive-Parallel reactions with a general stoichiometry. The model is capable of dealing with both reaction schemes, something that was not previously available. A single Damköhler number was found for both kinds of mixing sensitive reactions. This is encouraging since there has previously been a lot of debate on the formulation of the Damköhler number for these competing reactions, i.e. should it be based on the first or the second reaction. Also, having just one expression to describe mixing accurately reflects reality where mixing is the same regardless of the reaction scheme. The general expression for the Damköhler number, when applied to the classic reaction schemes, collapses to the expressions used in previous investigations by others, Cox et al. (1998) in particular. However, the two reaction schemes are very different and these differences are reflected in the specific reaction rate ratios for the two types of reaction stoichiometries that are to be used in the model.

The effects of mixing and reaction rate ratios on the yield of desired product were investigated for the classic competitive-consecutive and competitive-parallel reaction schemes. It was found that they are somewhat independent of each other; though both are proportional to the yield of desired product, the reaction rate ratio limits the final yield of desired product that is possible to attain but good mixing helps to achieve that yield. The rate of mixing also determines the rate at which this final yield is reached. The reaction rate ratio and the Damköhler number both need to be minimized to achieve the maximum yield of product. The results from the model agree with the expected results and the results of previous investigations when both mixing and reaction rate ratio are varied, i.e. improving the mixing and chemistry by minimizing the Damköhler number and the reaction rate ratio respectively is desirable and leads to improvements in yield of desired product.

This confirmation of the model allows for future work where the effects of stoichiometry, mixing and k_2/k_1 ratios and the interactions between them will be investigated with the intention of producing charts that may help in prediction of the yield for a general mixing sensitive reaction. Though the model allows for the investigation of the effects of initial concentrations of reactants, this was not done in the current study and this is another possible avenue for further exploration. It is also acknowledged that the 1D model is not a very accurate depiction of real turbulent mixing, but this investigation was meant to be a first foray into the effect of stoichiometry of mixing sensitive reactions, so simplicity was desirable. Added complexities like introducing stretching and using a lamellar 'barcode' model could possibly be integrated into the model in the future to better approximate the real industrial situation.

2.6 TABLES FOR CHAPTER 2.

Table 2-1. General Mixing Sensitive Reaction Schemes

$\boldsymbol{Competitive\ Consecutive}$ $(\boldsymbol{C-C})$	$\boldsymbol{Competitive\ Parallel}$ $(\boldsymbol{C-P})$
$A + \epsilon B \overset{k_1'}{\rightarrow} \alpha P$ $\beta P + \gamma B \overset{k_2'}{\rightarrow} S$	$A + \epsilon B \overset{k_1'}{\rightarrow} P$ $C + \gamma B \overset{k_2'}{\rightarrow} S$

Table 2-2. General initial conditions for C-C and C-P reaction schemes @ t^*=0.

	C-C			**C-P**	
	$-\frac{1}{2} \le x^* < 0$	$0 \le x^* \le \frac{1}{2}$		$-\frac{1}{2} \le x^* < 0$	$0 \le x^* \le \frac{1}{2}$
A	w_{A_0}	0	***A***	w_{A_0}	0
B	0	w_{B_0}	***B***	0	w_{B_0}
C	-	-	***C***	w_{C_0}	-
P	0	0	***P***	0	0
S	0	0	***S***	0	0
I	$1 - w_{A_0}$	$1 - w_{B_0}$	***I***	$1 - w_{A_0} - w_{C_0}$	$1 - w_{B_0}$

Table 2-3. Stoichiometric initial conditions based on w_{B_0} for C-C and C-P reaction schemes.

	C-C			**C-P**	
	$-\frac{1}{2} \le x^* < 0$	$0 \le x^* \le \frac{1}{2}$		$-\frac{1}{2} \le x^* < 0$	$0 \le x^* \le \frac{1}{2}$
A	$\frac{1}{\epsilon}(w_{B_0})$	0	***A***	$\frac{1}{\epsilon}(w_{B_0})$	0
B	0	w_{B_0}	***B***	0	w_{B_0}
C	-	-	***C***	$\frac{1}{\gamma}(w_{B_0})$	0
P	0	0	***P***	0	0
S	0	0	***S***	0	0
I	$1-\frac{1}{\epsilon}(w_{B_0})$	$1-w_{B_0}$	***I***	$1-\left(\frac{1}{\epsilon}+\frac{1}{\gamma}\right)(w_{B_0})$	$1-w_{B_0}$

Table 2-4. Numerical values for simulated C-C test cases. Stoichiometric coefficients $\alpha, \beta, \gamma, \epsilon$ were set to 1, representing the reaction: $A + B \overset{k_1'}{\rightarrow} P$, $P + B \overset{k_2'}{\rightarrow} S$ and initial mass fraction of species *B* was always 1 ($w_{B_0} = 1$).

C-C case	$\boldsymbol{\frac{k_2}{k_1} = \frac{1}{2}\frac{k_2'}{k_1'}}$	$\boldsymbol{Da = k_1'\left(\frac{\rho_T}{M}\right)\frac{L_B^2}{D_B}}$
1	10^{-5}	1
2	10^{-5}	10000
3	1	1
4	1	10000

Table 2-5. Numerical values for simulated C-P test cases. Stoichiometric coefficients γ, ϵ were set to 1, representing the reaction: $A + B \overset{k_1'}{\rightarrow} P$, $C + B \overset{k_2'}{\rightarrow} S$ and initial mass fraction of species *B* was always 0.5 ($w_{B_0} = 0.5$).

C-P case	$\boldsymbol{\frac{k_2}{k_1}} = \frac{k_2'}{k_1'}$	$\boldsymbol{Da} = k_1' \left(\frac{\rho_T}{M}\right) \frac{L_B^2}{D_B}$
1	10^{-5}	1
2	10^{-5}	10000
3	1	1
4	1	10000

2.7 FIGURES FOR CHAPTER 2.

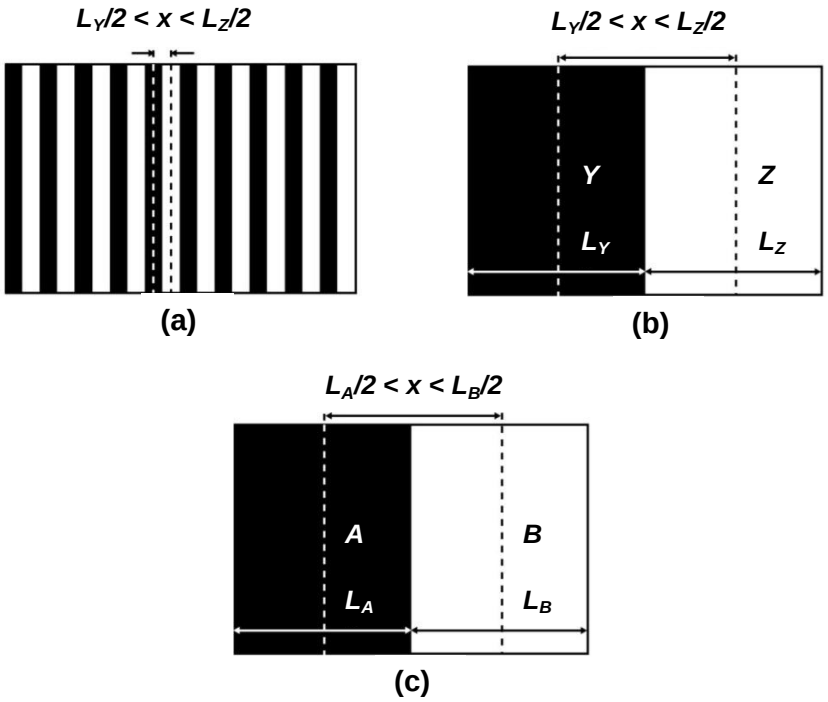

Figure 2-1. Geometry for proposed mixing model at time *t*=0.

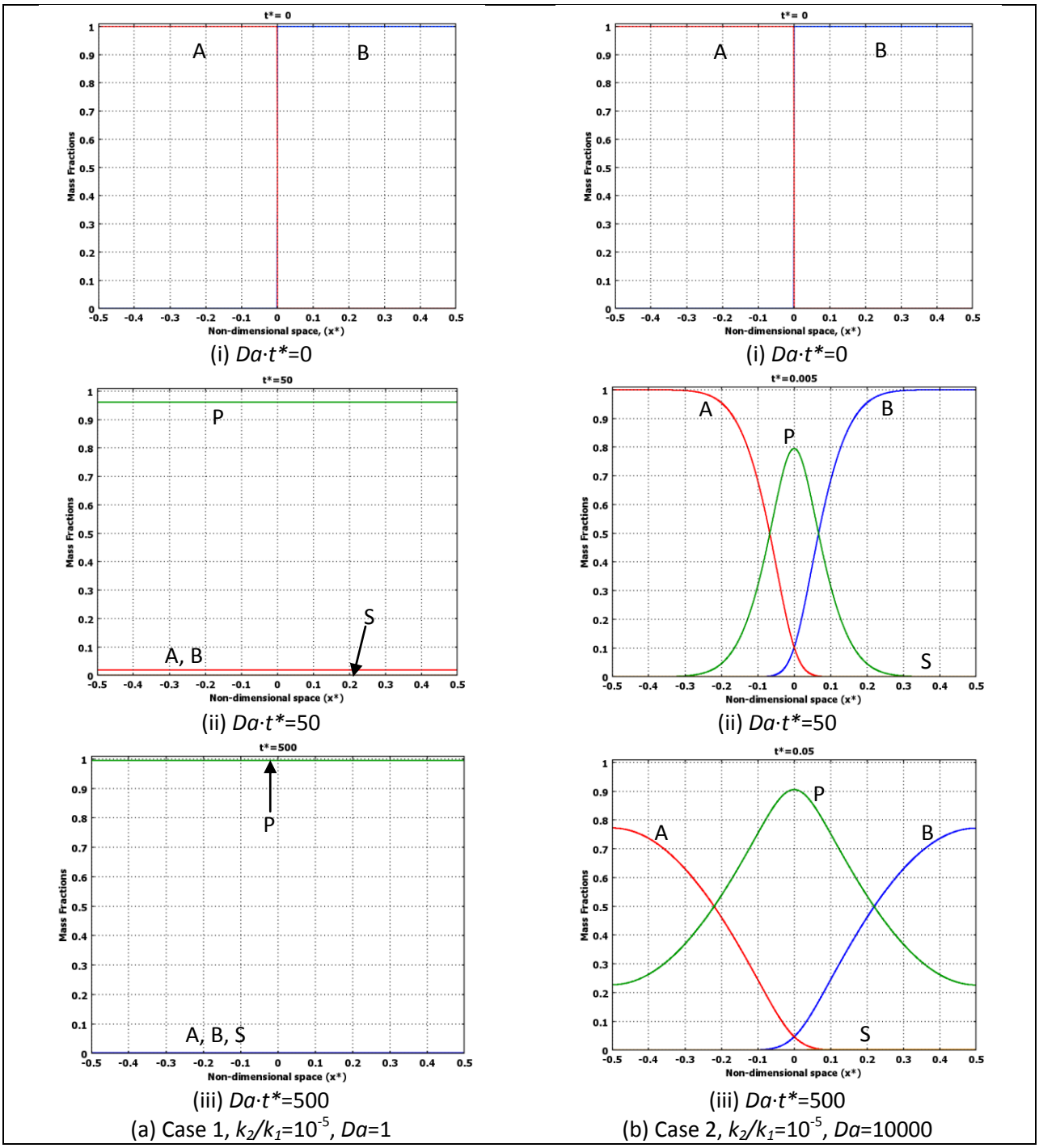

Figure 2-2. Spatial and temporal evolution of mass fractions for C-C Cases (a) 1 (k_2/k_1=10^{-5}, Da=1) and (b) 2 (k_2/k_1=10^{-5}, Da=10000).

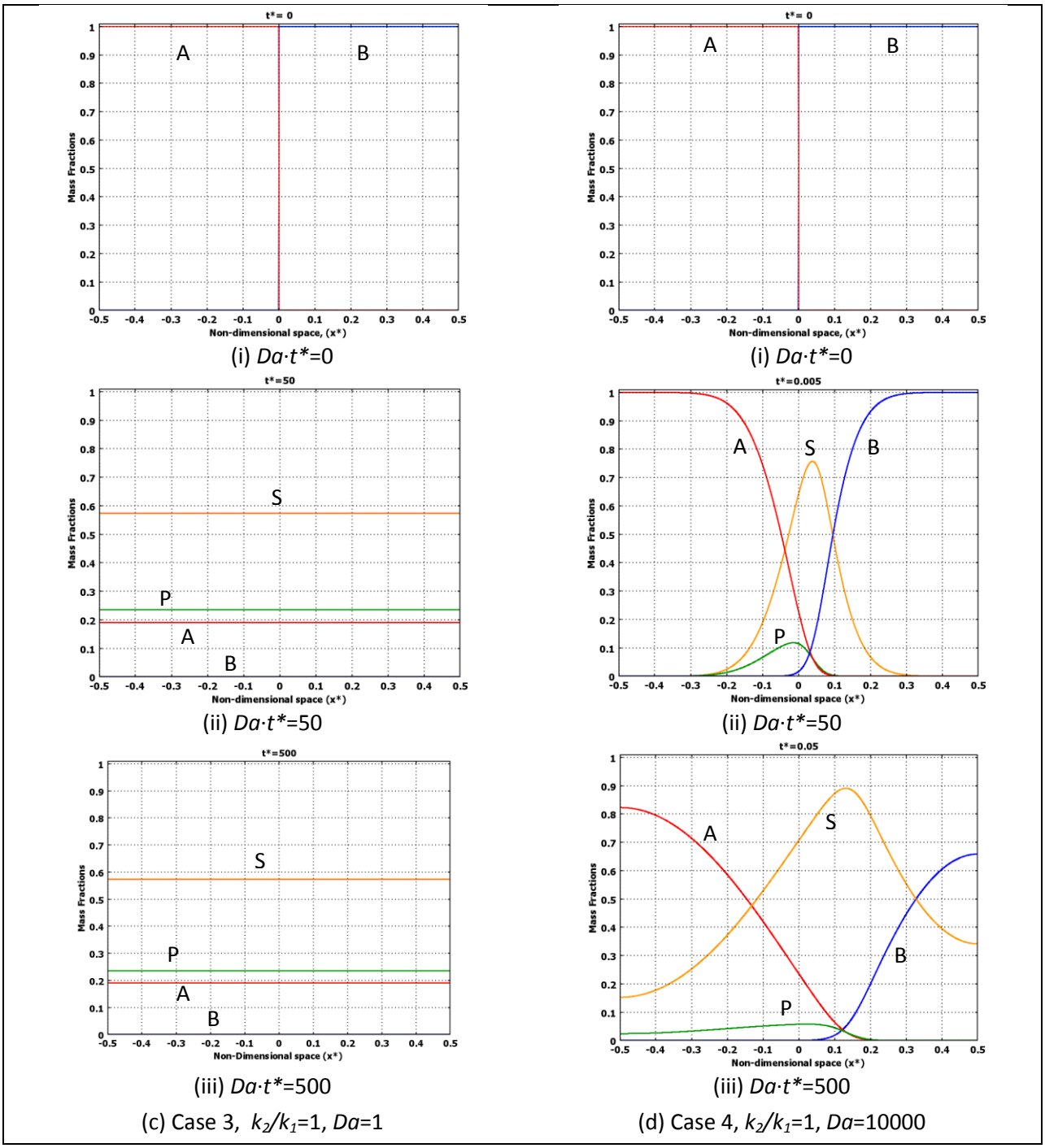

(c) Case 3, k_2/k_1=1, Da=1

(d) Case 4, k_2/k_1=1, Da=10000

Figure 2-2. Spatial and temporal evolution mass fractions of for C-C Cases (c) 3 (k_2/k_1=1, Da=1) and (d) 4 (k_2/k_1=1, Da=10000).

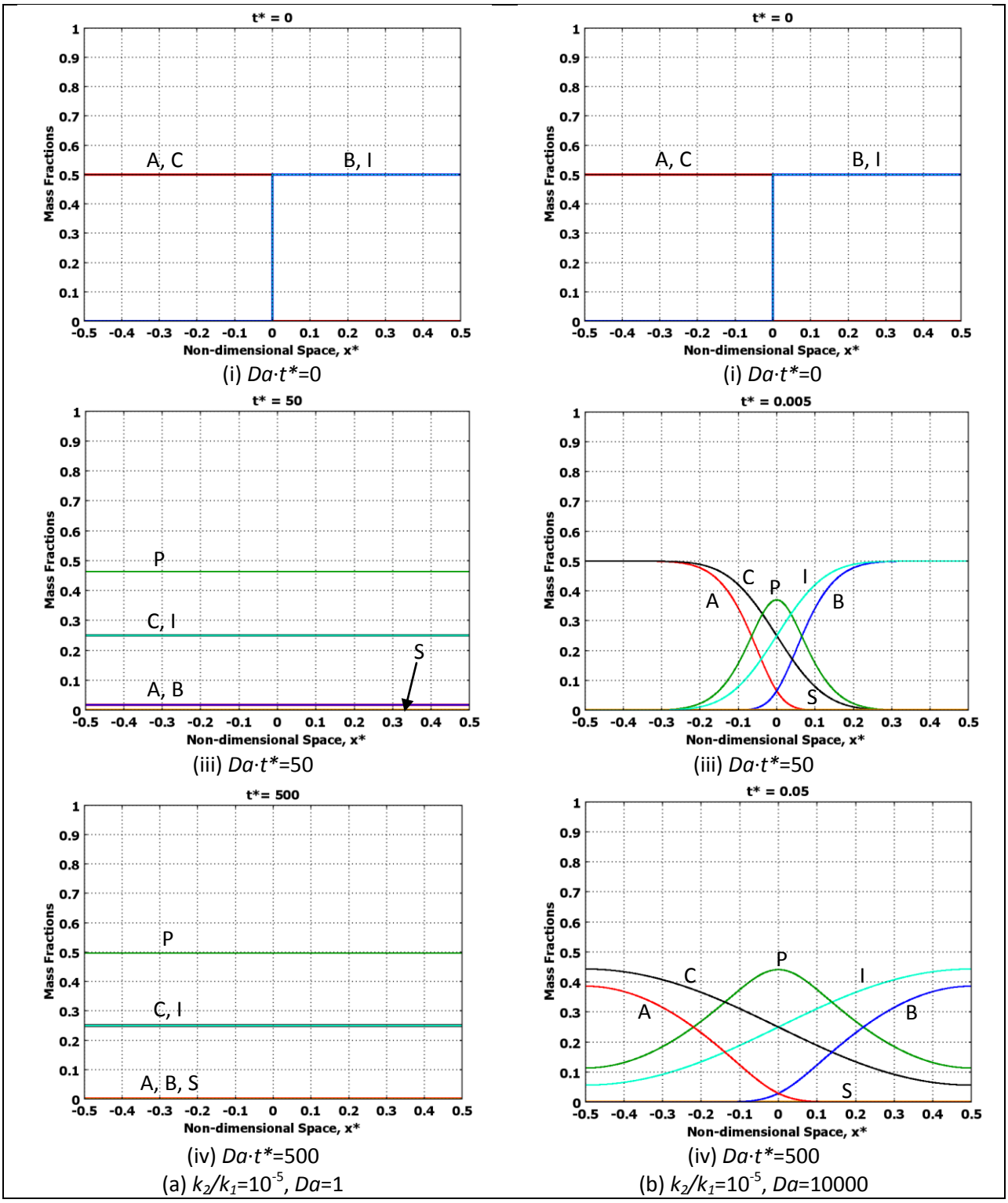

Figure 2-3. Spatial and temporal evolution of mass fractions for C-P Cases (a) 1, (k_2/k_1=10^{-5}, Da=1) (b) 2, (k_2/k_1=10^{-5}, Da=10000)

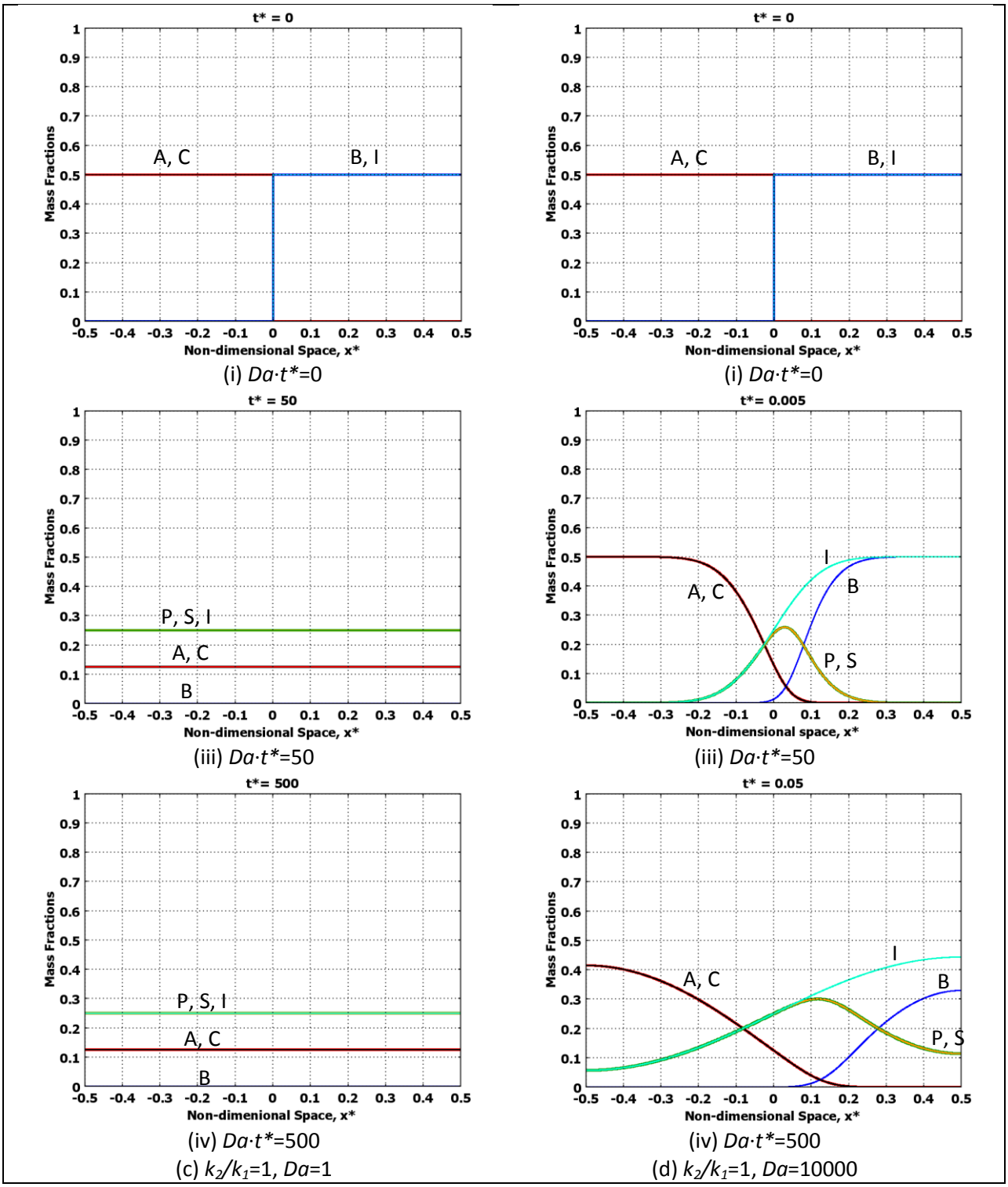

Figure 2-3. Spatial and temporal evolution of mass fractions for C-P Cases (c) 3, (k_2/k_1=1, *Da*=1) and (d) 4, (k_2/k_1=1, *Da*=10000)

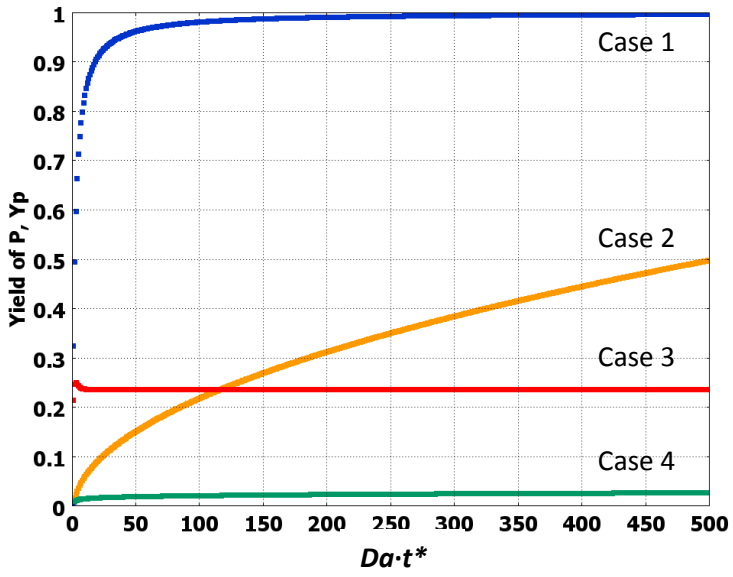

Figure 2-4. Yield of P versus time for the C-C cases.

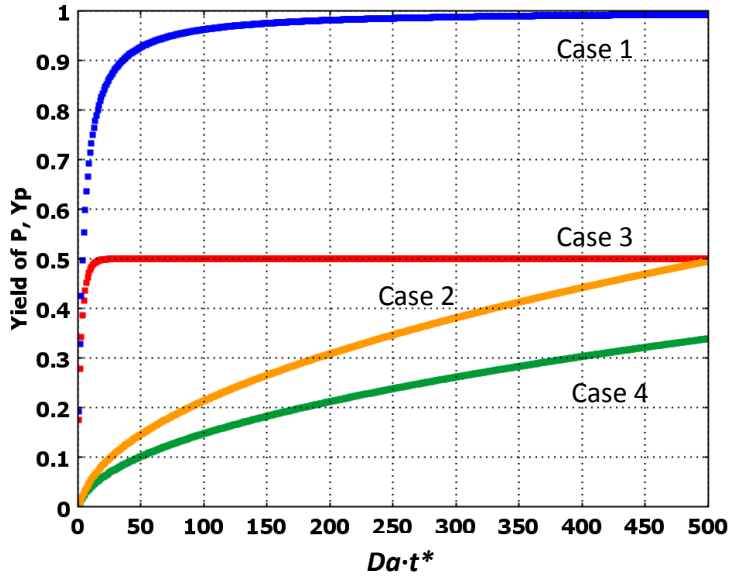

Figure 2-5. Yield of P versus time for the C-P cases.

3

Design Protocols for Mixing Sensitive Reactions

3.1 CHAPTER OVERVIEW

This chapter includes the detailed investigation of the effects of initial mixing condition (striation thickness), non-dimensional reaction rate ratio and reaction stoichiometry on the yield of desired product from a mixing sensitive reaction of two types: the Competitive-Consecutive reaction and the Competitive-Parallel reaction. This chapter includes the numerical solution of the equations, the cases studied and the results of the investigation. **Section 3.2** is a summary of the pertinent parameters. **Section 3.3** includes the numerical technique and solution of the equations and the various cases investigated. In **Section 3.4**, the results are presented and discussed in detail. **Section 3.5** concludes this chapter. **Sections 3.6** and **3.7** are the tables and figures for this chapter respectively.

3.2 MEASURES FOR DESIGN

In Chapter 2, a 1-D diffusion model for mixing sensitive reactions that could account for the effects of mixing, reaction rate ratio and reaction stoichiometry was developed. The model is capable of dealing with both Competitive-Consecutive and Competitive-Parallel type of mixing sensitive reaction, the general forms of which are given in Table 2-1.

Systems of Partial Differential Equations (PDEs) for the masses of the different species involved in the reaction and an inert were developed, out of which a general Damköhler number, common to both types of reaction schemes was found. The equation of the Damköhler number was found to be:

$$\boldsymbol{Da} = k_1^{'}\left(\frac{\rho_T}{M}\right)^{\epsilon}\frac{L_B^2}{D_B} = \frac{k_1^{'}\left(\frac{\rho_T}{M}\right)^{\epsilon}}{\left(\frac{D_B}{L_B^2}\right)} = \frac{rate\ of\ desired\ reaction}{rate\ of diffusion} \tag{3.1}$$

$$= (rate\ of\ desired\ fast\ reaction) * (diffusion\ \ time\ )$$

This Damköhler number is convenient because it is independent of the reaction scheme being investigated. The effect of stoichiometry on the Damköhler number is given by ϵ, the stoichiometric coefficient of the limiting reagent (*B)* in the desired reaction.

The effect of the relative reaction rates of the competing reactions is also of interest. The model provided non-dimensional reaction rate ratios for C-C and C-P reactions, which are as follows:

C-C:
$$\frac{\boldsymbol{k_2}}{\boldsymbol{k_1}} = \left[\frac{\beta}{\alpha}\left(\frac{\alpha}{1+\epsilon}\right)^{\beta}\left(\frac{\rho_T}{M}\right)^{\beta+\gamma-\epsilon-1}\right]\frac{k_2^{'}}{k_1^{'}} \tag{3.2}$$

C-P:
$$\frac{\boldsymbol{k_2}}{\boldsymbol{k_1}} = \left[\frac{\gamma}{\epsilon}\left(\frac{\rho_T}{M}\right)^{\gamma-\epsilon}\right]\frac{k_2^{'}}{k_1^{'}} \tag{3.3}$$

These non-dimensional reaction rate ratios are specific to the type of mixing sensitive reaction, i.e. C-C or C-P, and incorporate the effect of the relative reaction rates of the competing reactions as well as the effect of stoichiometry.

These two non-dimensional parameters, along with the stoichiometry, were varied in this investigation. For both the C-C and C-P simulations, the Damköhler number was varied from 0.01 to 10000 in x100 increments, where 0.01 is the best and 10000 is the worst mixing. The non-dimensional reaction rate ratio (k_2/k_1) was varied from 1 to 0.00001 in x10 increments, where 1 is the worst ratio and 0.00001 is the best ratio. For the C-C reactions, ϵ was always 1 and α, β, γ were given a value of either 1 or 2. For the C-P reactions, ϵ and γ were varied as 1 or 2. Table 3-1 shows the different C-C reaction scheme stoichiometries investigated, with the corresponding reaction rate ratios that take into account the stoichiometric effects. Table 3-2 shows the same terms for the C-P reaction schemes.

3.3 NUMERICAL DETAILS

Simulation of the systems of five or six PDEs for the C-C and C-P reaction schemes respectively were carried out using COMSOL 3.4, a Finite Element PDE Solver. It is worth noting that for the C-C reaction scheme only four of the equations are independent and for the C-P reaction scheme there are only five independent equations. The 1-D, transient, convection and diffusion mass transport model was used, with the mass fractions for each species specified as the independent variables. The default Lagrange-quadratic element was chosen. The specified 1-D geometry line of unit length was split equally into two sub-domains and a mesh of 2048 equally spaced elements with 2049 nodes was generated. The mesh was tested for grid dependence, and it was found that 1024 elements was sufficient resolution to ensure repeatable results to within the required tolerance of the solver, which was set to 10^{-6}. Since the geometry was only 1-D and the computational cost was minimal, a finer mesh than the minimum required resolution was used. The total time taken per simulation was approximately 30 seconds. The Boundary Conditions were specified for no net mass transfer across the boundaries (Equation 2.40).

Figure 3-1 shows the initial conditions for the C-C and C-P schemes. For the C-C cases, the initial conditions were chosen such that all of the mass initially present could be converted to desired product *P*. This was done by specifying a ratio of *A*:*B* as 1:1 in all

the simulations, with *A* and B being present in pure striations, i.e. $w_{A_0} = w_{B_0} = 1$. For the C-P scheme, owing to the parallel nature of the reactions, the initial conditions were a bit more complicated. They were chosen such that either *A* or *C* could consume the entire limiting reagent *B* by themselves, i.e. the initial ratios depended on the stoichiometric coefficients in the reaction scheme. In order to satisfy the constant mass concentration assumption of the model, it was necessary to include the inert in the C-P simulations. w_{B_0} and w_{IZ_0} were always set to 0.5, and $w_{A_0} w_{C_0}, w_{IY_0}$ were calculated accordingly.

The modelled equations allow for specification of the Damköhler number, the non-dimensional reaction rate ratio and the stoichiometry as values directly in the simulation. All possible combinations of the values of reaction rate ratio, Damköhler number and stoichiometry for the C-C reaction scheme (stoichiometries given in Table 3-1) and the C-P reaction scheme (stoichiometries given in Table 3-2) were investigated. This resulted in 192 converged cases for the C-C and 96 converged cases for the C-P reaction scheme, giving a total of 288 converged simulations.

The model is capable of handling all sorts of different initial conditions. The initial mass fraction ratios do not need to be stoichiometric; the analysis is just more convenient if they are. Any difference in mass fractions is replaced by the inert species. A requirement of the model is that the mass concentration of the system remains constant. If there is more or less *A* or *B*, the inert has to be adjusted to compensate for the increase/decrease of the reactant species. For example, the initial conditions for the C-C cases could have been 0.5 *A* and 0.5 *I* in mixture *Y*, and 0.5 *B* and 0.5 *I* for mixture *Z*. The ratio of *A*:*B* is still the same as before at 1:1, but the concentrations are now half of what they used to be. The choices for the stoichiometries of the C-C were chosen such that the ratio of stoichiometries is always 1:1. It is understood that there would be another 8 cases of stoichiometry for $\epsilon = 2$ (and subsequently a 192 more total cases), but those cases are not addressed here.

The transient simulations were run from *Da·t**=0 to *Da·t**=500 for all cases. *Da·t** is actually equivalent to a non-dimensional reaction time where $Da \cdot t^* = t/\tau_R$. Therefore,

running the simulations to $Da \cdot t^*$ =500 is the same as the simulations being run for 500 reaction times. This final value was chosen because it was found that for most cases the limiting reagent, *B,* was completely consumed by this time.

3.4 RESULTS AND DISCUSSION

The results obtained for the simulations are profiles of mass fraction for each of the species over the space x^* for all non-dimensional time t^*. Samples of these results were given in Chapter 2 (Figures 2-2 and 2-3).

Since the main objective of the process is to maximize the production of desired product *P*, the profiles of mass fraction of P are of most interest. Comparison of the total yield of desired product is difficult by direct observation of these profiles. In order to facilitate the comparison of different striation thickness, reaction rate ratios and stoichiometries on the yield, the profiles of mass fraction of P were integrated over the domain to obtain the total mass of desired product present within the system at any instant in time using the formula:

$$Y_P = \frac{mass\ of\ species\ P\ at\ t^*}{max\ mass\ of\ P\ obtainable} = \frac{\int_{-0.5}^{0.5} w_P dx^*(t^*)}{0.5 w_{B_o}\left(1+\frac{1}{\epsilon}\right)} \tag{3.4}$$

Following Y_P over time gives the progression of yield over time. The total production of *P* as time progresses can be observed in a plot of Y_P versus non-dimensional time $Da \cdot t^*$. Figures 2-4 and 2-5 in Chapter 2 show examples of such plots.

Since the primary interest is in the final yield of P that is obtainable, the final yields of *P* for all the simulations, i.e. at $Da \cdot t^*$=500, were collected and plotted for the different variables to assess the effects of each of the variables on the final yield of desired product.

The values of yield obtained for all the simulations were plotted for all the variables. The data and these figures can be found in Appendix A. Though all the figures showed the

same trends for the variables, only the figures that displayed them the most clearly are presented here.

3.4.1 Competitive-Consecutive (C-C) Reaction

Figures 3-2 (a) to (f) are semi-log plots of Y_P versus the Damköhler number for decreasing non-dimensional reaction rate ratio, k_2/k_1, values, each at time $Da \cdot t^*$=500. The curves on each of the plots represent the eight different C-C stoichiometry cases that have been investigated. The effects that are of interest for both kinds of reaction schemes are the effects of the Damköhler number, reaction rate ratio k_2/k_1 and the reaction stoichiometry.

3.4.1.1 Effect of Damköhler number (*Da*).

The plots in Figure 3-2 show a trend of decrease of yield of desired product with increasing Damköhler number. This trend is true for all stoichiometries and at all values of k_2/k_1. This suggests that a larger Damköhler number represents worse mixing and a smaller Damköhler number represents improved mixing. The figures also show that the value of yield for *Da*=1 and *Da*=0.01 is the same for all stoichiometries at all k_2/k_1. The yield at *Da*=100 and *Da*=10000 always decreases on the figures, regardless of the value of k_2/k_1. This suggests that *Da*≤1 is the well mixed limit. Figures 3-3 (a) and (b) further emphasize this point. They are sample plots of Y_P vs. k_2/k_1 for C-C stoichiometry case 2, the classic C-C stoichiometry, and case 7 respectively. The curves on the figures represent the Damköhler numbers that were investigated. The curves for *Da*=0.01 and *Da*=1 can be seen to lie exactly on top of one another, while increasing *Da* significantly drops yield at all k_2/k_1 for both cases. These trends are true for all the C-C stoichiometry cases, which can be seen in Appendix B. Therefore, it is concluded that *Da*=1 is the well mixed limit.

Going back to the plots in Figure 3-2, it is also worthwhile to notice that the yield at *Da*=10000 is always much lower than the well mixed yield irrespective of the value of k_2/k_1. This suggests that mixing is an independent effect that can significantly affect the

yield if it is poor. If the mixing is not good enough, the yield will always be lower than the well mixed situation given the same amount of elapsed time.

3.4.1.2 Effect of non-dimensional reaction rate ratio (k_2/k_1).

Looking at Figures 3-2 (a) to (f) together, it can be seen that as k_2/k_1 is decreased, the curves of yield of desired product obtainable for all of the stoichiometry cases at all values of Damköhler number move steadily upward, i.e. the yield always increases when k_2/k_1 is decreased. This result is as expected, since a smaller k_2/k_1 gives a slower undesired side reaction.

Moving from Figures 3-2 (a) to (f) as k_2/k_1 is decreased it is clear that the curves for the different stoichiometry cases grow steadily closer to one another, almost collapsing onto one curve at k_2/k_1=0.001 and collapsing completely onto one curve at k_2/k_1=0.0001. Figures 3-2 (e) and (f) are nearly identical. The collapse of stoichiometries is also shown in Figure 3-4 (a) to (c), which are semi-log plots of Y_P versus k_2/k_1 for all stoichiometries at (a) Da=1, (b) Da=100 and (c) Da=10000 at time $Da \cdot t^*$=500.

The yield increases significantly from k_2/k_1=1, where the yield varies from 0.23 to 0.75 even under well mixed conditions, to k_2/k_1=0.001, where the yield is essentially 99% and above at well mixed conditions (Da<=1) for all stoichiometries. At k_2/k_1=0.001 the individual stoichiometry curves collapse, eliminating the difference due to stoichiometry, while at k_2/k_1 =1 there is a large disparity between the yields of different stoichiometries.

Y_P can be seen to increase to 1 as k_2/k_1 decreases for all stoichiometries and the curves collapse at about k_2/k_1=0.001 for the well mixed cases, Da=1 and 0.01, and k_2/k_1=0.0001 for the badly mixed case, Da=10000. The yield of the badly mixed case remains at about half of what would be obtainable given a well mixed mixture. This brings up an interesting question: “Is it possible to get perfect yield of desired product, i.e. Y_P ~1, for Da=10000, a badly mixed case?”. In order to investigate this, the simulations for Da=10000 cases were re-run for a hundred times longer than before, i.e. they were run

to $Da \cdot t^*$=50000 instead of $Da \cdot t^*$=500. Figure 3-5 shows the results of these simulations. It can be seen that it is indeed possible to obtain a perfect yield with insufficient mixing, but this imposes a much more stringent k_2/k_1 requirement of k_2/k_1=0.00001 on the reaction. Under poor mixing conditions the effect of stoichiometry does not go away as easily with improving k_2/k_1 and the shapes of the curves change significantly. Although the yield at the good k_2/k_1 values gets better, the increase in yield for the worse k_2/k_1 ratios is very small considering that the time allowed for reaction was increased by 100 times. While it may be possible to obtain good yield for a bad mixing condition, the requirements for k_2/k_1 are more stringent and the time required is much longer, which directly impacts the required residence time in the reactor.

3.4.1.3 Effect of Stoichiometry.

Returning once again to Figures 3-2 (a) to (f) there is a clear effect of stoichiometry on the final yield of desired product, which changes with both the mixing and the non-dimensional reaction rate ratio.

At k_2/k_1=1 (Figure 3-2 (a)) there is a clear effect of stoichiometry evidenced by the separation of the curves from one another. These curves seem to come closer as the striation thickness increases. There is a clear distinction of stoichiometries, which Cases 7 and 8 having the highest yields, and therefore the most favourable stoichiometry, and Cases 1 and 2 having the lowest yields, meaning they have the least favourable stoichiometries. This is as expected since, as shown by the stoichiometries in Table 3-1, Cases 1 and 2 require only two molecules for the side reaction while Cases 7 and 8 require four molecules each. The additional molecules required places a mass transfer and collision probability limitation on the side reaction for Cases 7 and 8, hence making them more favourable for the desired reaction.. This separation remains intact for k_2/k_1=0.1 (Figure 3-2 (b)) and k_2/k_1=0.01 (Figure 3-2 (c)) but to a lesser extent and vanishes as k_2/k_1 decreases to 0.001 and below where the curves collapse onto each other. This suggests that the effect of stoichiometry vanishes for $k_2/k_1 \leq 0.001$ for good mixing ($Da \leq 1$ and Da=100) and is very small for poor mixing (Da=10000). At $k_2/k_1 \leq 0.0001$ all dependence of stoichiometry is gone for all k_2/k_1 and all Da. This

suggests that the design of the reaction should be such that $k_2/k_1 \leq 0.00001$ to guarantee that stoichiometry doesn't play a role at short elapsed times, i.e. $Da \cdot t^* = 500$. Figure 3-4 (a) to (c) also show this collapse of stoichiometry for short times. For the bad mixing condition that was allowed to proceed for a very long time, Figure 3-5, the effect of stoichiometry creeps back into the picture, affecting yield at previously adequate values of k_2/k_1. Therefore, it is possible that if the residence time is too long in a reactor with inadequate mixing, the stoichiometry effects will manifest themselves and affect production.

3.4.1.4 Summary of the effects on C-C reaction schemes.

As a summary, for Competitive-Consecutive reactions:

(a) $Da \leq 1$ is well mixed.
(b) $k_2/k_1 \leq 0.001$ with $Da \leq 100$ will provide good values of yield at $Da \cdot t^* = 500$.
(c) The effect of stoichiometry is a legitimate one, which can be large if the k_2/k_1 is unfavourable but vanishes at $k_2/k_1 \leq 0.001$ for short times and good mixing. At longer times with bad mixing conditions, this effect of stoichiometry reappears and requires a much smaller value of k_2/k_1.

3.4.2 Competitive-Parallel (C-P) Reaction

As with the C-C reaction scheme, the values of yield for the various simulations were plotted for all the variables involved. The data and figures can be found in Appendix A.

A similar set of figures to Figures 3-2 to 3-5 was chosen for consistency with the C-C analysis. Once again, the effects of interest are the Damköhler number, the non-dimensional reaction rate ratio k_2/k_1 and the reaction stoichiometry.

Figures 3-6 (a) to (f) are semi-log plots of yield of desired product versus the Damköhler number for decreasing values of k_2/k_1 respectively. The curves represent the four different stoichiometry cases investigated.

3.4.2.1 Effect of Damköhler number (*Da*).

The plots in Figure 3-6 show a trend of a decrease in Y_P with increasing Damköhler number, i.e. the mixing. This trend is true for all the stoichiometries at all values of k_2/k_1 except one: Case 3 at k_2/k_1=1 (Figure 3-6 (a)) which shows an increase in yield with increasing Damköhler number. Since the majority of cases do show the same trend as the C-C cases, it can once again be concluded that a larger value of Damköhler number represents worse mixing and a smaller value represents a better condition.

These figures also show that Y_P is the same at *Da*=0.01 and *Da*=1 for all values of k_2/k_1, once again implying that the well mixed limit is *Da*=1. Figure 3-7 (a) and (b) further support this conclusion. They are semi-log plots of Y_P vs k_2/k_1 for C-P stoichiometry cases 1 and 3 respectively. The curves show values of *Da* investigated. The curves for *Da*=0.01 and *Da*=1 lie exactly on top of each other while increasing *Da* drops the yield, as with the C-C cases (Figure 3-3). This confirms that *Da*=1 is the well mixed limit.

The same *Da* limit was found for both the C-C and C-P cases. *Da*≤1 is well mixed and *Da*>1 is imperfectly mixed. The fact that the same trends and effect of Damköhler number are seen for a different type of reaction altogether suggests that mixing is a physical effect that can be controlled regardless of the reaction being studied. At the same time mixing interacts strongly with the reaction stoichiometry and reaction rate ratio.

3.4.2.2 Effect of non-dimensional reaction rate ratio (k_2/k_1).

Looking at Figures 3-6 (a) to (f), it can be seen that as k_2/k_1 is decreased, the curves for all the stoichiometries move upwards, indicating that the yields for all the stoichiometry cases at all values of *Da* increase with this decrease in k_2/k_1. This again suggests that a smaller k_2/k_1 is favourable and a larger k_2/k_1 is unfavourable, similar to the C-C reaction scheme. For Cases 1 and 2 the maximum yield is approximately 1 and for cases 3 and 4 it is approximately 0.88. The curves for cases 1 and 2 collapse at k_2/k_1=0.001 (Figure 3-6 (d)) and at k_2/k_1=0.0001 for cases 3 and 4 (Figure 3-6 (e)). The yields are seen to increase

at all values of *Da* as k_2/k_1 is decreased from 1 to 0.00001 (from Figure 3-6 and more clearly in Figure 3-7). The largest improvement with improving k_2/k_1 is seen for Case 3, while Case 1 seems to improve the least.

These trends are also reflected in Figure 3-8 (a), (b) and (c) which are semi-log plots of Y_P versus k_2/k_1 for all four C-C stoichiometries at (a) *Da*=1, (b) *Da*=100 and (c) *Da*=10000 at time $Da \cdot t^*$=500. These figures show the yield increasing with improving k_2/k_1 with the final yields being different for cases 1 and 2 and cases 3 and 4, as previously noticed, suggesting an effect of stoichiometry on the maximum attainable yield at short times. The poorly mixed condition (*Da*=10000) provides yields of approximately half of the well mixed cases at this short time. Though the other well mixed cases may have reached completion at $Da \cdot t^*$=500, it is very possible that this is not the case for the bad mixing condition at *Da*=10000, since the yield is only at about 50%.

If the reaction is allowed to progress to long times ($Da \cdot t^*$=50000) for the bad mixing case, *Da*=10000, (Figure 3-9) it the yield can increase to above 90%, but only at an especially good k_2/k_1 ratio. The effect of stoichiometry on the maximum yield decreases at long times. The curves seem to collapse at k_2/k_1=0.00001, even though at the lower k_2/k_1's there is still an effect of stoichiometry. The cases also split away from each other at k_2/k_1's where they were equal at short times.

This suggests that if k_2/k_1 is very good but the stoichiometry of the C-P reaction is unknown, the best idea is to go with imperfect mixing for a very long time, though this may be restricted by the residence time of the reactor.

3.4.2.3 Effect of Stoichiometry.

Figures 3-6 (a) to (f) illustrate a significant effect of stoichiometry for the C-P case. At k_2/k_1=1 (Figure 3-6 (a)) the difference in yield for the different stoichiometries is enormous and there is a clear distinction between a favourable and unfavourable reaction stoichiometry (Case 2 and Case 3 respectively).This disparity decreases as k_2/k_1 decreases (Figures 3-6 (b) to (f)). However, the effect of stoichiometry never really goes

away since even at k_2/k_1=0.00001 there is still a difference in yield between cases 1 and 2 and cases 3 and 4 regardless of the mixing condition. This difference in maximum yield could be attributed to the coefficient of the limiting reagent in the desired reaction, ϵ, which takes a value of 1 for cases 1 and 2 and a value of 2 for cases 3 and 4. This means that though there is a collapse of the curves for similar stoichiometries, there is still a distinct difference between the stoichiometries of different types regardless of the Damköhler and k_2/k_1 values.

This is different from the C-C stoichiometries where the stoichiometries were seen to collapse (Figure 3-2 (a) to (e)) at $k_2/k_1 \leq 0.001$. This may be because for all the C-C cases investigated, the stoichiometric coefficient of the limiting reagent *B* in the desired reaction was always 1, so all the curves were seen to collapse, as for the C-P case with similar ϵ's.

The curves show a clear distinction between favourable stoichiometries (Case 2) and unfavourable stoichiometries (Case 3), where the difference between the two is that the stoichiometric coefficients of limiting reagent *B* in the desired and undesired reaction are reversed. This is particularly evident at k_2/k_1=1 (Figure 3-6(a)) with good mixing conditions ($Da \leq 100$), when the desired and undesired reactions are equally likely to take place. The Yield of *P* for Case 2 and Case 3 seems to flip, i.e. the amounts of *B* consumed in the desired and undesired reactions for Case 2 are just reversed for Case 3. This correspondingly changes the Yield of *P*, making one stoichiometry favourable and the other unfavourable. Cases 1 and 4 seem to be very similar, since the stoichiometric coefficients are all the same within each of them respectively.

At the worst k_2/k_1 ratio (Figure 3-6 (a), k_2/k_1 =1), the worsening of mixing (increasing *Da*) brings the curves for the four different stoichiometries closer to each other and improvement of mixing to drives the curves apart, i.e. the yield for the good stoichiometry gets better and the yield for the bad stoichiometry gets worse at well mixed conditions. Bad mixing tends to dampen the effect of stoichiometry on the yield for C-P reactions at unfavourable k_2/k_1. Curiously, worsening the mixing for the very unfavourable stoichiometry case, Case 3, improves the final yield. This is contrary to all

other instances and probably occurs because the poor mixing, i.e. pockets of high concentration of limiting reagent, favours the desired reaction since the dependence on the rate constant on concentration of limiting reagent is higher than the undesired reaction. For short times, there is a distinct difference in the final obtainable yield by a certain stoichiometry.

Though it may not seem like it at first, the C-P reaction scheme shows some intricacies that almost make it more complicated do deal with than the C-C reaction scheme. Careful consideration needs to be given to the stoichiometry, more so than the C-C reaction scheme, and the time allowed for reaction will need to be adjusted based on the stoichiometry, especially for stoichiometries of the form of Case 3 or 4.

In order to maximize yield for Cases 1 and 2, k_2/k_1 needs to be minimized (ideally below 0.001) and mixing made close to perfect. For Cases 3 and 4, if k_2/k_1 is greater than 0.001 maximum yield is obtained by mixing rapidly, but if k_2/k_1 is smaller than 0.001 the yield is maximized by mixing slowly but letting the reaction run for a VERY long time, at least a hundred times longer than for the well mixed cases.

3.4.2.4 Summary of the effects on C-P reaction schemes.

As a summary, for Competitive-Consecutive reactions:

(a) $Da \leq 1$ is perfectly well mixed. This is the same as for the C-C reaction scheme.
(b) For Cases 1 and 2, $k_2/k_1 \leq 0.001$ will provide maximum values of yield.
(c) From Figures 3-8 and 3-9, it can be concluded that for Cases 3 and 4, if $k_2/k_1 \geq 0.001$ maximum values of yield at short times are obtained with good mixing conditions and if $k_2/k_1 \leq 0.001$, maximum values of yield are obtained at very long times with bad mixing conditions.
(d) The effect of stoichiometry is very prevalent for C-P type reactions. Stoichiometry affects the maximum obtainable yield at short times for all mixing conditions and k_2/k_1, and at all $k_2/k_1 \geq 0.00001$ for long times with a bad mixing condition.

3.4.3 Phase plots of variables for C-C and C-P reaction schemes for the purpose of design.

The purpose of design graphs, in the context of mixing sensitive reactions, is to provide a direct method of predicting the yield of desired product without extensive calculations and investigation of the different variables. For our purposes, design graphs would incorporate the effects of stoichiometry, mixing and k_2/k_1 and the combinations of the three that could possibly give a certain specified yield of desired product. The purpose of the graphs would be to assist in the design of the following problem:

" If one has a certain mixing sensitive reaction and a target yield of desired product in mind, what range of values of non-dimensional reaction rate ratio and Damköhler would be required to ensure that the target yield of desired product will be obtained? If one of the variables is inadequate, is it still possible to obtain the said target yield? If it is possible, how much do the other variables need to change to accommodate for that inadequacy, if at all?"

The figures should allow for a design space to be established within which decisions can be made based on different criterions and restrictions.

Figures 3-10 and 3-11 are examples of such design curves for the C-C and C-P reaction schemes respectively. They show phase plots of Damköhler number (*x* axis) versus the non-dimensional reaction rate ratio (y axis) for yields of desired product of (a) 85% or more, (b) 95% or more and (c) 99% or more at a time of $Da \cdot t^* = 500$. They are set up such that the axis intersection (origin) represents the most favourable conditions for both k_2/k_1 and Damköhler number. The figures have marked regions of required k_2/k_1 and *Da* for the different stoichiometries to obtain the specified yield. These figures are essentially a filtered summary of the results presented in the previous sections. The effect of stoichiometry quickly becomes evident as the yield desired is raised. For the C-C cases, the regions common to all stoichiometries become smaller, i.e. the requirements on the k_2/k_1 and *Da* become a lot more stringent. Similarly, for C-P cases 3 and 4, yields greater than 90% were unachievable at short times, so those stoichiometries do not show up in Figures 3-11 (b) and (c)

For these reaction schemes it is suggested that *Da* be kept below 100, but then k_2/k_1 needs to be set accordingly to achieve the required yield and vice versa Not all stoichiometries may be able provide that yield for the chosen conditions, for example:
For a C-C reaction scheme, a *Da*=100 and desired yield of 99% and above (Figure 3-10 (c)), a k_2/k_1<=0.0001 will provide that yield for all stoichiometries; but if k_2/k_1 >0.0001 then only C-C stoichiometry Cases 3, 5, 6, 7 or 8 will provide a 99% yield. The C-P figures can be read in the same way.

In order to link these results to physical process variables, we could assume that our diffusion time is equal to the Batchelor time scale which, by definition, is equivalent to the Kolmogorov time scale. Replacing the expression for the Kolmogorov time scale in our definition of *Da* gives:

$$Da = k_1^{'} \left(\frac{\rho_T}{M}\right)^{\epsilon} \left(\frac{\nu}{\varepsilon_D}\right)^{\frac{1}{2}} \tag{3.5}$$

where ν is the kinematic viscosity and ε_D is local rate of dissipation of Turbulent Kinetic Energy (TKE) per mass. Rearranging for ε_D gives:

$$\varepsilon_D = \nu \left(\frac{k_1^{'} \left(\frac{\rho_T}{M}\right)^{\epsilon}}{Da} \right)^2 \tag{3.6}$$

This can be used to compare an existing equipment specification the *Da* and reaction rate ratio from the phase plot. For example, for a C-C reaction of the type Case 1 ($\epsilon = 1$), using typical values for water ($\nu = 1 \times 10^{-6}$ m^2/s, $\rho_T = 1000$ kg/m^3, $M = 18$ kg/kmole), the range of ε_D for 1 ≤*Da* ≤ 10000 will be:

$$3.09 \times 10^{-11} k_1^{'2} \leq \varepsilon_D \leq 3.09 \times 10^{-3} k_1^{'2}$$

3.5 CONCLUSIONS

The three effects of initial mixing condition, non-dimensional reaction rate ratio and reaction stoichiometry were investigated in detail using a 1D transient reaction-diffusion model for the Competitive-Consecutive (C-C) and Competitive-Parallel (C-P) form of mixing sensitive reactions. Several cases were investigated for each variable and the effects of each of the variables on the final yield of desired product were investigated. It was found that a smaller value of Damköhler number and non dimensional reaction rate ratio were desirable to obtain maximum yield of desired product for both the C-C and C-P reaction schemes. It was also found that the stoichiometry of the reaction can affect the final yield of desired product considerably, and needs to be taken into consideration in the design of reactors for such reactions. There are favourable and unfavourable stoichiometries for both types of reaction schemes. The stoichiometric coefficient of the limiting reagent in the desired reaction affects the required mixing condition to ensure a good yield of desired product. The stoichiometry also affects the non-dimensional reaction rate ratio, k_2/k_1, and the requirements of the absolute reaction rates for each of the reactions changes with the reaction stoichiometry. The following ranges were found for the investigated variables:

- $Da \leq 1$ is well mixed for both the C-C and C-P type of mixing sensitive reaction.
- For the C-C type reaction, $k_2/k_1 \leq 0.001$ with $Da \leq 100$ will provide good values of yield at short times, i.e. $Da \cdot t^* = 500$.
- For C-P Cases 1 and 2, $k_2/k_1 \leq 0.001$ will provide maximum values of yield. For Cases 3 and 4, if $k_2/k_1 \geq 0.001$ maximum values of yield at short times are obtained with good mixing conditions. If $k_2/k_1 \leq 0.001$, maximum values of yield are obtained at very long times with bad mixing conditions.
- For the C-C reaction scheme the effect of stoichiometry is a legitimate one, which can be large if the k_2/k_1 is unfavourable but vanishes at $k_2/k_1 \leq 0.001$ for short times and good mixing. At longer times with bad mixing conditions, this effect of stoichiometry reappears and requires a much smaller value of k_2/k_1. The effect of stoichiometry is also important for C-P type reactions. It affects

the maximum obtainable yield at short times for all mixing conditions and k_2/k_1, and at all $k_2/k_1 \geq 0.00001$ for long times with a bad mixing condition.

Overall, all three variables need to be given consideration if one is to design a reactor for such mixing sensitive reactions. However, the mixing model used is primitive and unrealistic and doesn't take into account the true nature of turbulent fluid flow and mixing that occurs in real reactor systems. Though this work strives to provide predictions of yield for the different conditions presented, the main aim was only to guide the reader on how to deal with the various variables and variable interactions that are present in reacting flows in order to better design a reactor for C-C and C-P mixing sensitive reactions. The intention of the authors is to explore the importance of the previously un-investigated effect the stoichiometry can have on the yield of desired product and to provide forms of the Damköhler number and reaction rate ratio for C-C and C-P mixing sensitive reactions with a general stoichiometry. This work was not intended to provide perfectly accurate predictions of yield of desired product. Experiments and fine tuning through trial and error when designing a reactor for these reactions are still recommended and will most definitely be required until a more realistic model can be implemented, such as the Engulfment model by Baldyga and Bourne (1999). Till then, the hope is that this work will reduce the number of experiments and trials that will need to be performed in order to adequately design a reactor for the C-C and C-P type of mixing sensitive reaction.

3.6 TABLES FOR CHAPTER 3

Table 3-1. Stoichiometries of reaction schemes and the corresponding non-dimensional reaction rate ratio for the eight different C-C reactions. *Da* was always $Da = k_1^{'}\left(\frac{\rho_T}{M}\right)\frac{L_B^2}{D_B}$.

Case	Reaction Scheme	$\epsilon, \alpha, \beta, \gamma$	$\frac{k_2}{k_1}$
1	$A + B \overset{k_1^{'}}{\rightarrow} 2\mathrm{P}$ $P + B \overset{k_2^{'}}{\rightarrow} S$	1, 2, 1, 1	$\frac{1}{2}\frac{k_2^{'}}{k_1^{'}}$
2	$A + B \overset{k_1^{'}}{\rightarrow} \mathrm{P}$ $P + B \overset{k_2^{'}}{\rightarrow} S$	1, 1, 1, 1	$\frac{1}{2}\frac{k_2^{'}}{k_1^{'}}$
3	$A + B \overset{k_1^{'}}{\rightarrow} \mathrm{P}$ $2P + B \overset{k_2^{'}}{\rightarrow} S$	1, 1, 2, 1	$\frac{1}{2}\left(\frac{\rho_T}{M}\right)\frac{k_2^{'}}{k_1^{'}}$
4	$A + B \overset{k_1^{'}}{\rightarrow} 2\mathrm{P}$ $2P + B \overset{k_2^{'}}{\rightarrow} S$	1, 2, 2, 1	$\left(\frac{\rho_T}{M}\right)\frac{k_2^{'}}{k_1^{'}}$
5	$A + B \overset{k_1^{'}}{\rightarrow} 2\mathrm{P}$ $P + 2B \overset{k_2^{'}}{\rightarrow} S$	1, 2, 1, 2	$\frac{1}{2}\left(\frac{\rho_T}{M}\right)\frac{k_2^{'}}{k_1^{'}}$
6	$A + B \overset{k_1^{'}}{\rightarrow} \mathrm{P}$ $P + 2B \overset{k_2^{'}}{\rightarrow} S$	1, 1, 1, 2	$\frac{1}{2}\left(\frac{\rho_T}{M}\right)\frac{k_2^{'}}{k_1^{'}}$
7	$A + B \overset{k_1^{'}}{\rightarrow} \mathrm{P}$ $2P + 2B \overset{k_2^{'}}{\rightarrow} S$	1, 1, 2, 2	$\frac{1}{2}\left(\frac{\rho_T}{M}\right)^2\frac{k_2^{'}}{k_1^{'}}$
8	$A + B \overset{k_1^{'}}{\rightarrow} 2\mathrm{P}$ $2P + 2B \overset{k_2^{'}}{\rightarrow} S$	1, 2, 2, 2	$\left(\frac{\rho_T}{M}\right)^2\frac{k_2^{'}}{k_1^{'}}$

Table 3-2. Stoichiometries of reaction schemes and the corresponding non-dimensional reaction rate ratio and Damköhler number for the four different C-P reactions.

Case	Reaction Scheme	ϵ, γ	$\frac{k_2}{k_1}$	Da
1	$A + B \overset{k_1'}{\rightarrow} \mathrm{P}$ $C + B \overset{k_2'}{\rightarrow} S$	1, 1	$\frac{k_2'}{k_1'}$	$k_1' \left(\frac{\rho_T}{M}\right) \frac{L_B^2}{D_B}$
2	$A + B \overset{k_1'}{\rightarrow} \mathrm{P}$ $C + 2B \overset{k_2'}{\rightarrow} S$	1, 2	$2\left(\frac{\rho_T}{M}\right) \frac{k_2'}{k_1'}$	$k_1' \left(\frac{\rho_T}{M}\right) \frac{L_B^2}{D_B}$
3	$A + 2B \overset{k_1'}{\rightarrow} \mathrm{P}$ $C + B \overset{k_2'}{\rightarrow} S$	2, 1	$\frac{1}{2}\left(\frac{\rho_T}{M}\right)^{-1} \frac{k_2'}{k_1'}$	$k_1' \left(\frac{\rho_T}{M}\right)^2 \frac{L_B^2}{D_B}$
4	$A + 2B \overset{k_1'}{\rightarrow} \mathrm{P}$ $C + 2B \overset{k_2'}{\rightarrow} S$	2, 2	$\frac{k_2'}{k_1'}$	$k_1' \left(\frac{\rho_T}{M}\right)^2 \frac{L_B^2}{D_B}$

3.7 FIGURES FOR CHAPTER 3

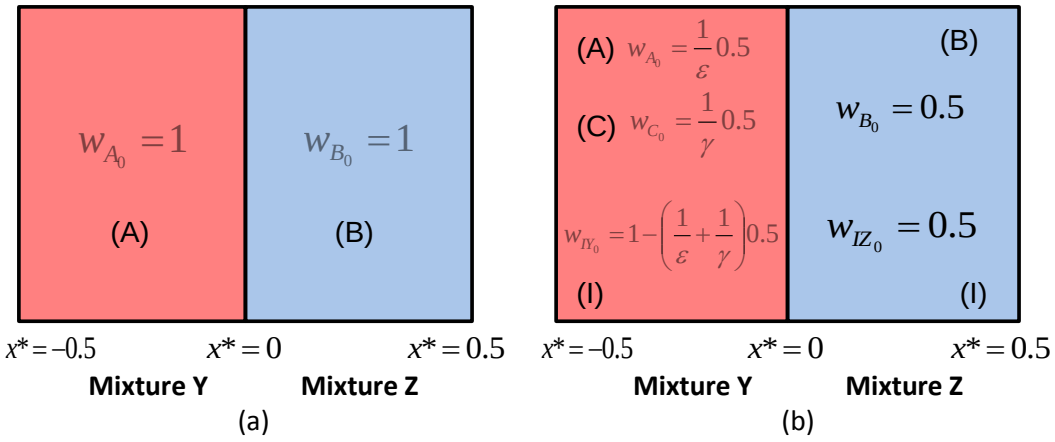

Figure 3-1. Initial conditions for (a) C-C and (b) C-P reaction scheme simulations.

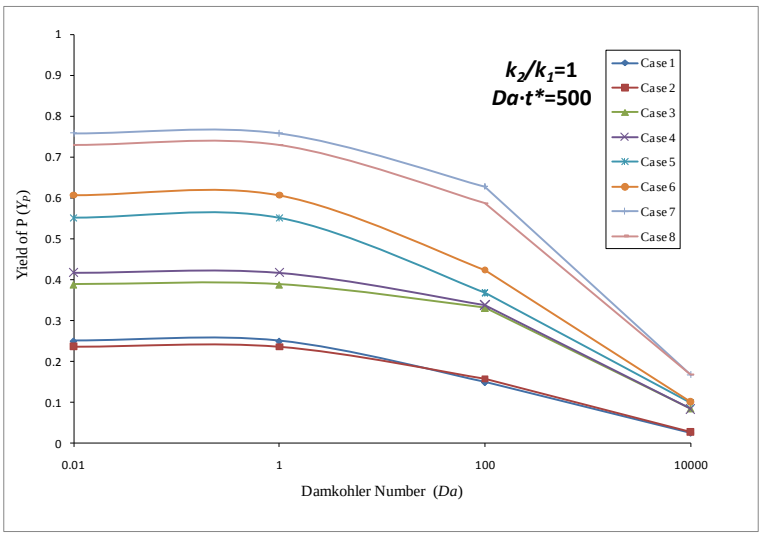

(a) k_2/k_1 = 1

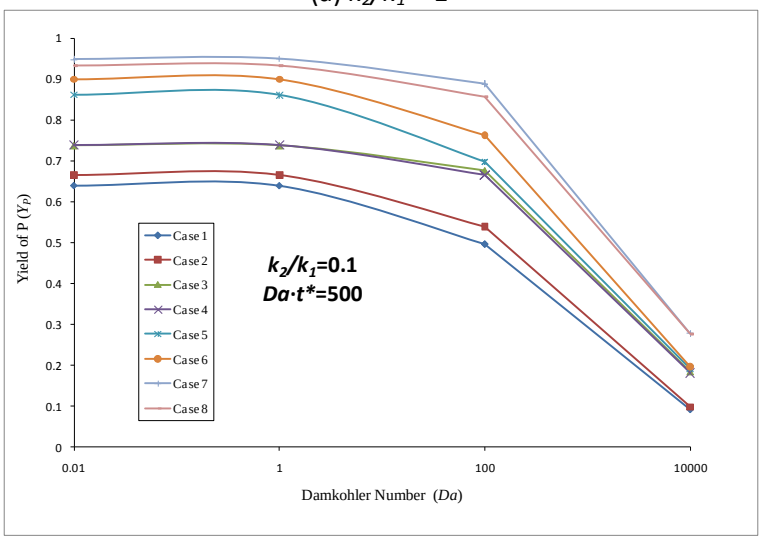

(b) k_2/k_1 = 0.1

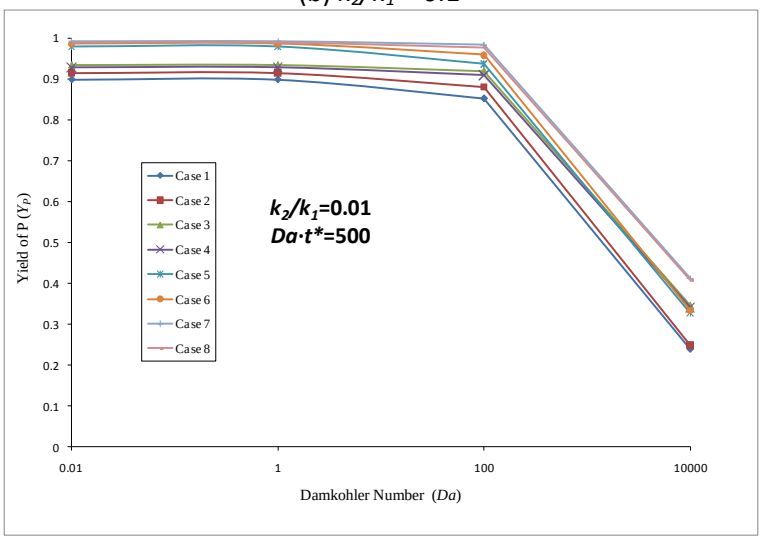

(c) k_2/k_1 = 0.01

Figure 3-2. Plots of Yield of *P* vs. *Da* for decreasing k_2/k_1 ratios for the C-C cases.

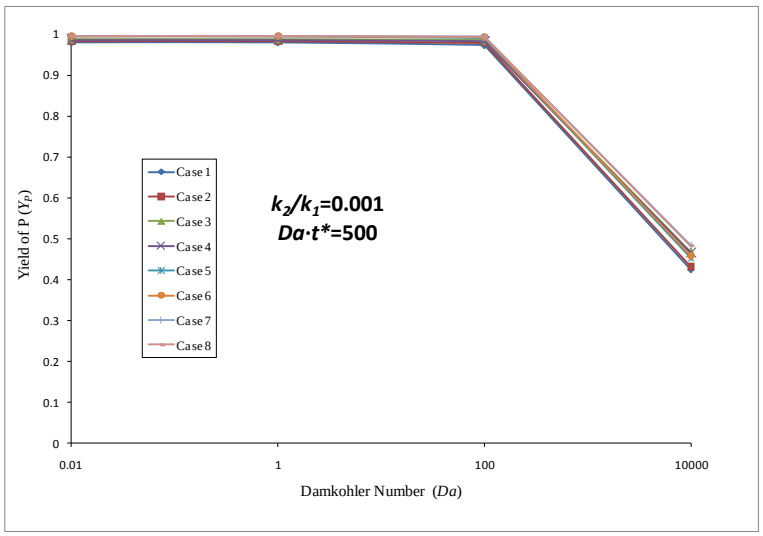

(d) k_2/k_1 = 0.001

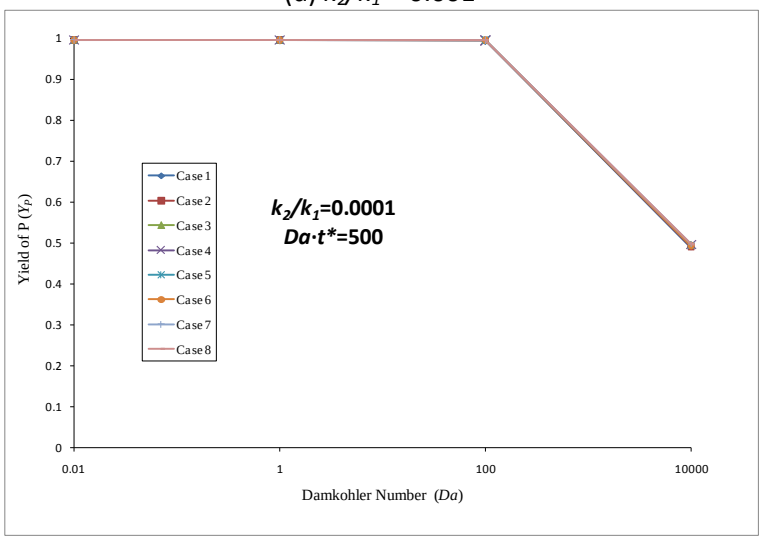

(e) k_2/k_1 = 0.0001

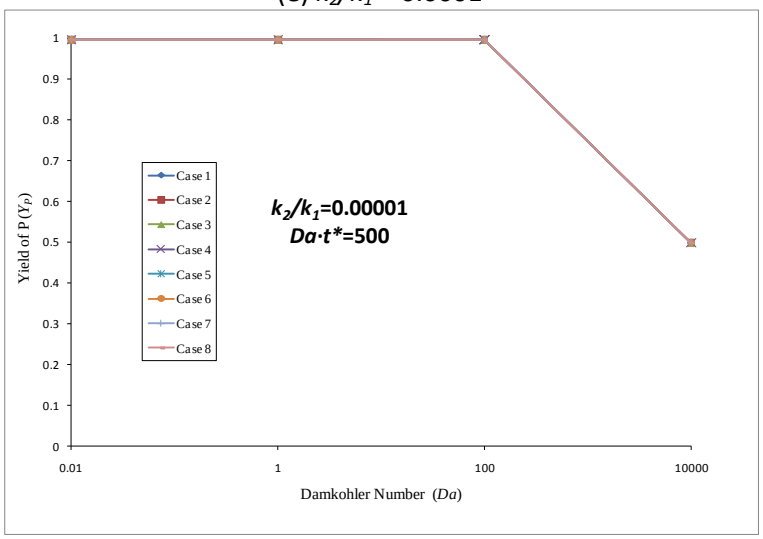

(f) k_2/k_1 = 0.00001

Figure 3-2. Plots of Yield of *P* vs. *Da* for decreasing k_2/k_1 ratios for the C-C cases.

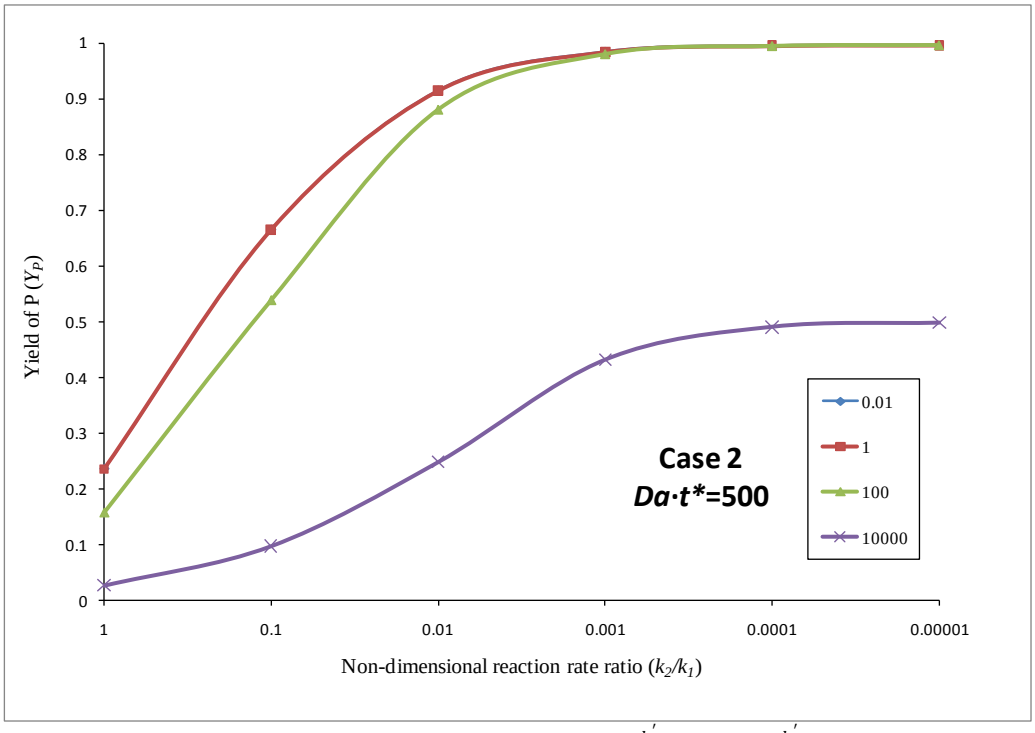

(a) C-C Stoichiometry Case 2: $A + B \overset{k_1'}{\rightarrow} \mathrm{P}\,;\, P + B \overset{k_2'}{\rightarrow} S$

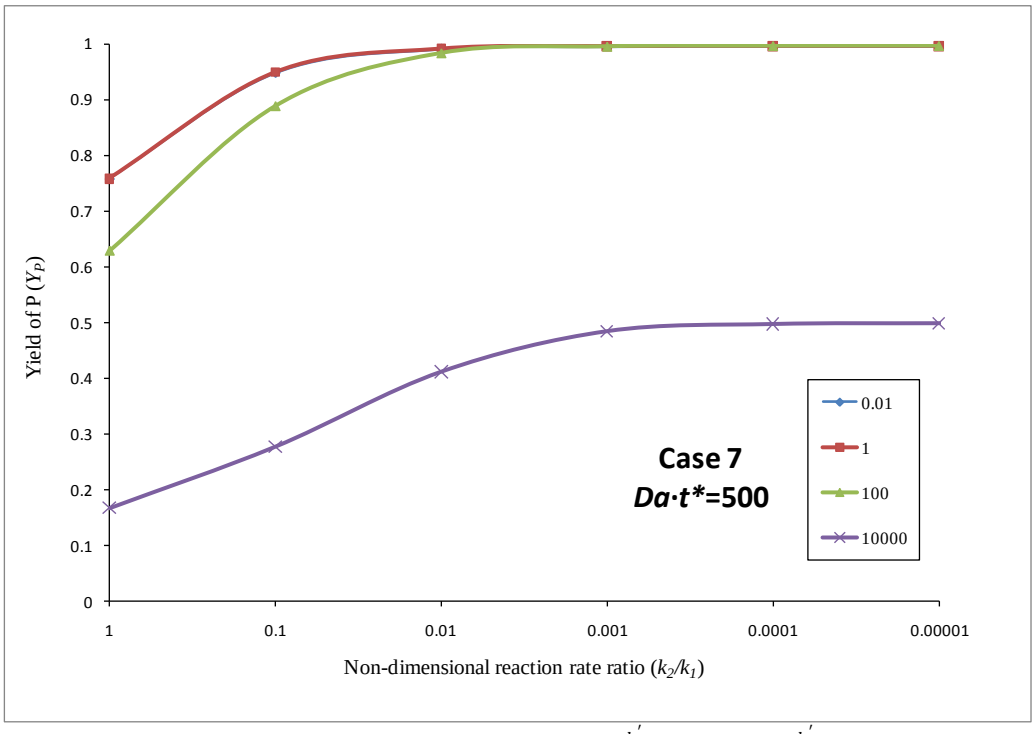

(b) C-C Stoichiometry Case 7: $A + B \overset{k_1'}{\rightarrow} \mathrm{P}\,;\, 2P + 2B \overset{k_2'}{\rightarrow} S$

Figure 3-3. Plots of Yield of *P* vs. k_2/k_1 for two sample C-C stoichiometries. The curves represent the different *Da*. Curves for *Da*=0.01 lie exactly under the curves for *Da*=1.

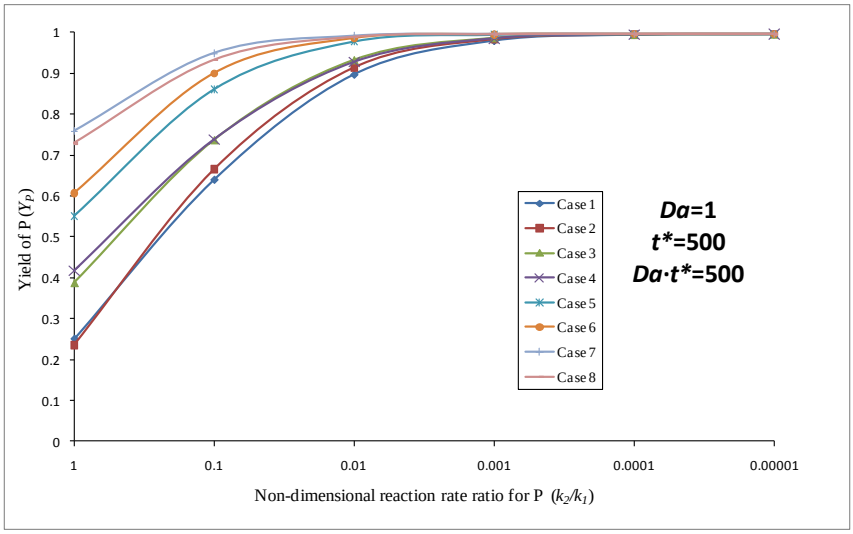

(a) *Da* = 1

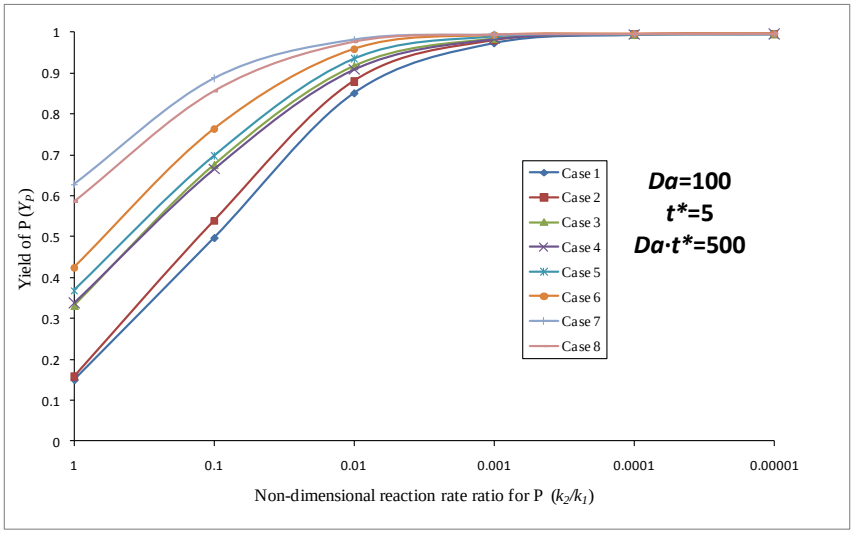

(b) *Da* = 100

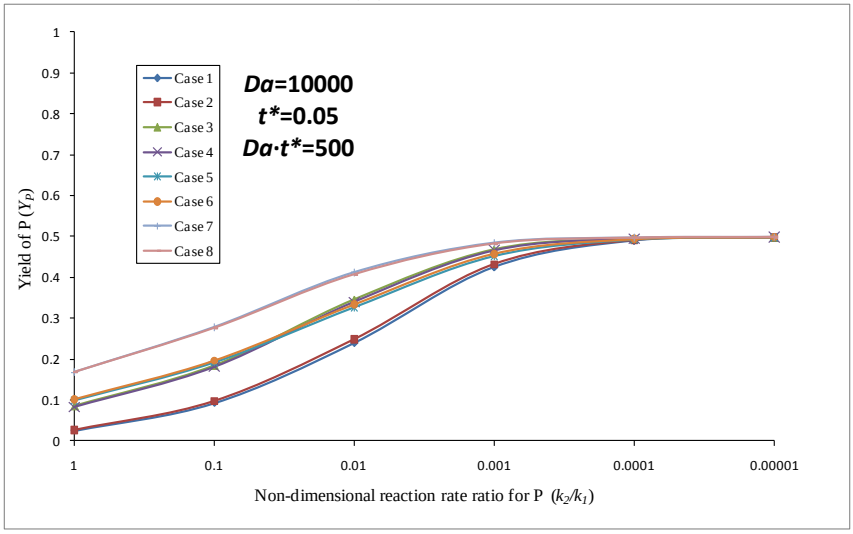

(c) *Da* = 10000

Figure 3-4. Plots of Yield of *P* vs. k_2/k_1 for various *Da* at $Da \cdot t^*$=500 for C-C cases.

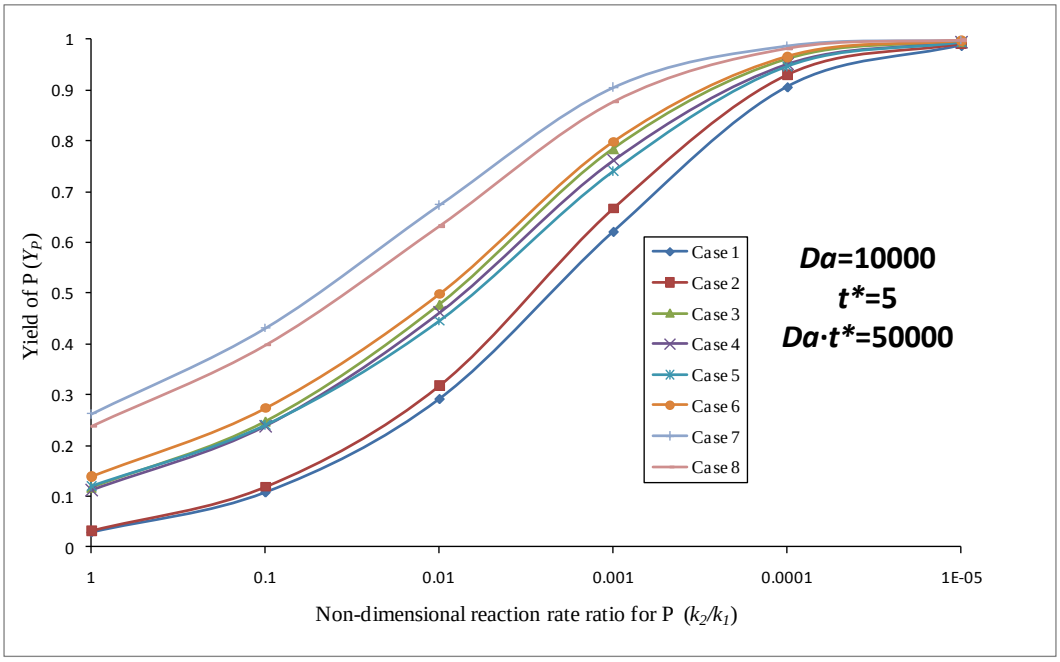

Figure 3-5 Plot of Yield of *P* vs.k_2/k_1 for *Da*=10000 at *Da*·*t**=50000 for C-C cases

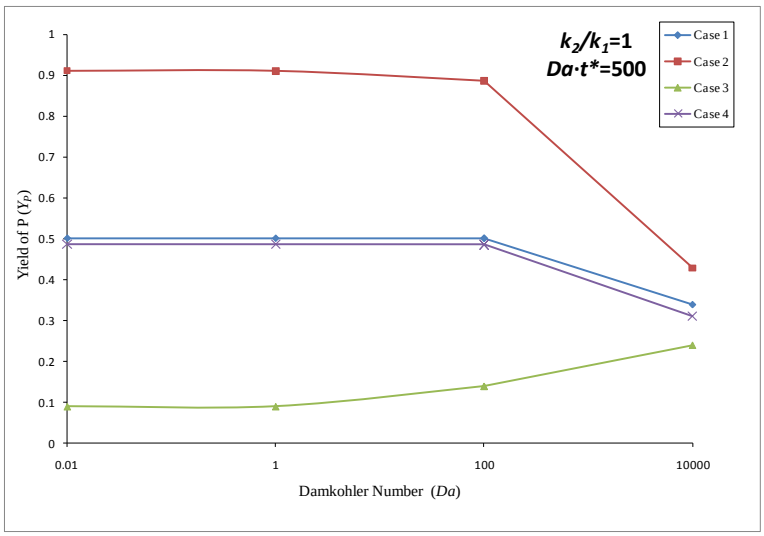

(a) k_2/k_1 = 1

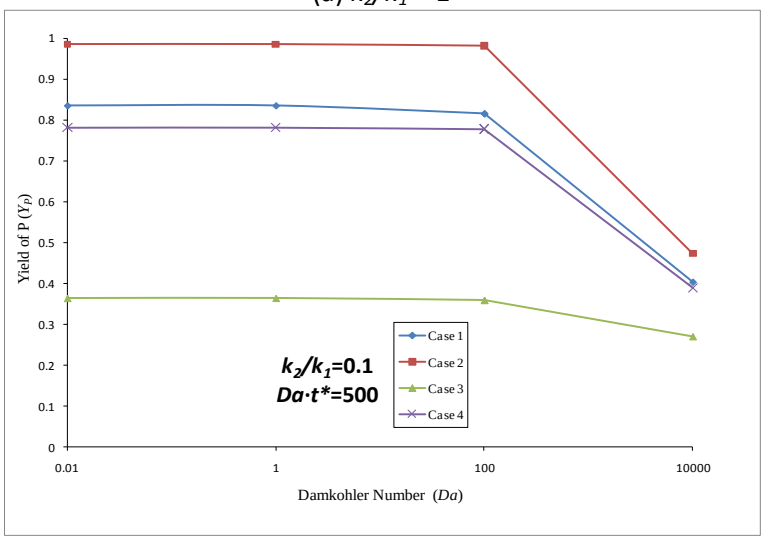

(b) k_2/k_1 = 0.1

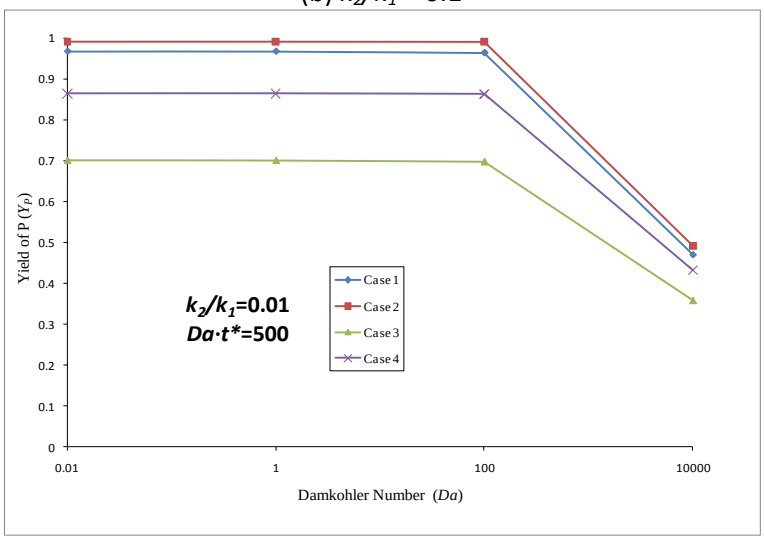

(c) k_2/k_1 = 0.01

Figure 3-6. Plots of Yield of *P* vs. *Da* for decreasing k_2/k_1 ratios for the C-P cases.

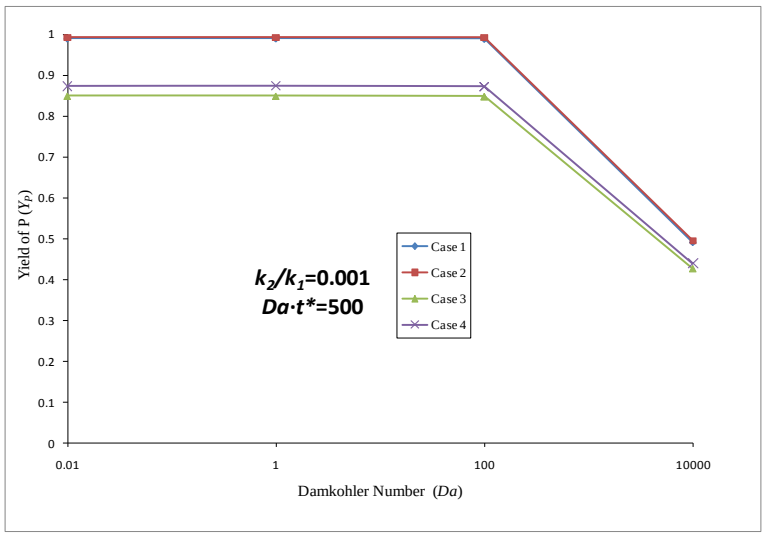

(d) k_2/k_1 = 0.001

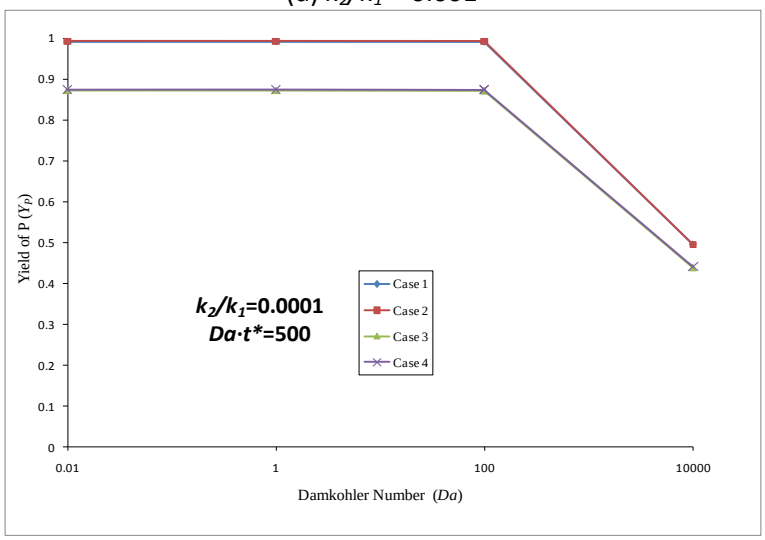

(e) k_2/k_1 = 0.0001

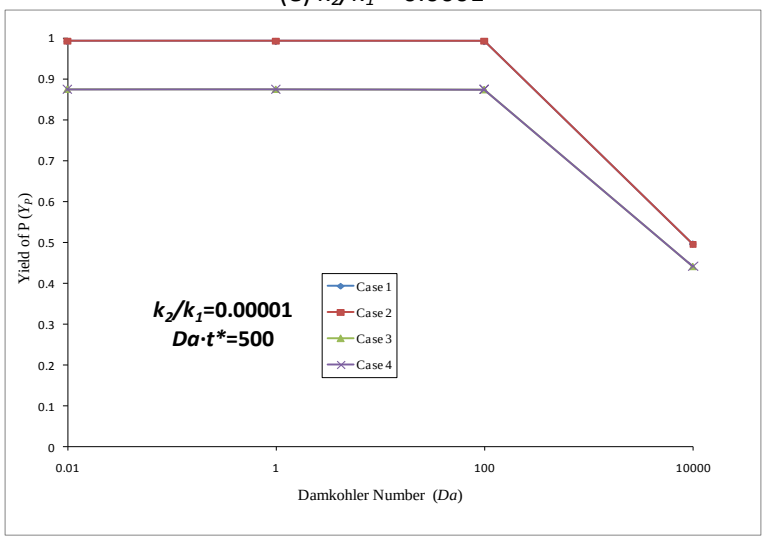

(f) k_2/k_1 = 0.00001

Figure 3-6. Plots of Yield of *P* vs. *Da* for decreasing k_2/k_1 ratios for the C-P cases.

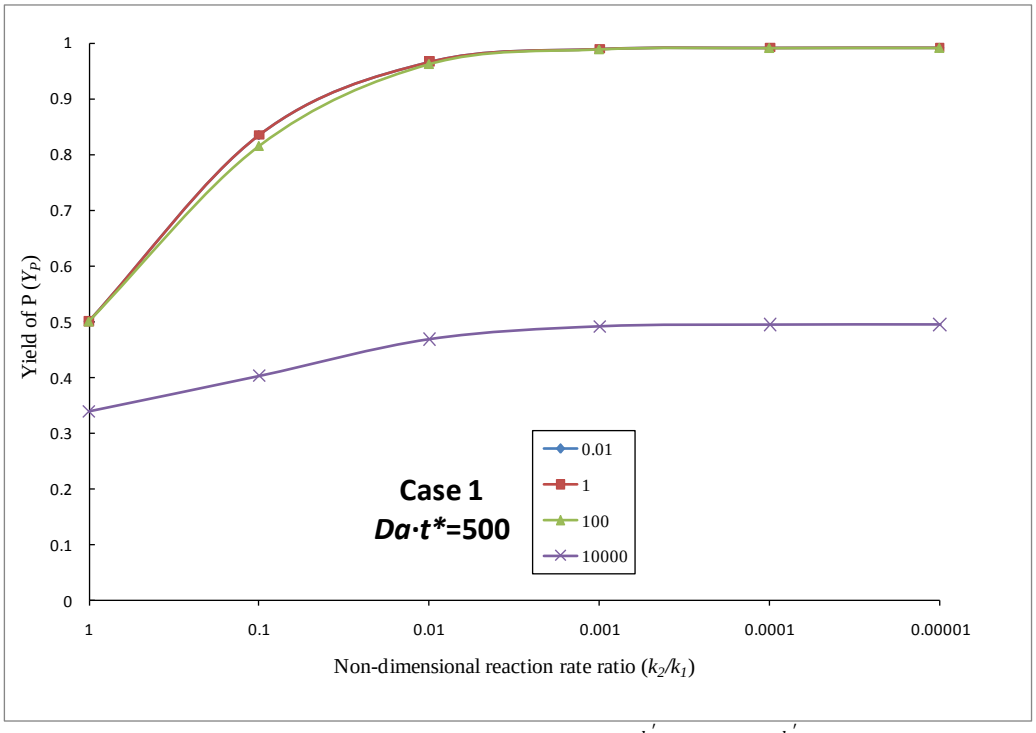

(a) C-P Stoichiometry Case 1: $A + B \overset{k_1'}{\rightarrow} \mathrm{P}\,;\, C + B \overset{k_2'}{\rightarrow} S$

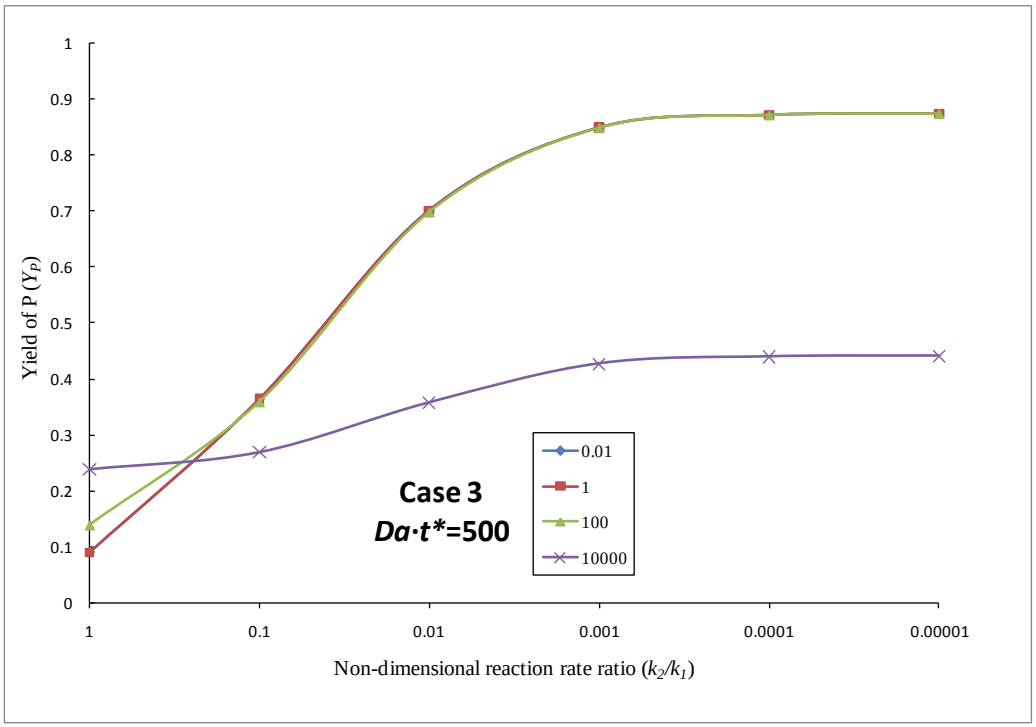

(b) C-P Stoichiometry Case 3: $A + 2B \overset{k_1'}{\rightarrow} \mathrm{P}\,;\, C + B \overset{k_2'}{\rightarrow} S$

Figure 3-7. Plots of Yield of *P* vs. k_2/k_1 for two sample C-P stoichiometries. The curves represent the different *Da*. Curves for *Da*=0.01 lie exactly under the curves for *Da*=1.

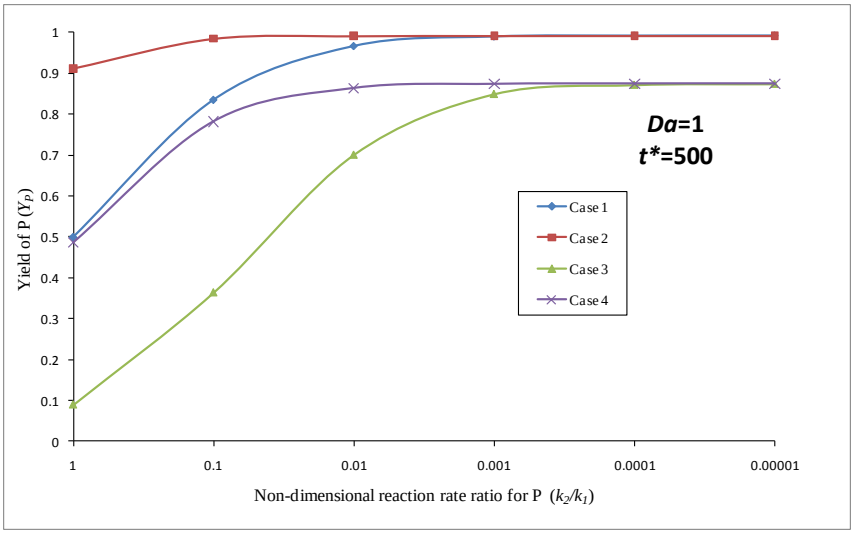

(a) *Da* = 1

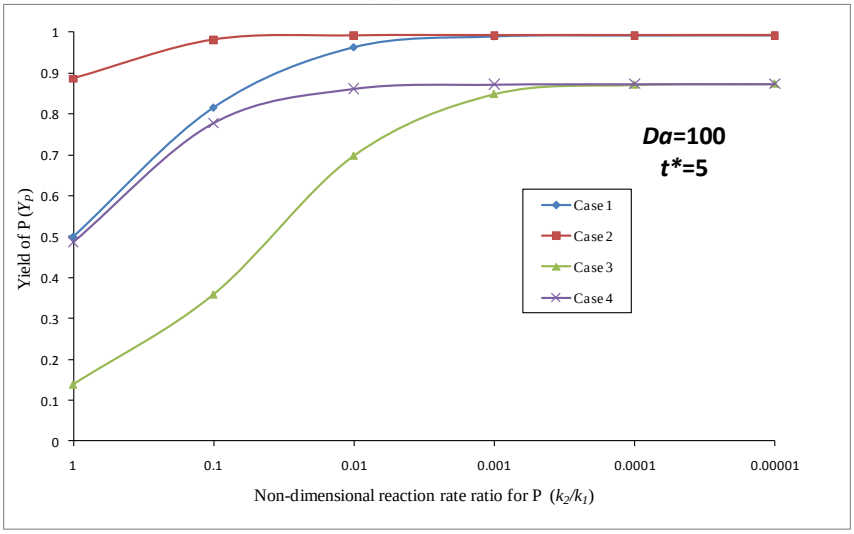

(b) *Da* = 100

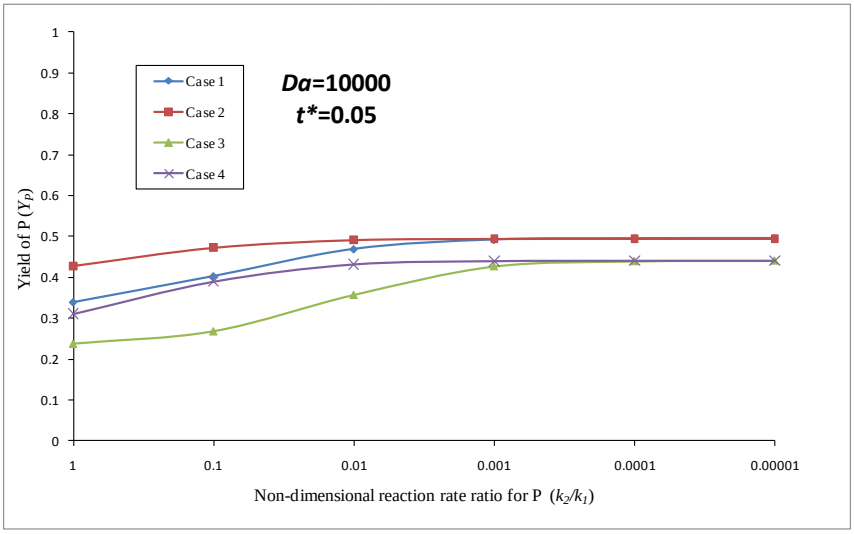

(c) *Da* = 10000

Figure 3-8. Plots of Yield of *P* vs. k_2/k_1 for various *Da* at $Da \cdot t^* = 500$ for C-P cases.

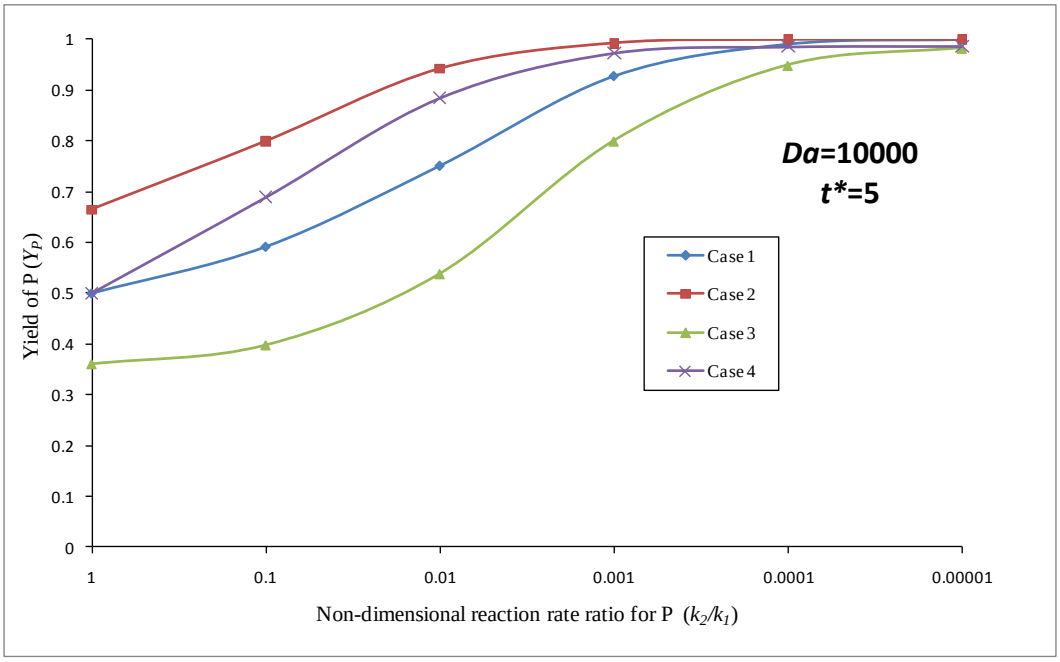

Figure 3-9. Plot of Yield of *P* vs.k_2/k_1 for *Da*=10000 at *Da*·*t**=50000 for C-P cases

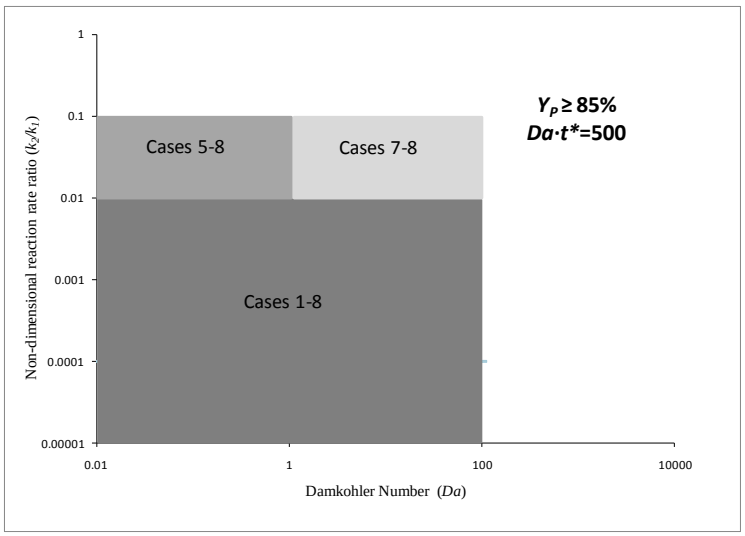

(a) Y_P is at least 0.85 (85%)

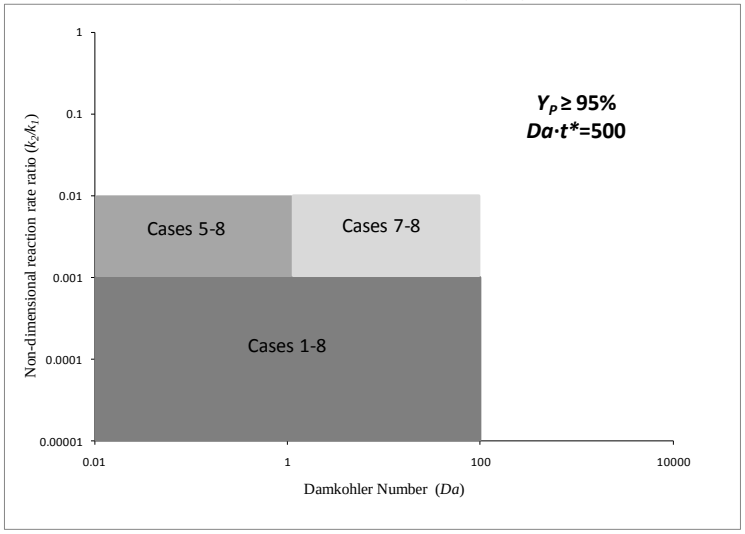

(b) Y_P is at least 0.95 (95%)

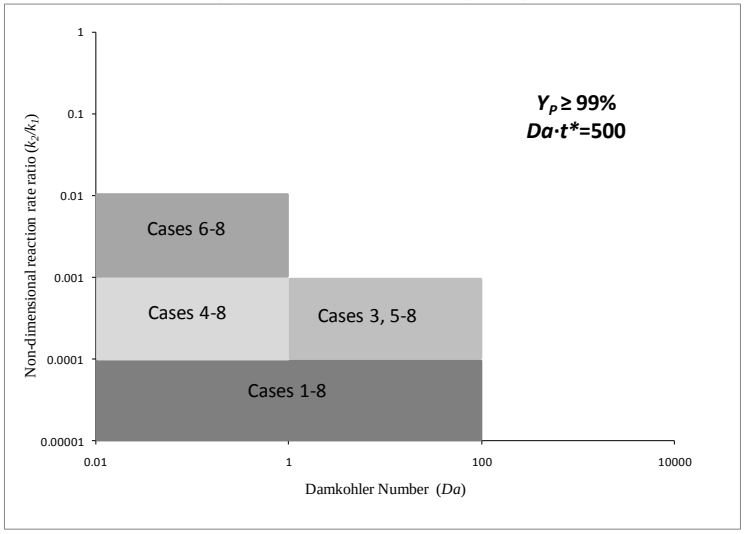

(c) Y_P is at least 0.99 (99%)

Figure 3-10. Design spaces for Yield of *P* for *Da* and k_2/k_1 at $Da \cdot t^*$=500 for C-C cases.

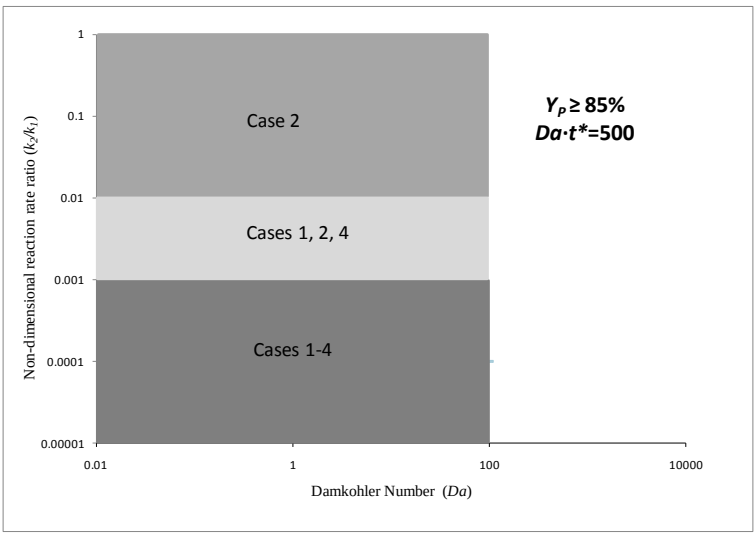

(a) Y_P is at least 0.85 (85%)

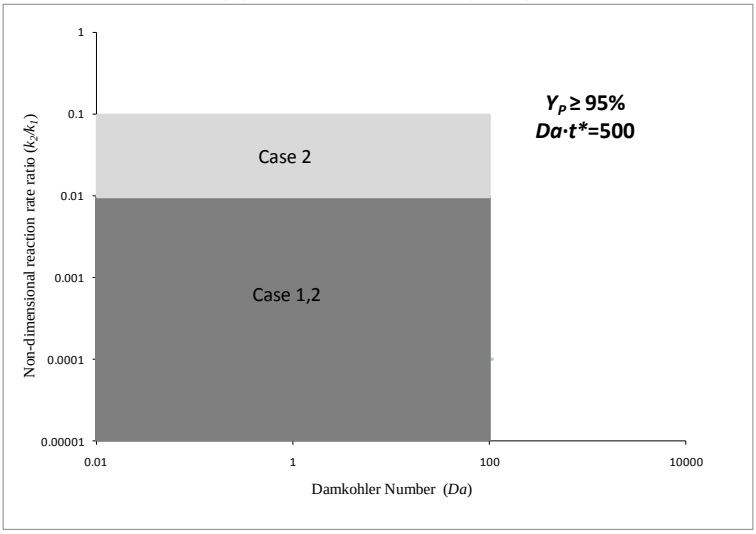

(b) Y_P is at least 0.95 (95%)

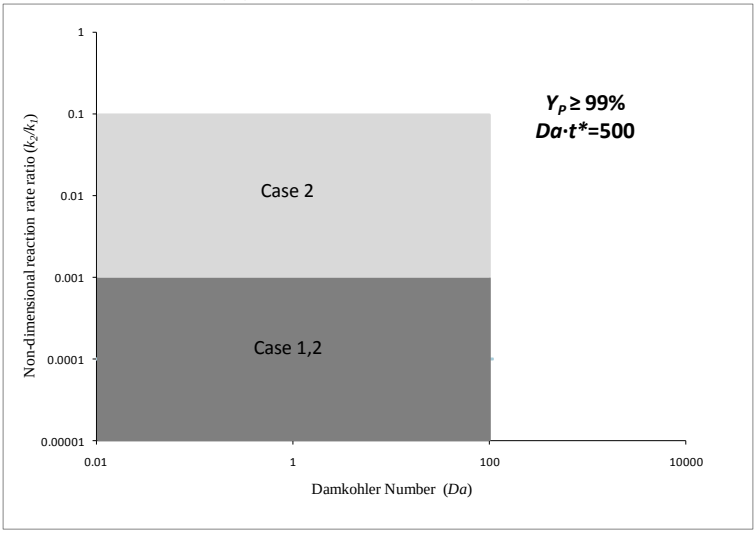

(c) Y_P is at least 0.99 (99%)

Figure 3-11. Design spaces for Yield of *P* for *Da* and k_2/k_1 at $Da \cdot t^*$=500 for C-P cases.

4

Conclusions and Future Work

4.1 CONCLUSIONS

Mixing sensitive reactions are reactions which are particularly sensitive to the rate at which the reactants are brought together, i.e. how fast they are mixed. Two types of mixing sensitive reactions have been studied: the Competitive-Consecutive reaction scheme, which involves two competing reactions where the second unwanted reaction consumes the desired product from the first reaction, and the Competitive-Parallel reaction scheme where two reactions compete for a limiting reagent to form a desired and undesired product. The effect of mixing and relative reaction rates of the competing reactions have been investigated previously and it is known that mixing can affect the product distribution significantly. However, though these reactions have been studied in the past, the work has been concentrated on the investigation of a single stoichiometry for each of the reaction schemes. This work intended to investigate whether the stoichiometry of the reaction plays a major role in the final yield of desired product obtainable.

A model was developed that successfully captured the effect of mixing, via the Damköhler number, the relative reaction rates, via a non-dimensional reaction rate ratio, and the stoichiometry of the reaction. General forms of the reactions were assumed and mass balance equations were derived. From the equations a general form of the Damköhler number that was common for both reaction types and all stoichiometries and a non-dimensional reaction rate ratio that was specific to each

reaction type were obtained. Both expressions exhibit a dependence on the stoichiometric coefficients of the reaction scheme. There is also an effect of stoichiometry evident in the modelling equations.

It was found that minimizing the Damköhler number and the non-dimensional reaction rate ratio would maximize the yield of desired product of the reaction for both Competitive-Consecutive and Competitive-Parallel reaction schemes. The stoichiometry of the reaction affected the requirements of well mixed Damkohler number and reaction rate ratio that would guarantee maximum yield of desired product. These qualitative descriptions were given quantitative ranges through an extensive investigation of the variables and were found to be:

- $Da \leq 1$ is well mixed for both the C-C and C-P type of mixing sensitive reaction.
- For the C-C type reaction, $k_2/k_1 \leq 0.001$ with $Da \leq 100$ will provide good values of yield at short times, i.e. $Da \cdot t^* = 500$.
- For C-P Cases 1 and 2, $k_2/k_1 \leq 0.001$ will provide maximum values of yield. For Cases 3 and 4, if $k_2/k_1 \geq 0.001$ maximum values of yield at short times are obtained with good mixing conditions. If $k_2/k_1 \leq 0.001$, maximum values of yield are obtained at very long times with bad mixing conditions.
- For the C-C reaction scheme the effect of stoichiometry is a legitimate one, which can be large if the k_2/k_1 is unfavourable but vanishes at $k_2/k_1 \leq 0.001$ for short times and good mixing. At longer times with bad mixing conditions, this effect of stoichiometry reappears and requires a much smaller value of k_2/k_1. The effect of stoichiometry is also important for C-P type reactions. It affects the maximum obtainable yield at short times for all mixing conditions and k_2/k_1, and at all $k_2/k_1 \geq 0.00001$ for long times with a bad mixing condition.

These results were interpreted into charts of requirements for mixing and relative rate ratio developed for desired values of yield for both types of reaction schemes. Overall, all three variables need to be given consideration if one is to design a reactor for such mixing sensitive reactions. However, the mixing model used is primitive and unrealistic

and doesn't take into account the true nature of turbulent fluid flow and mixing that occurs in real reactor systems.

This confirmation of the model allows for future work where the effects of stoichiometry, more realistic mixing models and k_2/k_1 ratios and the interactions between them will be investigated with the intention of producing charts that may help in prediction of the yield for a general mixing sensitive reaction. Though the model allows for investigation of the effects of initial concentrations of reactants, this was not done in the current study and this is another possible avenue for further exploration. It is also acknowledged that the 1D model is not a very accurate depiction of real turbulent mixing, but this investigation was meant to be a first foray into the effect of stoichiometry of mixing sensitive reactions, so simplicity was desirable. Added complexities like introducing stretching and using a lamellar 'barcode' model could possibly be integrated into the model in the future to better approximate the real industrial situation.

4.2 FUTURE WORK

Possible recommendations for future work are as follows:

- Introduce more complex models of fluid flow into the model such as taking into account laminar stretching of the striations, 2D deformations and eventually 3D deformation, similar to the collective work of Cox et al and Baldyga and Bourne. The eventual goal would be to somehow integrate the reaction diffusion equations into the Engulfment model of Baldyga and Bourne (1999), since this is regarded as the best micro mixing model currently available.

- Introduce more complex forms of the rate expressions used for the reactions, i.e. use the full Arrhenius form of the rate constants instead of assuming them to be constant. This would include the effects of temperature on the reaction rate.

- Compare the results of this study to some real experimental data for micro mixing reactions with varied stoichiometries and see if similar trends are observed in the yield of desired product. This would allow us to obtain ranges of the Damköhler number which are encountered experimentally, which could then be directly used in the model instead of using the suggested theoretical values.

- Eventually relate this Lagrangian micro-mixing model to the more complex CFD models, similar to how viscous sub layer models are used for computational modelling of turbulent flows.

- Expand the model to include the meso-mixing length scales, so that the assumption of being below the Kolmogorov length scale can be challenged and that the model more accurately represents the real system, where diffusion occurs at the same time as reduction of scale of segregation instead of being turned on after a convenient scale is obtained. This could possibly be done using a Gaussian distribution of reactants instead of uniform slabs, like Cox et al did previously, but would also require the inclusion of reaction effects with reduction of scale instead of just diffusion before reaction occurs.

- Possibly figure out a better way of defining what a 'fast' and 'slow' reaction is by using the rate of reaction instead of just the rate constants.

- Figure out how reactions can be integrated into spatial statistical measures of mixing for the intensity, scale and reduction of segregation.

- Possibly extend the model to heterogeneous reactions instead of just reactions in a homogeneous phase.

- Changing the initial conditions of the reactant concentrations to other than stoichiometric could be interesting as well.

5

References

Baldyga, J., & Bourne, J. R. (1992). Interactions Between Mixing on Various Scales in Stirred Tank Reactors. *Chemical Engineering Science , 47* (8), 1839-1848.

Baldyga, J., & Bourne, J. R. (1999). *Turbulent Mixing and Chemical Reactions.* Chichester, England: Wiley.

Baldyga, J., & Pohorecki, R. (1995). Turbulent micromixing in chemical reactors - a review. *The Chemical Engineering Journal , 58*, 183-195.

Baldyga, J., Bourne, J. R., & Hearn, S. J. (1997). Interaction between chemical reactions and mixing on various scales. *Chemical Engineering Science , 52* (4), 457-466.

Bhattacharya, S. (2005). Performance Improvement of Stirred Tank Reactors with Surface Feed, PhD Thesis, University of Alberta, Canada.

Clifford, M. J. (1999). A Gaussian model for reaction and diffusion in a lamellar structure. *Chemical Engineering Science , 54*, 303-310.

Clifford, M. J., & Cox, S. M. (1999). A simple model for a two-stage chemical reaction with diffusion. *IMA Journal of Applied Mathematics , 63*, 307-318.

Clifford, M. J., Cox, S. M., & Roberts, E. P. (1998a). The influence of segregation on the yield for a series-parallel reaction. *Chemical Engineering Science , 53*, 1791-1801.

Clifford, M. J., Cox, S. M., & Roberts, E. P. (1998b). Lamellar modelling of reaction, diffusion and mixing in a two-dimensional flow. *Chemical Engineering Journal , 71*, 49-56.

Clifford, M. J., Cox, S. M., & Roberts, E. P. (1999). Reaction and diffusion in a lamellar structure: the effect of the lamellar arrangement upon yield. *Physica A , 262*, 294-306.

Clifford, M. J., Cox, S. M., & Roberts, E. P. (2000). The influence of a lamellar structure upon the yield of a chemical reaction. *Trans IChemE , 78* (Part A), 371-377.

Cornell, S., & Droz, M. (1997). Exotic Reaction fronts in the steady state. *Physica D , 103*, 348-356.

Cox, S. M. (2004). Chaotic mixing of a competitive-consecutive reaction. *Physica D , 199*, 369-386.

Cox, S. M., & Finn, M. D. (2001). Behavior of the reaction front between initially segregated species in a two-stage reaction. *Physical Review E , 63*.

Cox, S. M., Clifford, M. J., & Roberts, E. P. (1998). A two-stage reaction with initially separated reactants. *Physica A , 256*, 65-86.

Danckwerts, P. V. (1953). The Definition and Measurement of Some Characteristics of Mixtures. *Applied Scientific Research* , *A3*, 279-296.

Danckwerts, P. V. (1958). The effect of incomplete mixing on homogeneous reactions. *Chemical Engineering Science*, *8*, 93-102.

Fogler, H. S. (1999). *Elements of Chemical Reaction Engineering* (3 ed.). Upper Saddle River, New Jersey, USA: Prentice Hall.

Fox, R. O. (1998). On the relationship between Lagrangian micromixing models and computational fluid dynamics. *Chemical Engineering and Processing , 37*, 521-535.

Fox, R. O. (2003). Computational models for turbulent reacting flows. Cambridge, U.K. : Cambridge University Press.

Hecht, I., & Taitelbaum, H. (2006). Perturbation analysis for competing reactions with initially separated components. *Physical Review E , 74*.

Levenspiel, O. (1972). *Chemical Reaction Engineering* (2 ed.). New York, New York, USA: Wiley.

Muzzio, F. J., & Liu, M. (1996). Chemical reactions in chaotic flows. *The Chemical Engineering Journal , 64*, 117-127.

Patterson, G. K., Paul, E. L., Kresta, S. M., & Etchells III, A. W. (2004). Mixing and Chemical Reactions. In E. L. Paul, V. A. Atiemo-Obeng, & S. M. Kresta (Eds.), *Handbook of Industrial Mixing - Science and Practice.* Hoboken, New Jersey, USA: Wiley.

Paul, E. L., Atiemo-Obeng, V. A., & Kresta, S. M. (Eds.). (2004). *Handbook of Industrial Mixing - Science and Practice.* Hoboken, New Jersey, USA: Wiley.

Sinder, M. (2002). Theory for competing reactions with initially separated components. *Physical Review E , 65*.

Sinder, M., Pelleg, J., Sokolovsky, V., Mecrovich, V. (2003). Competing reactions with initially separated components in the asymtotic time region. *Physical Review E*, *68*.

Taitelbaum, H., Vilensky, B., Lin, A., Yen, A., Koo, Y.-E. L., & Kopelman, R. (1996). Competing Reactions with Initially Separated Components. *Physical Review Letters , 77*, 1640-1643.

Van Vliet, E., Derksen, J. J., Van den Akker, H. E. A. (2001). Modelling of parallel competitive reactions in homogeneous turbulence using a filtered density function approach for large eddy simulations. *Proceedings of the 3rd Interational Symposium on Computational Techniques for Fluid/Thermal/Chemical Systems with Industrial Applications* , Atlanta, Georgia, USA.

Villermaux, J., & Falk, L. (1994). A Generalized Mixing Model for Initial Contacting of Reactive Fluids. *Chemical Engineering Science , 49* (24B), 5127-5140.

A

Appendix A

A.1 Summary

This Appendix includes all figures of results plotted for Chapter 3 with the tables of the corresponding Y_P data obtained from COMSOL. **Section A.2** includes all the Competitive-Consecutive reaction scheme figures and corresponding data. **Section A.3** includes all the Competitive-Parallel reaction scheme figures and corresponding data.

A.2 Competitive-Consecutive Reaction Scheme

A.2.1 Plots and data of Y_P versus Damkohler number with curves of the stoichiometry cases for different non-dimensional reaction rate ratios.

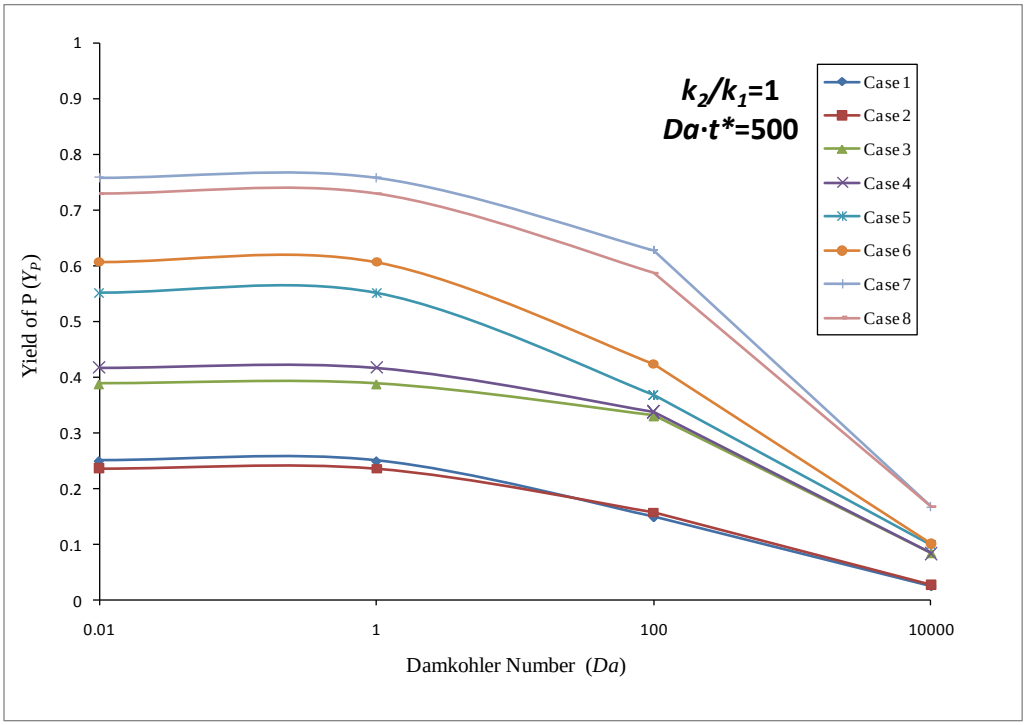

Figure A-1. Plot of Yield of *P* vs *Da* for k_2/k_1=1 at $Da \cdot t^*$=500 for C-C cases

Table A-1. Data for Yield of *P* vs *Da* for k_2/k_1=1 at $Da \cdot t^*$=500 for C-C cases

$k_2/k_1 = 1$ $Da \cdot t^* = 500$

Yield of *P*

Da	**0.01**	**1**	**100**	**10000**
Case 1	0.249963	0.249711	0.14922	0.024851
Case 2	0.235999	0.235911	0.157405	0.026988
Case 3	0.388095	0.388004	0.33079	0.084261
Case 4	0.417059	0.41684	0.33762	0.083383
Case 5	0.550825	0.550456	0.367454	0.098157
Case 6	0.606914	0.606508	0.423812	0.101564
Case 7	0.758424	0.758376	0.627822	0.167712
Case 8	0.728555	0.728506	0.586622	0.168112

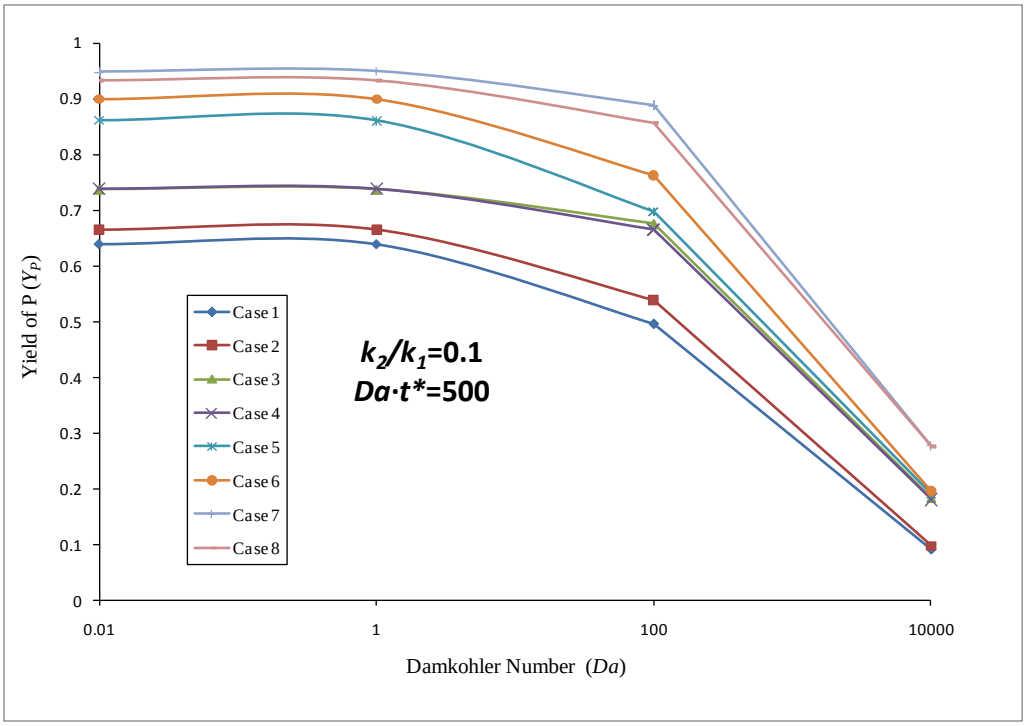

Figure A-2. Plot of Yield of *P* vs *Da* for k_2/k_1=0.1 at *Da*·*t**=500 for C-C cases

Table A-2. Data for Yield of *P* vs *Da* for k_2/k_1=0.1 at *Da*·*t**=500 for C-C cases

k_2/k_1 = 0.1 **Da·t* = 500**

Yield of *P*

Da	**0.01**	**1**	**100**	**10000**
Case 1	0.639787	0.639525	0.496778	0.09228
Case 2	0.664954	0.665156	0.538323	0.097642
Case 3	0.73741	0.737319	0.67567	0.183469
Case 4	0.737926	0.737867	0.664878	0.181215
Case 5	0.860791	0.860663	0.697308	0.191248
Case 6	0.899378	0.899307	0.762701	0.196048
Case 7	0.9478932	0.948907	0.887687	0.277811
Case 8	0.932667	0.932597	0.856184	0.276192

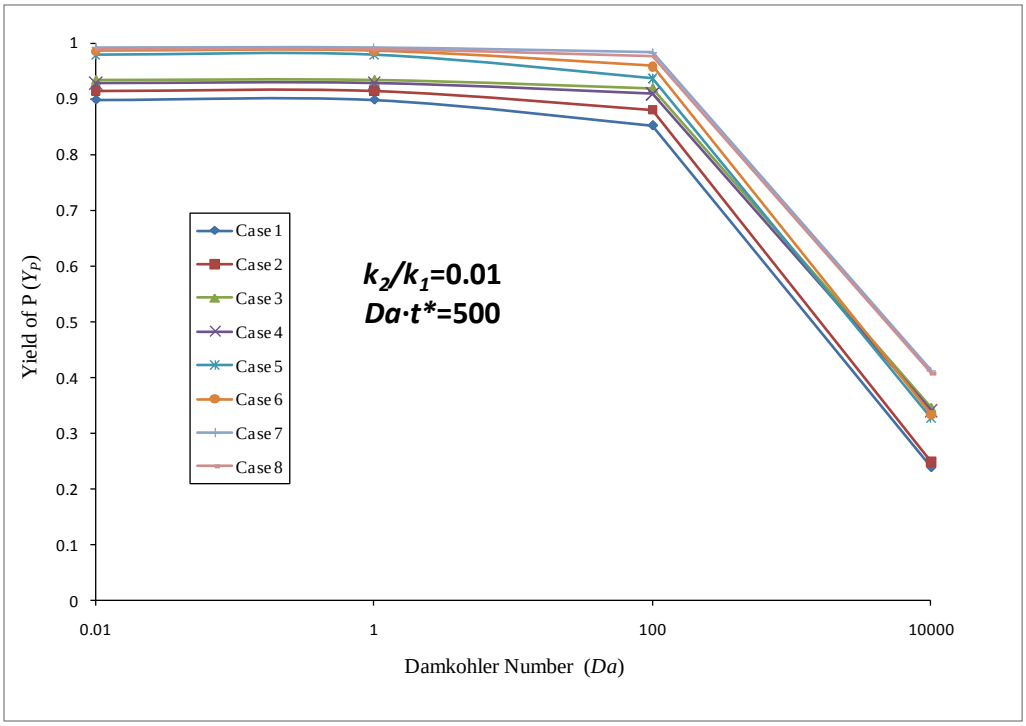

Figure A-3. Plot of Yield of *P* vs *Da* for k_2/k_1=0.01 at *Da*·*t**=500 for C-C cases

Table A-3. Data for Yield of *P* vs *Da* for k_2/k_1=0.01 at *Da*·*t**=500 for C-C cases

k_2/k_1 = 0.01 *Da*·*t = 500**

Yield of *P*

Da	**0.01**	**1**	**100**	**10000**
Case 1	0.897284	0.897207	0.851133	0.239003
Case 2	0.914385	0.91439	0.880128	0.248073
Case 3	0.933045	0.933027	0.917807	0.345446
Case 4	0.927368	0.927491	0.908424	0.340221
Case 5	0.977843	0.977854	0.935599	0.326346
Case 6	0.985152	0.985142	0.958186	0.333472
Case 7	0.991068	0.991066	0.982766	0.411861
Case 8	0.989124	0.989115	0.976673	0.407097

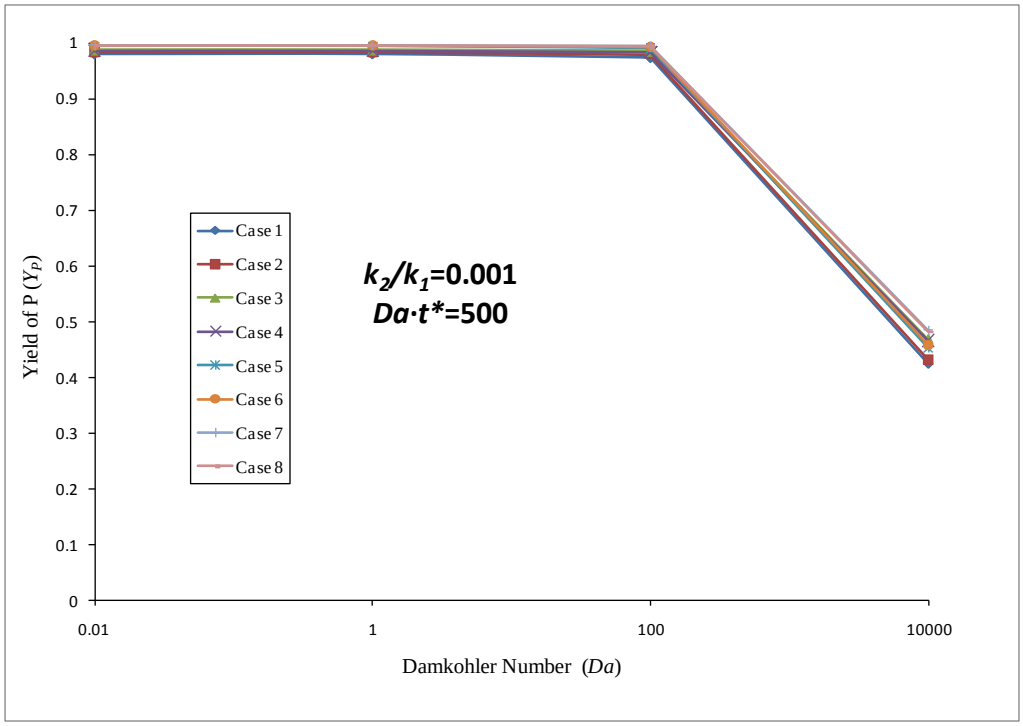

Figure A-4. Plot of Yield of *P* vs *Da* for k_2/k_1=0.001 at *Da*·*t**=500 for C-C cases

Table A-4. Data for Yield of *P* vs *Da* for k_2/k_1=0.001 at *Da*·*t**=500 for C-C cases

k_2/k_1 = 0.001 *Da*·*t = 500**

Yield of *P*

Da	**0.01**	**1**	**100**	**10000**
Case 1	0.979887	0.979874	0.973593	0.424367
Case 2	0.983928	0.983916	0.979649	0.431537
Case 3	0.986885	0.986899	0.984904	0.468575
Case 4	0.985424	0.98544	0.982962	0.466019
Case 5	0.994477	0.994481	0.990553	0.452073
Case 6	0.99502	0.995013	0.992593	0.457815
Case 7	0.995513	0.995525	0.994617	0.484262
Case 8	0.995346	0.995359	0.994164	0.482465

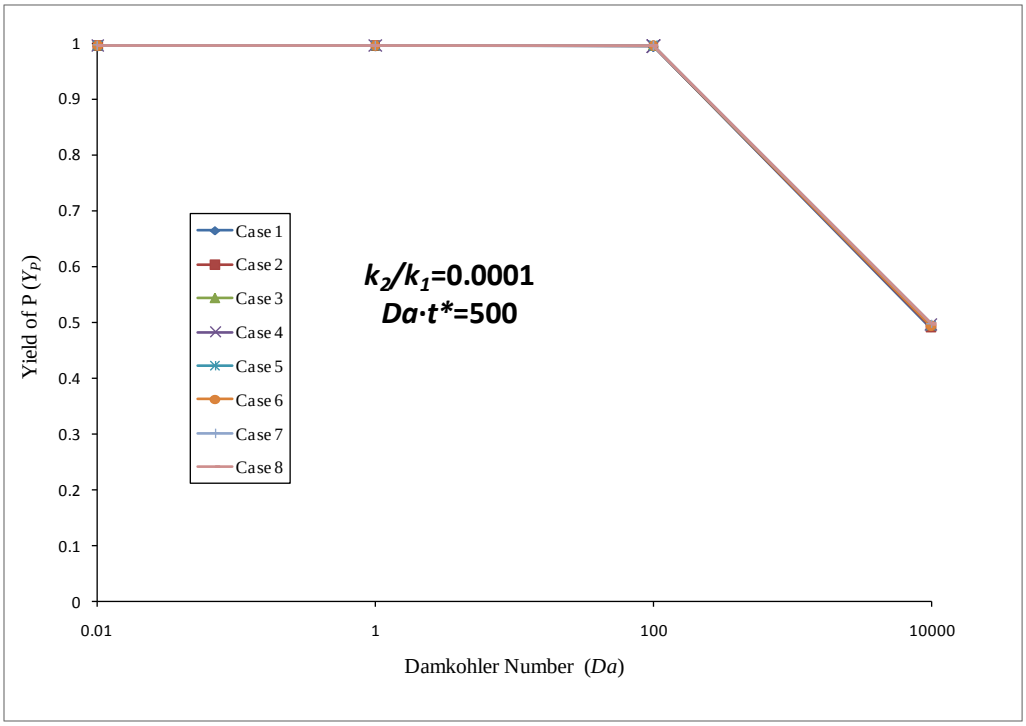

Figure A-5. Plot of Yield of *P* vs *Da* for k_2/k_1=0.0001 at *Da*·*t**=500 for C-C cases

Table A-5. Data for Yield of *P* vs *Da* for k_2/k_1=0.0001 at *Da*·*t**=500 for C-C cases

k_2/k_1 = 0.0001 *Da*·*t = 500**

Yield of *P*

Da	**0.01**	**1**	**100**	**10000**
Case 1	0.9943	0.994312	0.993629	0.489204
Case 2	0.994708	0.99472	0.994189	0.490376
Case 3	0.99503	0.995042	0.994721	0.495172
Case 4	0.994857	0.994869	0.994508	0.494831
Case 5	0.995857	0.995869	0.995411	0.492587
Case 6	0.995906	0.995919	0.995573	0.493571
Case 7	0.995956	0.995969	0.995763	0.496988
Case 8	0.99594	0.995953	0.995721	0.496765

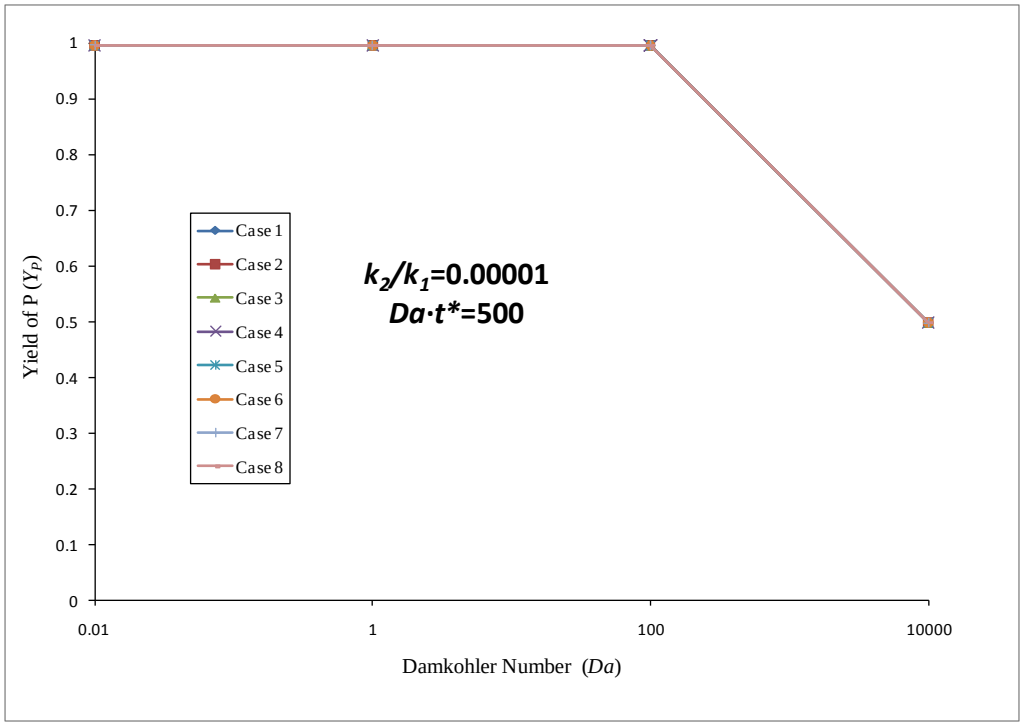

Figure A-6. Plot of Yield of *P* vs *Da* for k_2/k_1=0.00001 at $Da \cdot t^*$=500 for C-C cases

Table A-6. Data for Yield of *P* vs *Da* for k_2/k_1=0.00001 at $Da \cdot t^*$=500 for C-C cases

k_2/k_1 = 0.00001 $Da \cdot t^*$ = 500

Yield of *P*

Da	**0.01**	**1**	**100**	**10000**
Case 1	0.995834	0.995847	0.995665	0.497568
Case 2	0.995875	0.995888	0.995719	0.497694
Case 3	0.995907	0.99592	0.995772	0.498185
Case 4	0.99589	0.995902	0.995751	0.498149
Case 5	0.995991	0.996004	0.995843	0.497913
Case 6	0.995996	0.996009	0.995858	0.49802
Case 7	0.996001	0.996014	0.995877	0.498369
Case 8	0.995999	0.996012	0.995873	0.498346

A.2.2 Plots and data of Y_P versus Damkohler number with curves of non-dimensional reaction rate ratios for individual stoichiometry cases.

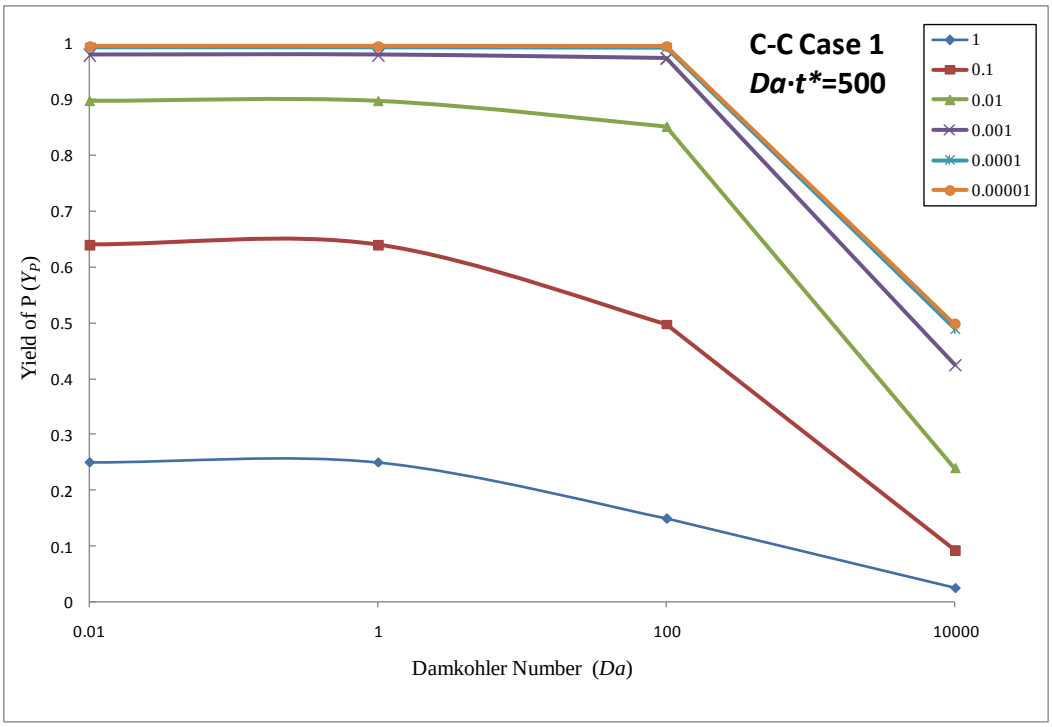

Figure A-7. Plot of Yield of *P* vs *Da* for C-C Case 1 for all k_2/k_1 at $Da \cdot t^*$=500

Table A-7. Data for Yield of *P* vs *Da* for C-C Case 1 for all k_2/k_1 at $Da \cdot t^*$=500

C-C Case 1 $Da \cdot t^* = 500$

Yield of *P*

k_2/k_1	*Da*	0.01	1	100	10000
1		0.249963	0.249711	0.14922	0.024851
0.1		0.639787	0.639525	0.496778	0.09228
0.01		0.897284	0.897207	0.851133	0.239003
0.001		0.979887	0.979874	0.973593	0.424367
0.0001		0.9943	0.994312	0.993629	0.489204
0.00001		0.995834	0.995847	0.995665	0.497568

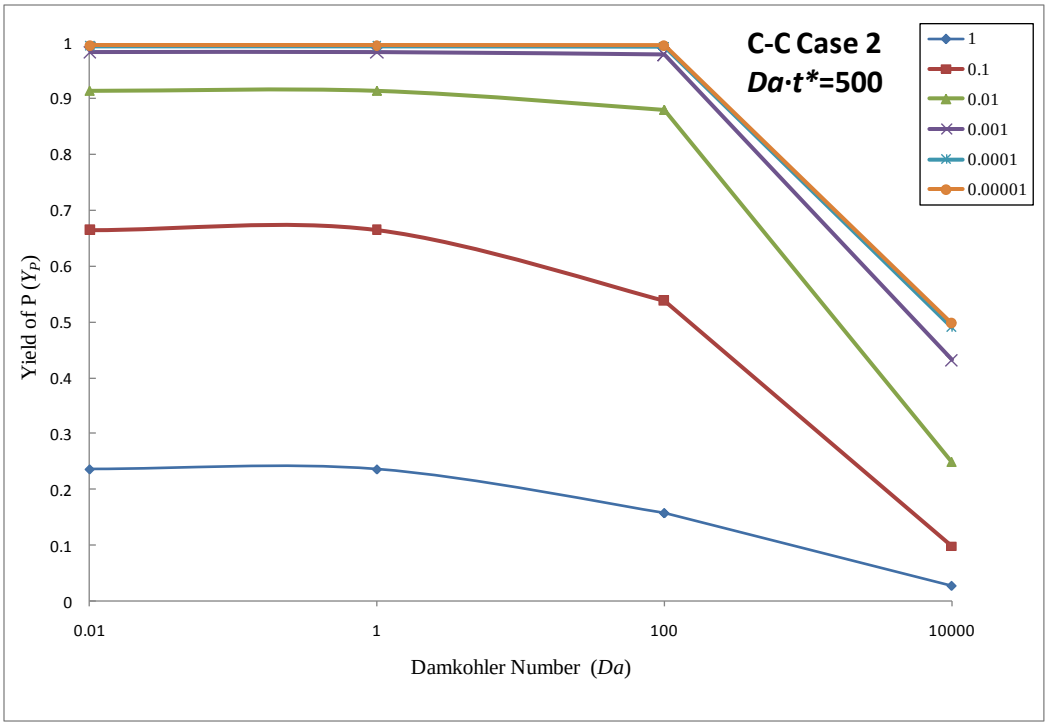

Figure A-8. Plot of Yield of *P* vs *Da* for C-C Case 2 for all k_2/k_1 at $Da \cdot t^*$=500

Table A-8. Data for Yield of *P* vs *Da* for C-C Case 2 for all k_2/k_1 at $Da \cdot t^*$=500

C-C Case 2 $Da \cdot t^* = 500$

Yield of *P*

k_2/k_1	*Da*	0.01	1	100	10000
1		0.235999	0.235911	0.157405	0.026988
0.1		0.664954	0.665156	0.538323	0.097642
0.01		0.914385	0.91439	0.880128	0.248073
0.001		0.983928	0.983916	0.979649	0.431537
0.0001		0.994708	0.99472	0.994189	0.490376
0.00001		0.995875	0.995888	0.995719	0.497694

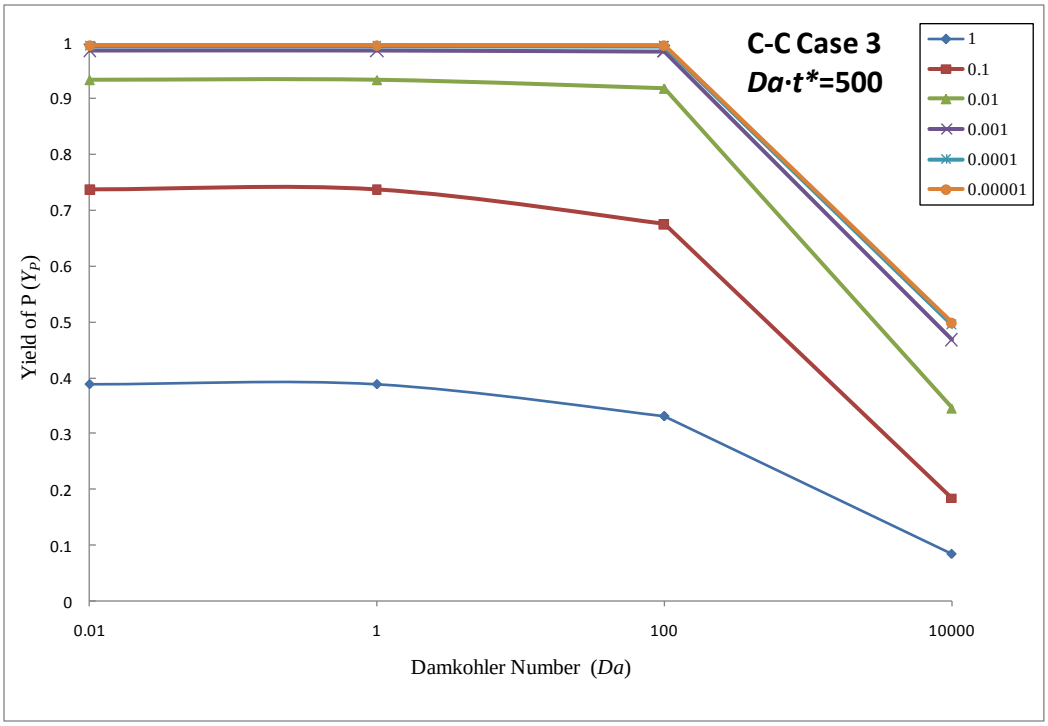

Figure A-9. Plot of Yield of *P* vs *Da* for C-C Case 3 for all k_2/k_1 at $Da \cdot t^*$=500

Table A-9. Data for Yield of *P* vs *Da* for C-C Case 3 for all k_2/k_1 at $Da \cdot t^*$=500

C-C Case 3 $Da \cdot t^* = 500$

Yield of *P*

k_2/k_1	*Da*	0.01	1	100	10000
1		0.388095	0.388004	0.33079	0.084261
0.1		0.73741	0.737319	0.67567	0.183469
0.01		0.933045	0.933027	0.917807	0.345446
0.001		0.986885	0.986899	0.984904	0.468575
0.0001		0.99503	0.995042	0.994721	0.495172
0.00001		0.995907	0.99592	0.995772	0.498185

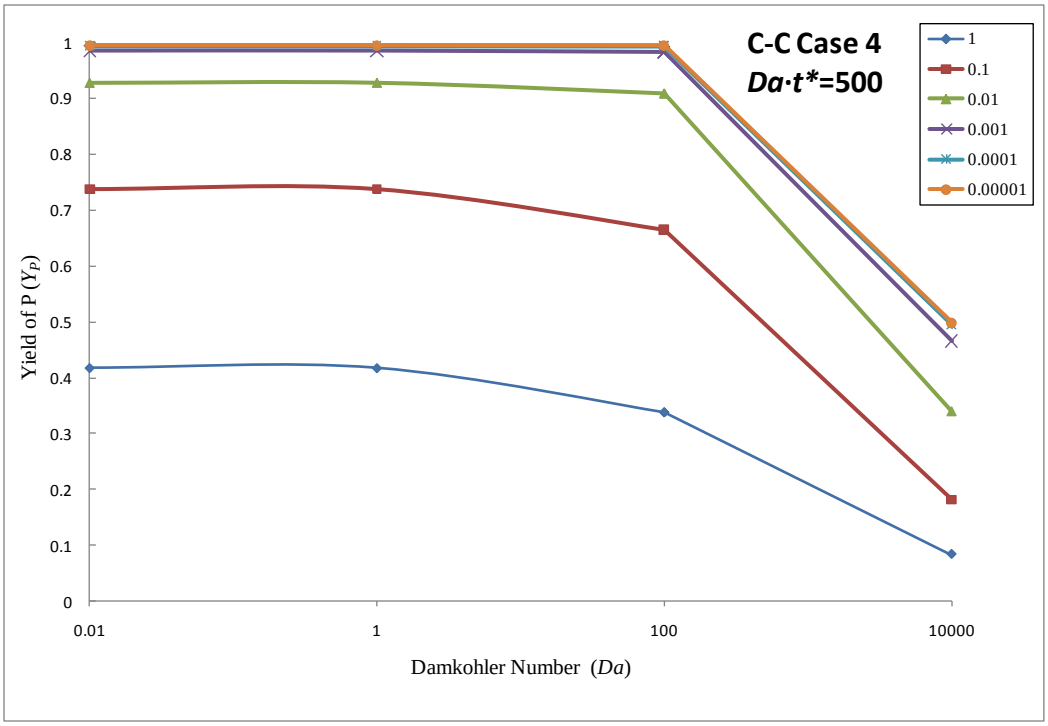

Figure A-10. Plot of Yield of *P* vs *Da* for C-C Case 4 for all k_2/k_1 at $Da \cdot t^*$=500

Table A-10. Data for Yield of *P* vs *Da* for C-C Case 4 for all k_2/k_1 at $Da \cdot t^*$=500

C-C Case 4 $Da \cdot t^* = 500$

Yield of *P*

k_2/k_1	*Da*	0.01	1	100	10000
1		0.417059	0.41684	0.33762	0.083383
0.1		0.737926	0.737867	0.664878	0.181215
0.01		0.927368	0.927491	0.908424	0.340221
0.001		0.985424	0.98544	0.982962	0.466019
0.0001		0.994857	0.994869	0.994508	0.494831
0.00001		0.99589	0.995902	0.995751	0.498149

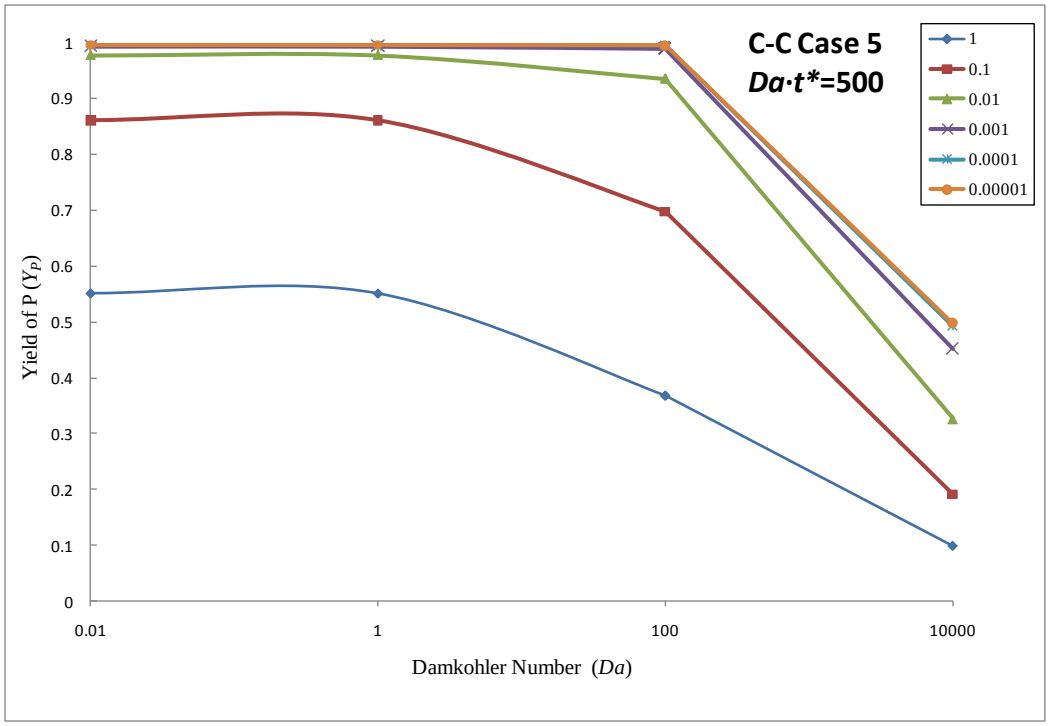

Figure A-11. Plot of Yield of *P* vs *Da* for C-C Case 5 for all k_2/k_1 at $Da \cdot t^*$=500

Table A-11. Data for Yield of *P* vs *Da* for C-C Case 5 for all k_2/k_1 at $Da \cdot t^*$=500

C-C Case 5 $Da \cdot t^* = 500$

Yield of *P*

k_2/k_1	*Da*	0.01	1	100	10000
1		0.550825	0.550456	0.367454	0.098157
0.1		0.860791	0.860663	0.697308	0.191248
0.01		0.977843	0.977854	0.935599	0.326346
0.001		0.994477	0.994481	0.990553	0.452073
0.0001		0.995857	0.995869	0.995411	0.492587
0.00001		0.995991	0.996004	0.995843	0.497913

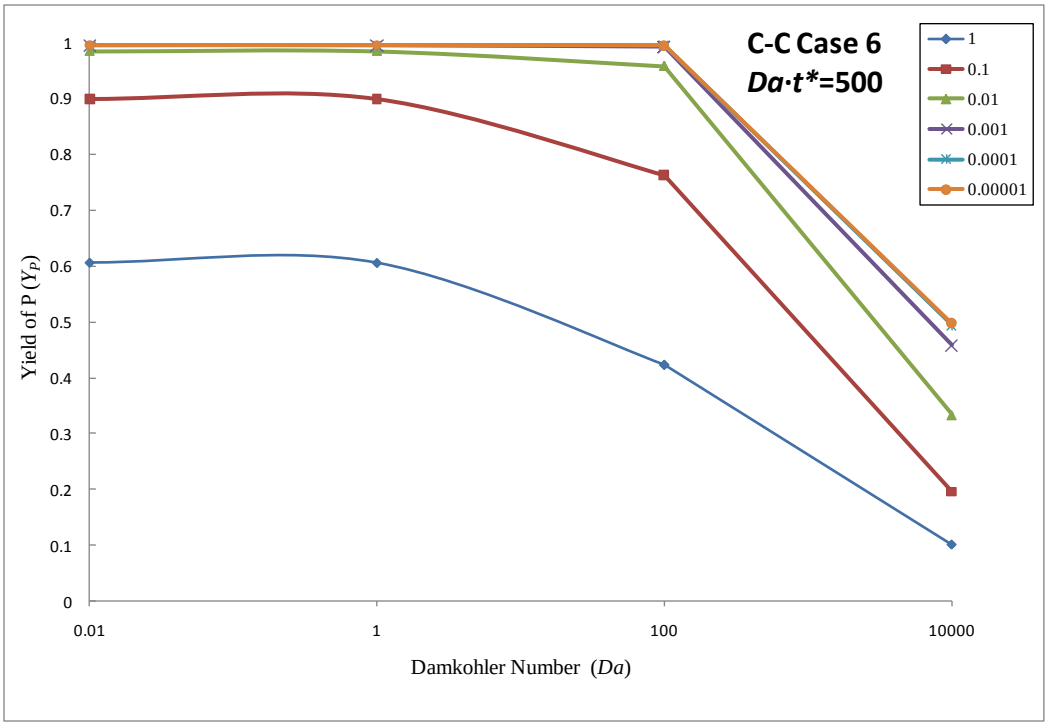

Figure A-12. Plot of Yield of *P* vs *Da* for C-C Case 6 for all k_2/k_1 at $Da \cdot t^*$=500

Table A-12. Data for Yield of *P* vs *Da* for C-C Case 6 for all k_2/k_1 at $Da \cdot t^*$=500

C-C Case 6 $Da \cdot t^* = 500$

Yield of *P*

k_2/k_1	*Da*	0.01	1	100	10000
1		0.606914	0.606508	0.423812	0.101564
0.1		0.899378	0.899307	0.762701	0.196048
0.01		0.985152	0.985142	0.958186	0.333472
0.001		0.99502	0.995013	0.992593	0.457815
0.0001		0.995906	0.995919	0.995573	0.493571
0.00001		0.995996	0.996009	0.995858	0.49802

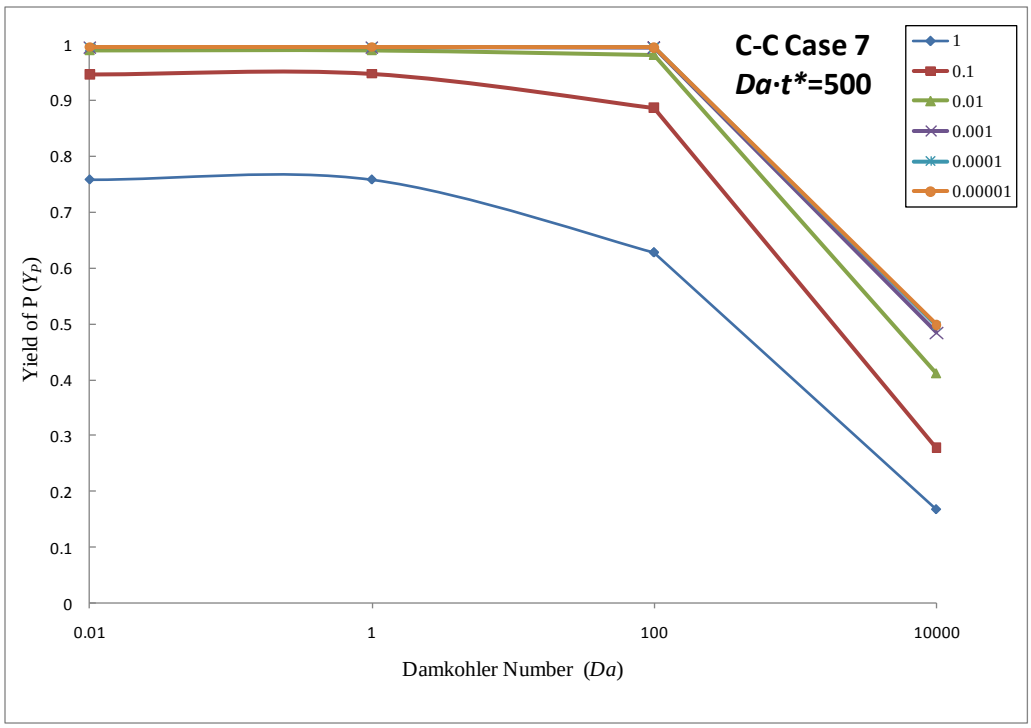

Figure A-13. Plot of Yield of *P* vs *Da* for C-C Case 7 for all k_2/k_1 at $Da \cdot t^*$=500

Table A-13. Data for Yield of *P* vs *Da* for C-C Case 7 for all k_2/k_1 at $Da \cdot t^*$=500

C-C Case 7 $Da \cdot t^* = 500$

Yield of *P*

k_2/k_1	*Da*	0.01	1	100	10000
1		0.758424	0.758376	0.627822	0.167712
0.1		0.947893	0.948907	0.887687	0.277811
0.01		0.991068	0.991066	0.982766	0.411861
0.001		0.995513	0.995525	0.994617	0.484262
0.0001		0.995956	0.995969	0.995763	0.496988
0.00001		0.996001	0.996014	0.995877	0.498369

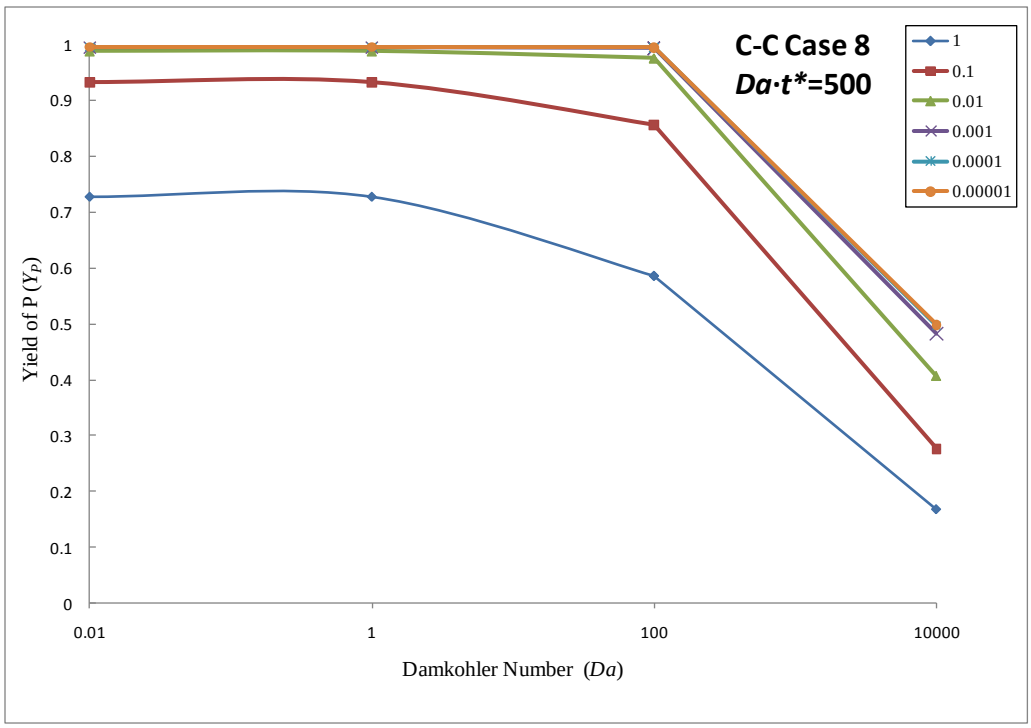

Figure A-14. Plot of Yield of *P* vs *Da* for C-C Case 8 for all k_2/k_1 at $Da \cdot t^*$=500

Table A-14. Data for Yield of *P* vs *Da* for C-C Case 8 for all k_2/k_1 at $Da \cdot t^*$=500

C-C Case 8 $Da \cdot t^* = 500$

Yield of *P*

k_2/k_1	*Da*	0.01	1	100	10000
1		0.728555	0.728506	0.586622	0.168112
0.1		0.932667	0.932597	0.856184	0.276192
0.01		0.989124	0.989115	0.976673	0.407097
0.001		0.995346	0.995359	0.994164	0.482465
0.0001		0.99594	0.995953	0.995721	0.496765
0.00001		0.995999	0.996012	0.995873	0.498346

A.2.3 Plots and data of Y_P versus non-dimensional reaction rate ratio with curves of the stoichiometry cases for different Damkohler numbers.

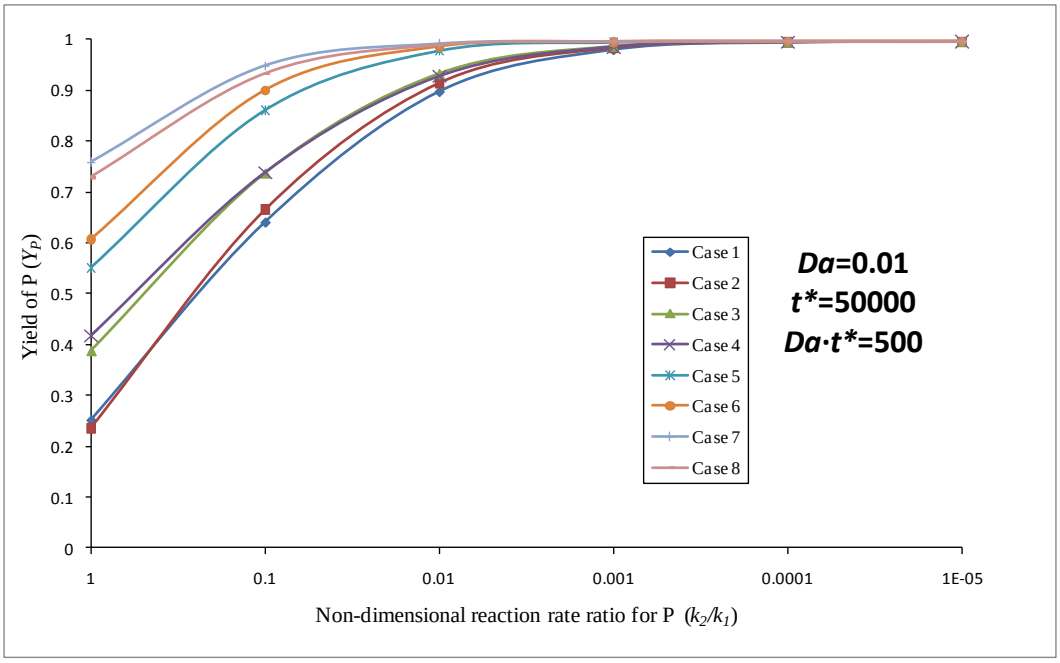

Figure A-15. Plot of Yield of *P* vs k_2/k_1 for *Da*=0.01 at *Da*·*t**=500 for C-C cases

Table A-15. Data for Yield of *P* vs k_2/k_1 for *Da*=0.01 at *Da*·*t**=500 for C-C cases

***Da* = 0.01** ***t**= 50000** ***Da*·*t**= 500**

Yield of *P*

k_2/k_1	1	0.1	0.01	0.001	0.0001	0.00001
Case 1	0.249963	0.639787	0.897284	0.979887	0.9943	0.995834
Case 2	0.235999	0.664954	0.914385	0.983928	0.994708	0.995875
Case 3	0.388095	0.73741	0.933045	0.986885	0.99503	0.995907
Case 4	0.417059	0.737926	0.927368	0.985424	0.994857	0.99589
Case 5	0.550825	0.860791	0.977843	0.994477	0.995857	0.995991
Case 6	0.606914	0.899378	0.985152	0.99502	0.995906	0.995996
Case 7	0.758424	0.9478932	0.991068	0.995513	0.995956	0.996001
Case 8	0.728555	0.932667	0.989124	0.995346	0.99594	0.995999

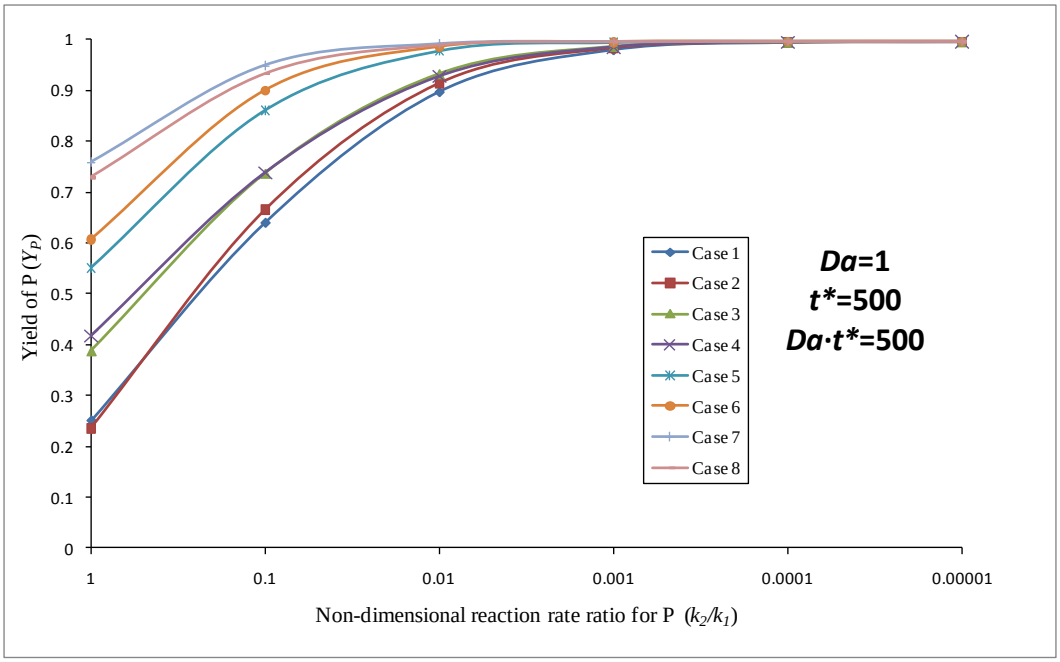

Figure A-16. Plot of Yield of *P* vs k_2/k_1 for *Da*=1 at *Da*·*t**=500 for C-C cases

Table A-16. Data for Yield of *P* vs k_2/k_1 for *Da*=1 at *Da*·*t**=500 for C-C cases

***Da* = 1** ***t** = 500** ***Da*·*t** = 500**

Yield of *P*

k_2/k_1	1	0.1	0.01	0.001	0.0001	0.00001
Case 1	0.249711	0.639525	0.897207	0.979874	0.994312	0.995847
Case 2	0.235911	0.665156	0.91439	0.983916	0.99472	0.995888
Case 3	0.388004	0.737319	0.933027	0.986899	0.995042	0.99592
Case 4	0.41684	0.737867	0.927491	0.98544	0.994869	0.995902
Case 5	0.550456	0.860663	0.977854	0.994481	0.995869	0.996004
Case 6	0.606508	0.899307	0.985142	0.995013	0.995919	0.996009
Case 7	0.758376	0.948907	0.991066	0.995525	0.995969	0.996014
Case 8	0.728506	0.932597	0.989115	0.995359	0.995953	0.996012

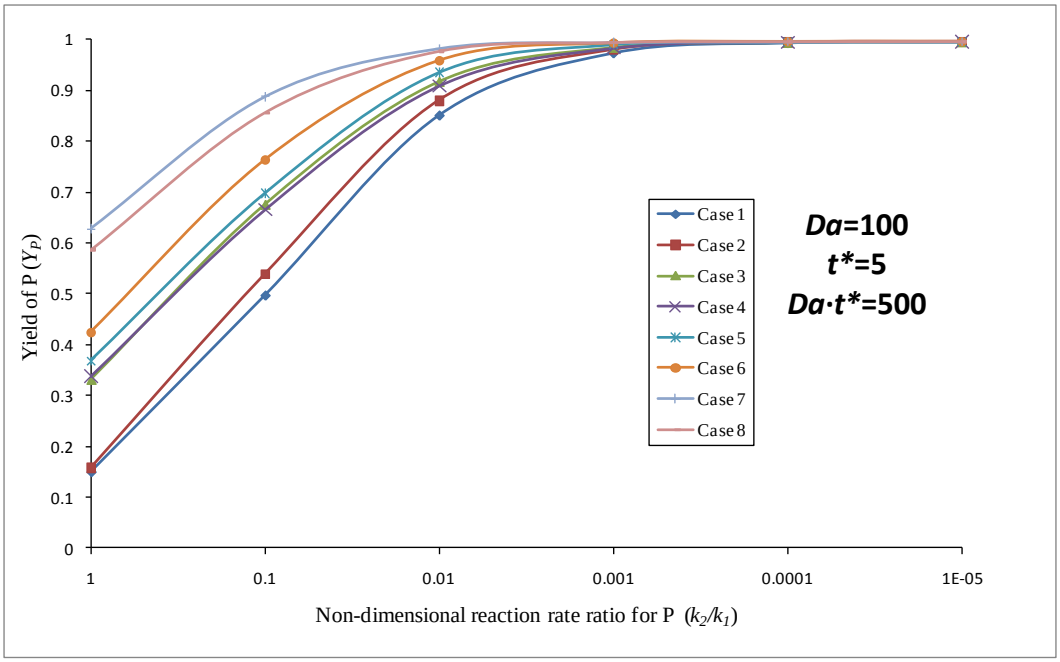

Figure A-17. Plot of Yield of *P* vs k_2/k_1 for *Da*=100 at *Da*·*t**=500 for C-C cases

Table A-17. Data for Yield of *P* vs k_2/k_1 for *Da*=100 at *Da*·*t**=500 for C-C cases

***Da* = 100** ***t**= 5* ***Da*·*t**= 500**

Yield of *P*

k_2/k_1	1	0.1	0.01	0.001	0.0001	0.00001
Case 1	0.14922	0.496778	0.851133	0.973593	0.993629	0.995665
Case 2	0.157405	0.538323	0.880128	0.979649	0.994189	0.995719
Case 3	0.33079	0.67567	0.917807	0.984904	0.994721	0.995772
Case 4	0.33762	0.664878	0.908424	0.982962	0.994508	0.995751
Case 5	0.367454	0.697308	0.935599	0.990553	0.995411	0.995843
Case 6	0.423812	0.762701	0.958186	0.992593	0.995573	0.995858
Case 7	0.627822	0.887687	0.982766	0.994617	0.995763	0.995877
Case 8	0.586622	0.856184	0.976673	0.994164	0.995721	0.995873

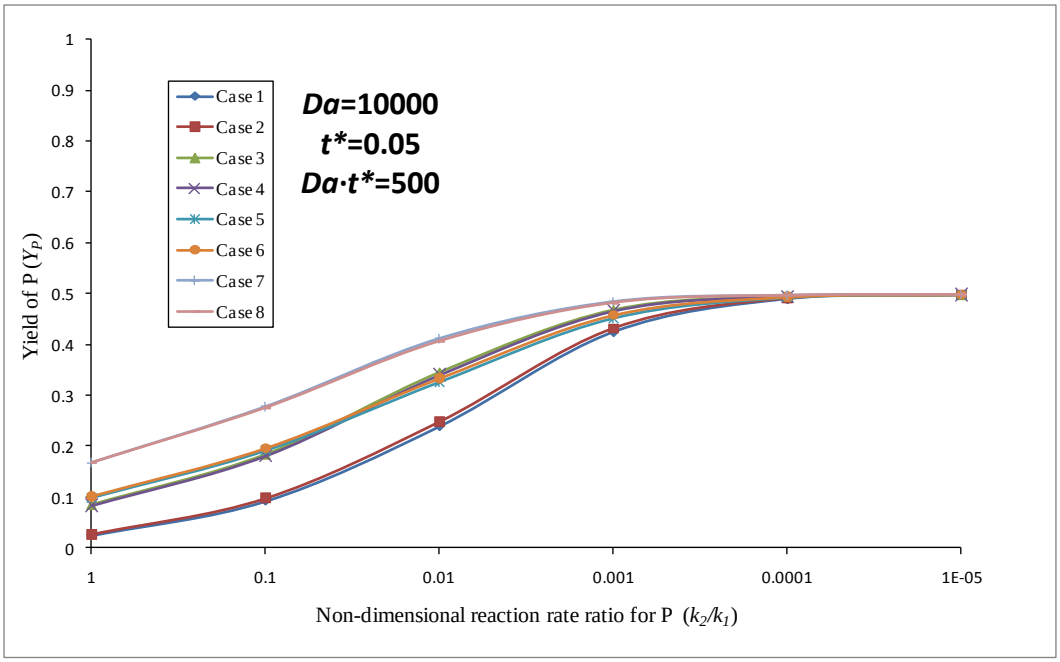

Figure A-18. Plot of Yield of *P* vs k_2/k_1 for *Da*=10000 at *Da*·*t**=500 for C-C cases

Table A-18. Data for Yield of *P* vs k_2/k_1 for *Da*=10000 at *Da*·*t**=500 for C-C cases

***Da* = 10000 *t** = 0.05 *Da*·*t** = 500**

Yield of *P*

k_2/k_1	1	0.1	0.01	0.001	0.0001	0.00001
Case 1	0.024851	0.09228	0.239003	0.424367	0.489204	0.497568
Case 2	0.026988	0.097642	0.248073	0.431537	0.490376	0.497694
Case 3	0.084261	0.183469	0.345446	0.468575	0.495172	0.498185
Case 4	0.083383	0.181215	0.340221	0.466019	0.494831	0.498149
Case 5	0.098157	0.191248	0.326346	0.452073	0.492587	0.497913
Case 6	0.101564	0.196048	0.333472	0.457815	0.493571	0.49802
Case 7	0.167712	0.277811	0.411861	0.484262	0.496988	0.498369
Case 8	0.168112	0.276192	0.407097	0.482465	0.496765	0.498346

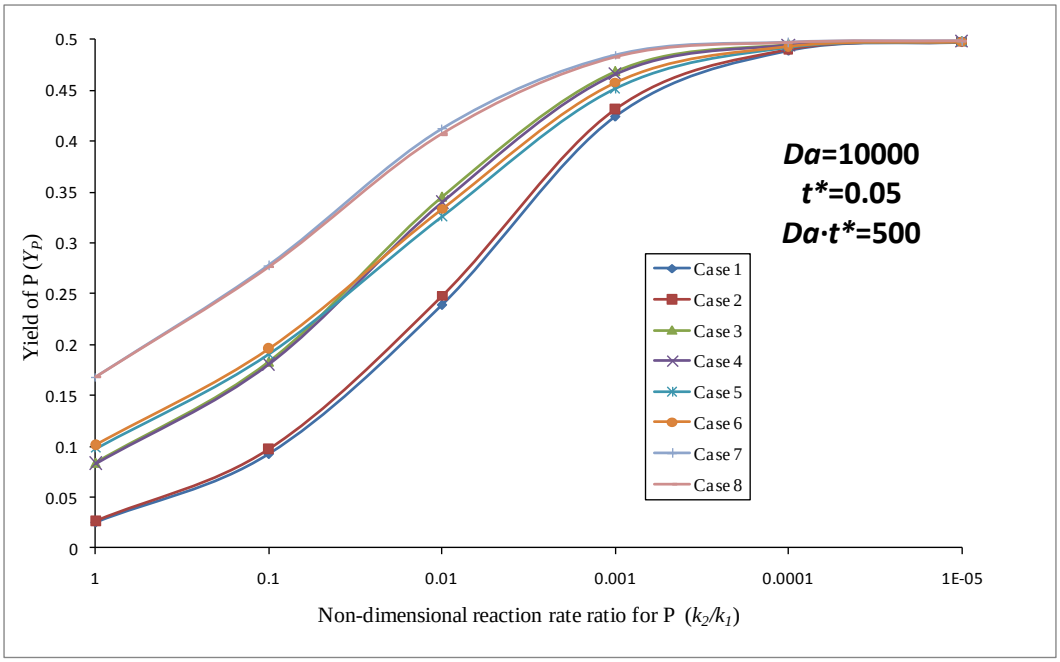

Figure A-19. Plot of Yield of *P* vs k_2/k_1 for *Da*=10000 at *Da*·*t**=500 for C-C cases with Y_P axis going only to 0.5

Table A-19. Data for Yield of *P* vs k_2/k_1 for *Da*=10000 at *Da*·*t**=500 for C-C cases with Y_P axis going only to 0.5

***Da* = 10000 *t** = 0.05 *Da*·*t** = 500**

Yield of *P*

k_2/k_1	1	0.1	0.01	0.001	0.0001	0.00001
Case 1	0.024851	0.09228	0.239003	0.424367	0.489204	0.497568
Case 2	0.026988	0.097642	0.248073	0.431537	0.490376	0.497694
Case 3	0.084261	0.183469	0.345446	0.468575	0.495172	0.498185
Case 4	0.083383	0.181215	0.340221	0.466019	0.494831	0.498149
Case 5	0.098157	0.191248	0.326346	0.452073	0.492587	0.497913
Case 6	0.101564	0.196048	0.333472	0.457815	0.493571	0.49802
Case 7	0.167712	0.277811	0.411861	0.484262	0.496988	0.498369
Case 8	0.168112	0.276192	0.407097	0.482465	0.496765	0.498346

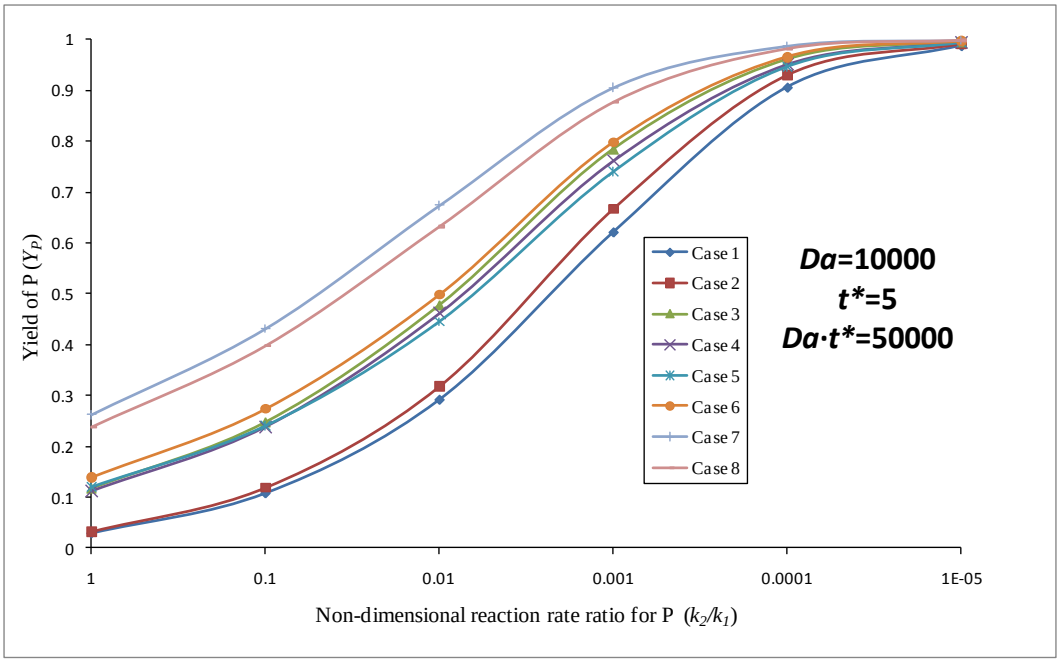

Figure A-20. Plot of Yield of *P* vs k_2/k_1 for *Da*=10000 at *Da*·*t**=50000 for C-C cases

Table A-20. Data for Yield of *P* vs k_2/k_1 for *Da*=10000 at *Da*·*t**=50000 for C-C cases

***Da* = 10000** ***t** = 5** ***Da*·*t** = 50000**

Yield of *P*

k_2/k_1	1	0.1	0.01	0.001	0.0001	0.00001
Case 1	0.028499	0.107265	0.291422	0.621006	0.906043	0.987718
Case 2	0.032119	0.118645	0.317798	0.667117	0.930252	0.991616
Case 3	0.116416	0.246822	0.47728	0.784174	0.960497	0.995482
Case 4	0.11228	0.238653	0.461476	0.761209	0.950781	0.994066
Case 5	0.119554	0.239844	0.445205	0.739948	0.946514	0.993814
Case 6	0.139685	0.273998	0.498485	0.798072	0.9657	0.996258
Case 7	0.261931	0.431196	0.673557	0.905328	0.987231	0.998671
Case 8	0.23845	0.397939	0.632099	0.876415	0.981336	0.998012

A.2.4 Plots and data of Y_P versus non-dimensional reaction rate ratio with curves of Damkohler numbers for individual stoichiometry cases.

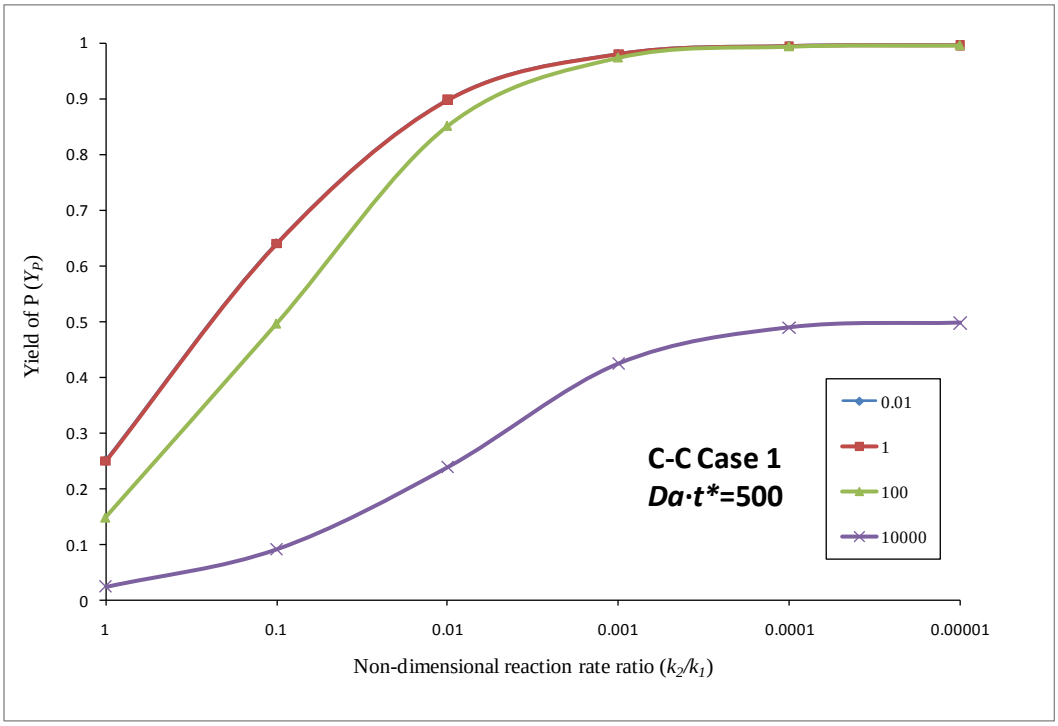

Figure A-21. Plot of Yield of *P* vs k_2/k_1 for C-C Case 1 for all *Da* at *Da*·*t**=500

Table A-21. Data for Yield of *P* vs k_2/k_1 for C-C Case 1 for all *Da* at *Da*·*t**=500

C-C Case 1 *Da*·*t = 500**

Yield of *P*

Da	k_2/k_1	1	0.1	0.01	0.001	0.0001	0.00001
0.01		0.249963	0.639787	0.897284	0.979887	0.9943	0.995834
1		0.249711	0.639525	0.897207	0.979874	0.994312	0.995847
100		0.14922	0.496778	0.851133	0.973593	0.993629	0.995665
10000		0.024851	0.09228	0.239003	0.424367	0.489204	0.497568

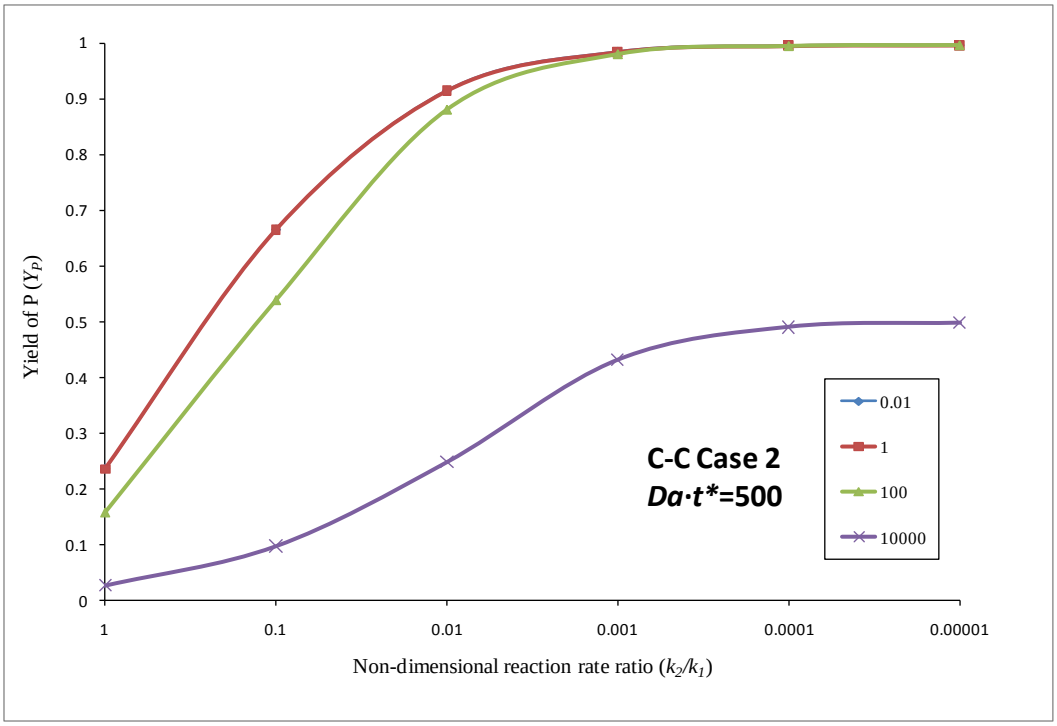

Figure A-22. Plot of Yield of *P* vs k_2/k_1 for C-C Case 2 for all *Da* at *Da*·*t**=500

Table A-22. Data for Yield of *P* vs k_2/k_1 for C-C Case 2 for all *Da* at *Da*·*t**=500

C-C Case 2 *Da*·*t = 500**

Yield of *P*

Da	k_2/k_1	**1**	**0.1**	**0.01**	**0.001**	**0.0001**	**0.00001**
0.01		0.235999	0.664954	0.914385	0.983928	0.994708	0.995875
1		0.235911	0.665156	0.91439	0.983916	0.99472	0.995888
100		0.157405	0.538323	0.880128	0.979649	0.994189	0.995719
10000		0.026988	0.097642	0.248073	0.431537	0.490376	0.497694

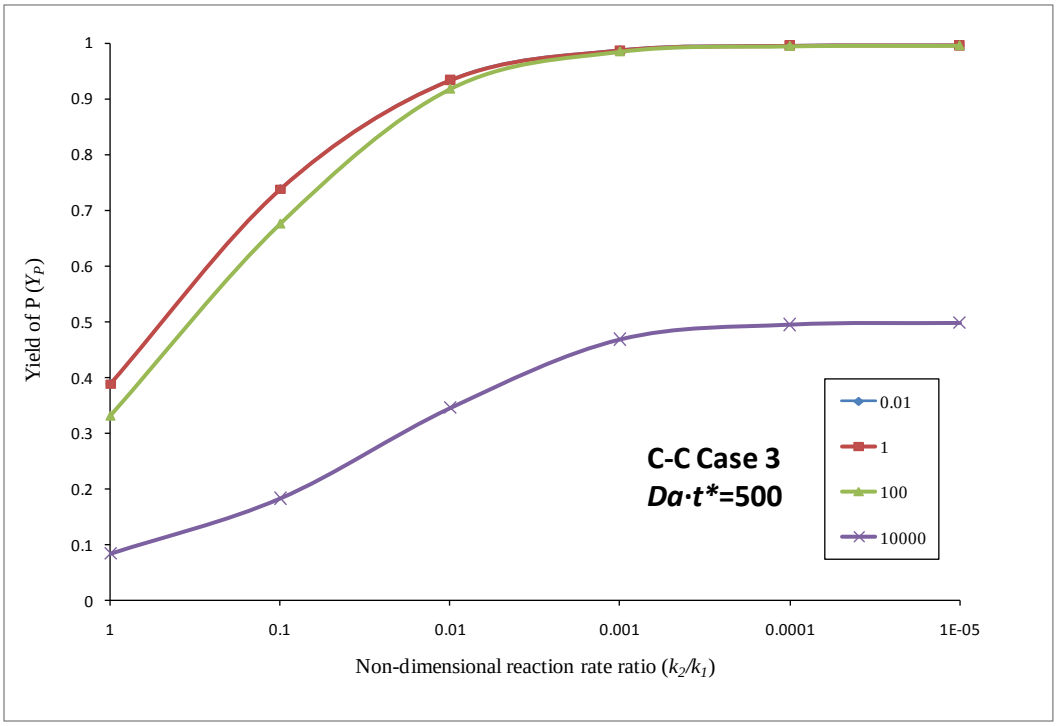

Figure A-23. Plot of Yield of *P* vs k_2/k_1 for C-C Case 3 for all *Da* at *Da*·*t**=500

Table A-23. Data for Yield of *P* vs k_2/k_1 for C-C Case 3 for all *Da* at *Da*·*t**=500

C-C Case 3 *Da*·*t = 500**

Yield of *P*

Da	k_2/k_1	**1**	**0.1**	**0.01**	**0.001**	**0.0001**	**0.00001**
0.01		0.388095	0.73741	0.933045	0.986885	0.99503	0.995907
1		0.388004	0.737319	0.933027	0.986899	0.995042	0.99592
100		0.33079	0.67567	0.917807	0.984904	0.994721	0.995772
10000		0.084261	0.183469	0.345446	0.468575	0.495172	0.498185

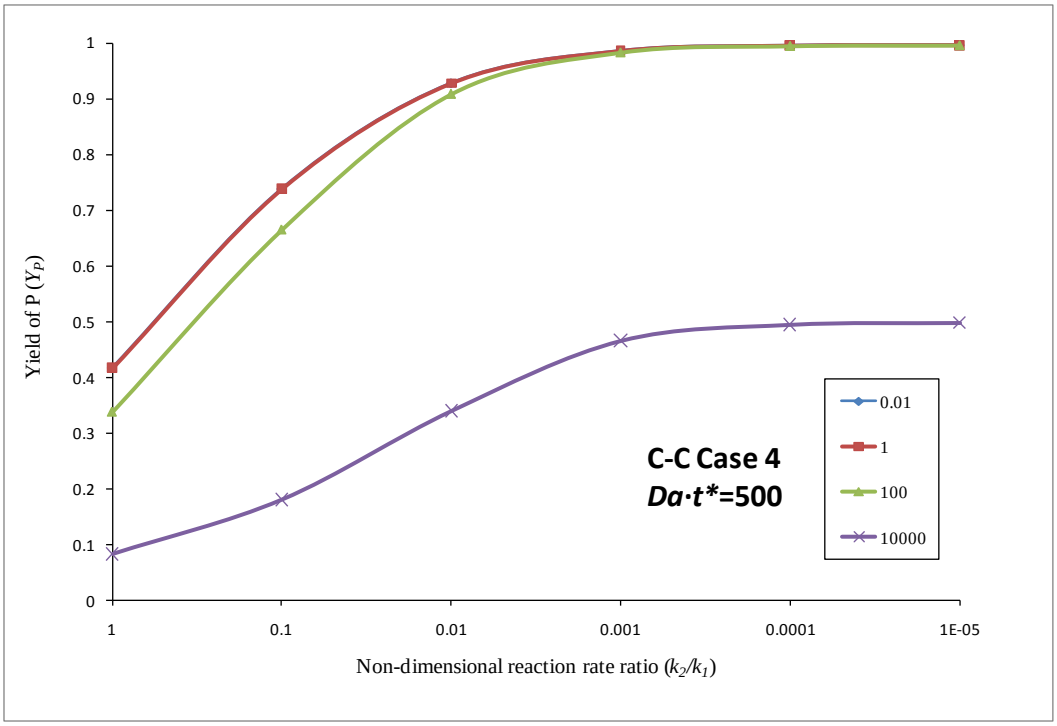

Figure A-24. Plot of Yield of *P* vs k_2/k_1 for C-C Case 4 for all *Da* at $Da \cdot t^*$=500

Table A-24. Data for Yield of *P* vs k_2/k_1 for C-C Case 4 for all *Da* at $Da \cdot t^*$=500

C-C Case 4 $Da \cdot t^* = 500$

Yield of *P*

Da	**k_2/k_1**	**1**	**0.1**	**0.01**	**0.001**	**0.0001**	**0.00001**
0.01		0.417059	0.737926	0.927368	0.985424	0.994857	0.99589
1		0.41684	0.737867	0.927491	0.98544	0.994869	0.995902
100		0.33762	0.664878	0.908424	0.982962	0.994508	0.995751
10000		0.083383	0.181215	0.340221	0.466019	0.494831	0.498149

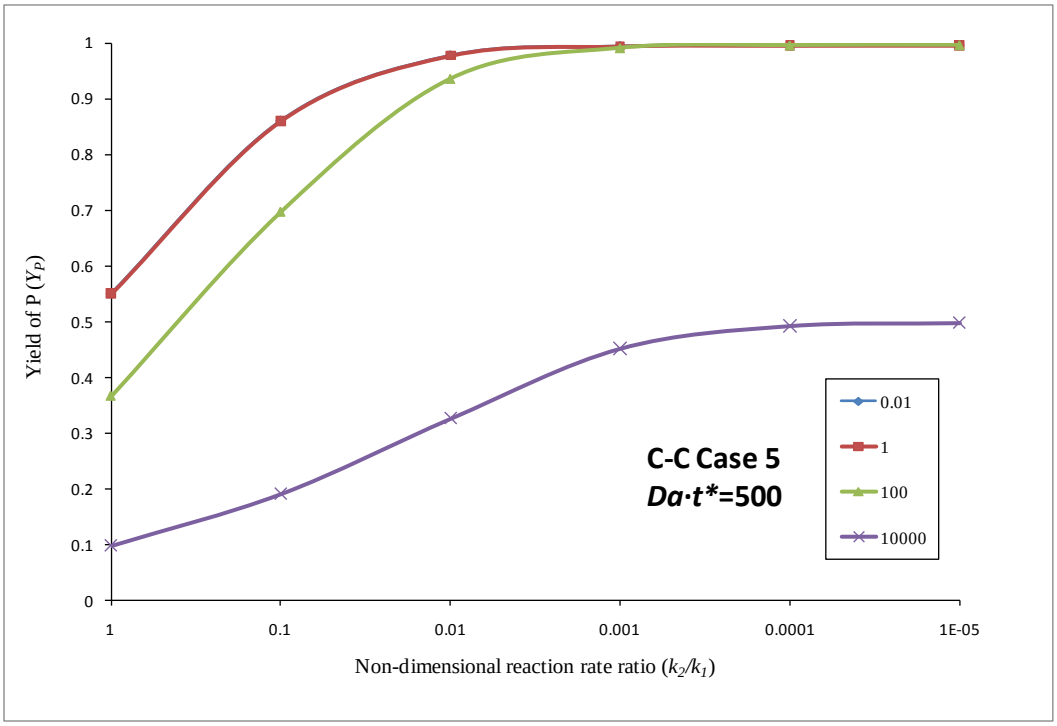

Figure A-25. Plot of Yield of *P* vs k_2/k_1 for C-C Case 5 for all *Da* at $Da \cdot t^*$=500

Table A-25. Data for Yield of *P* vs k_2/k_1 for C-C Case 5 for all *Da* at $Da \cdot t^*$=500

C-C Case 5 $Da \cdot t^* = 500$

Yield of *P*

Da	k_2/k_1	**1**	**0.1**	**0.01**	**0.001**	**0.0001**	**0.00001**
0.01		0.550825	0.860791	0.977843	0.994477	0.995857	0.995991
1		0.550456	0.860663	0.977854	0.994481	0.995869	0.996004
100		0.367454	0.697308	0.935599	0.990553	0.995411	0.995843
10000		0.098157	0.191248	0.326346	0.452073	0.492587	0.497913

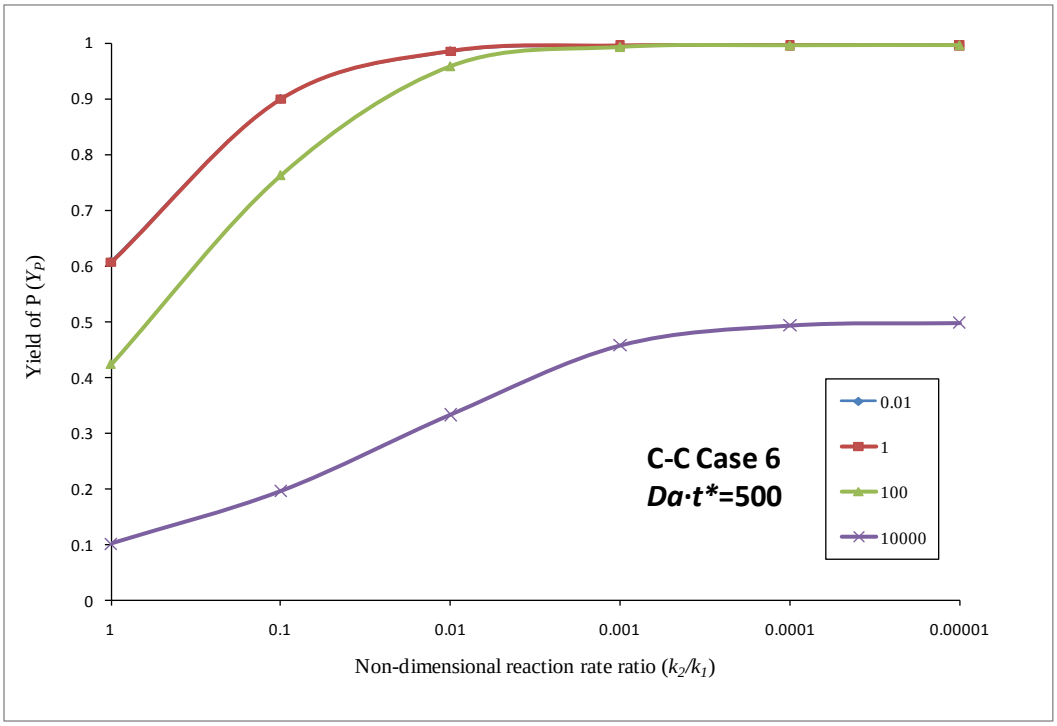

Figure A-26. Plot of Yield of *P* vs k_2/k_1 for C-C Case 6 for all *Da* at *Da*·*t**=500

Table A-26. Data for Yield of *P* vs k_2/k_1 for C-C Case 6 for all *Da* at *Da*·*t**=500

C-C Case 6 *Da*·*t = 500**

Yield of *P*

Da	k_2/k_1	**1**	**0.1**	**0.01**	**0.001**	**0.0001**	**0.00001**
0.01		0.606914	0.899378	0.985152	0.99502	0.995906	0.995996
1		0.606508	0.899307	0.985142	0.995013	0.995919	0.996009
100		0.423812	0.762701	0.958186	0.992593	0.995573	0.995858
10000		0.101564	0.196048	0.333472	0.457815	0.493571	0.49802

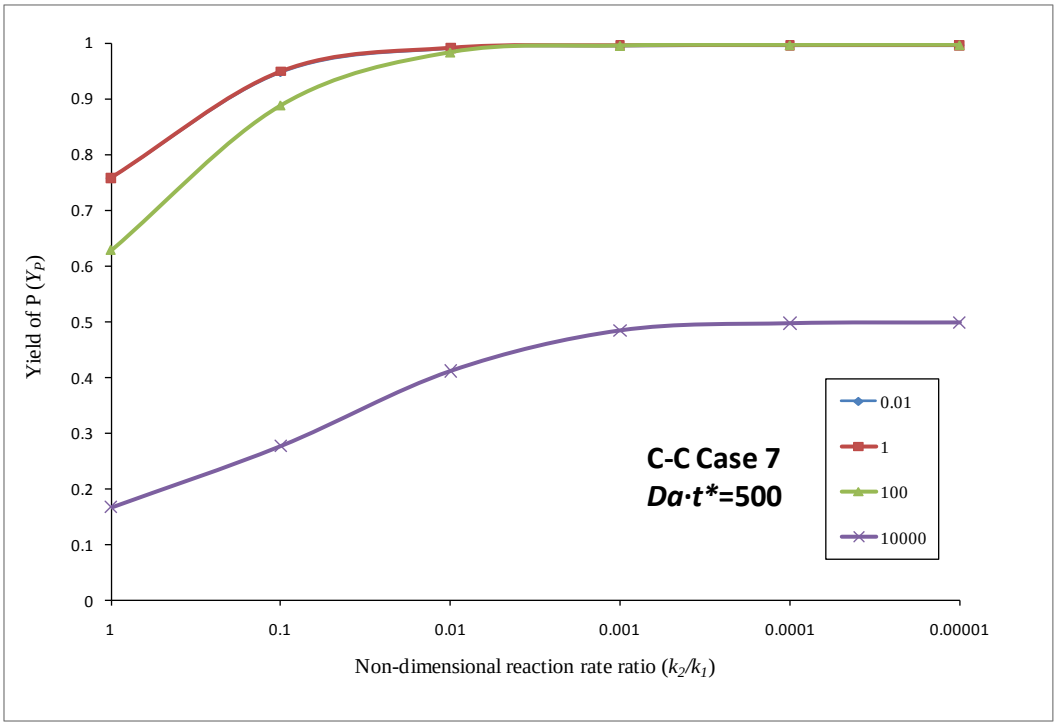

Figure A-27. Plot of Yield of *P* vs k_2/k_1 for C-C Case 7 for all *Da* at *Da*·*t**=500

Table A-27. Data for Yield of *P* vs k_2/k_1 for C-C Case 7 for all *Da* at *Da*·*t**=500

C-C Case 7 *Da*·*t = 500**

Yield of *P*

Da	k_2/k_1	**1**	**0.1**	**0.01**	**0.001**	**0.0001**	**0.00001**
0.01		0.758424	0.947893	0.991068	0.995513	0.995956	0.996001
1		0.758376	0.948907	0.991066	0.995525	0.995969	0.996014
100		0.627822	0.887687	0.982766	0.994617	0.995763	0.995877
10000		0.167712	0.277811	0.411861	0.484262	0.496988	0.498369

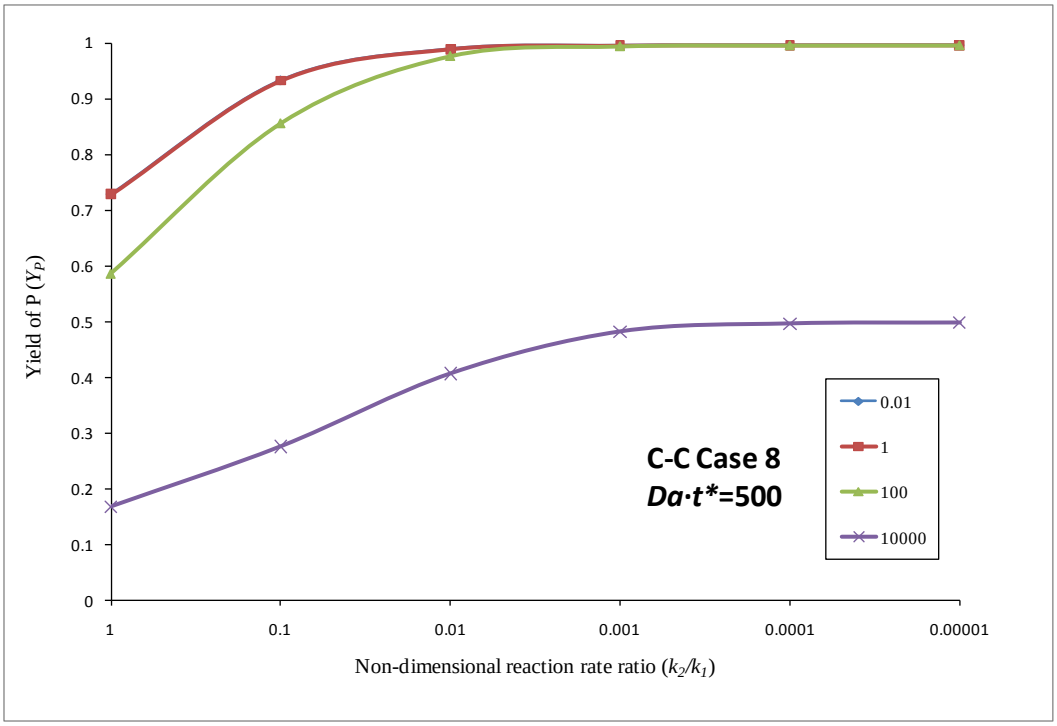

Figure A-28. Plot of Yield of *P* vs k_2/k_1 for C-C Case 8 for all *Da* at *Da*·*t**=500

Table A-28. Data for Yield of *P* vs k_2/k_1 for C-C Case 8 for all *Da* at *Da*·*t**=500

C-C Case 8 *Da*·*t = 500**

Yield of *P*

Da	k_2/k_1	**1**	**0.1**	**0.01**	**0.001**	**0.0001**	**0.00001**
0.01		0.728555	0.932667	0.989124	0.995346	0.99594	0.995999
1		0.728506	0.932597	0.989115	0.995359	0.995953	0.996012
100		0.586622	0.856184	0.976673	0.994164	0.995721	0.995873
10000		0.168112	0.276192	0.407097	0.482465	0.496765	0.498346

A.3 Competitive-Parallel Reaction Scheme

A.3.1 Plots and data of Y_P versus Damkohler number with curves of the stoichiometry cases for different non-dimensional reaction rate ratios.

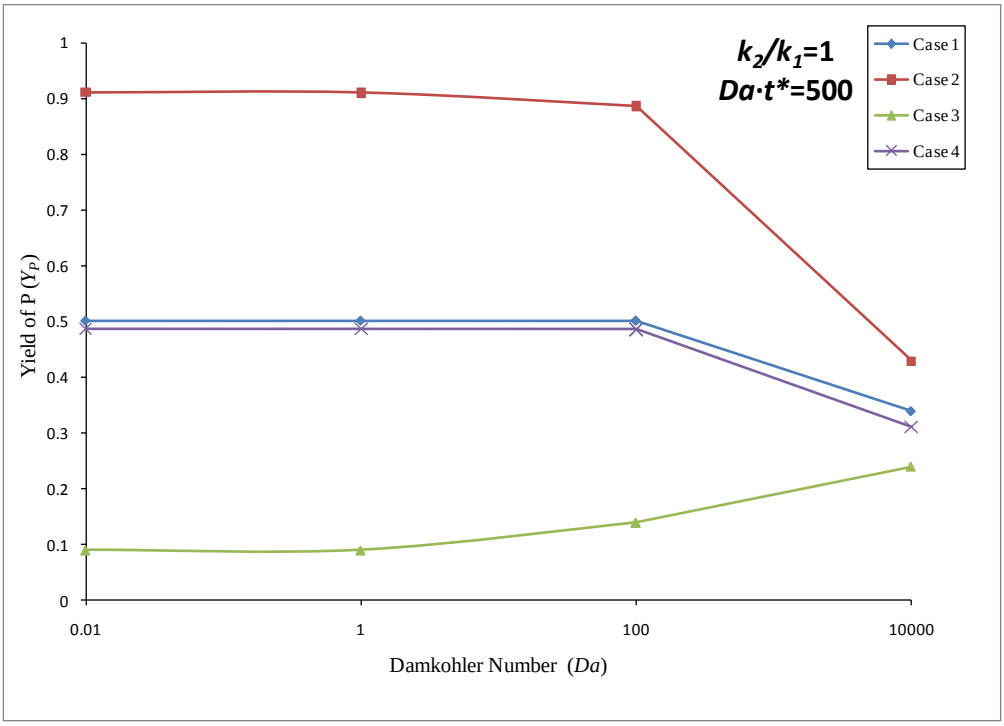

Figure A-29. Plot of Yield of *P* vs *Da* for k_2/k_1=1 at $Da \cdot t^*$=500 for C-P cases

Table A-29. Data for Yield of *P* vs *Da* for k_2/k_1=1 at $Da \cdot t^*$=500 for C-P cases

$k_2/k_1 = 1$ $\quad$ $Da \cdot t^* = 500$

	Yield of *P*			
Da	**0.01**	**1**	**100**	**10000**
Case 1	0.5	0.5	0.5	0.339086
Case 2	0.910664	0.910649	0.886249	0.428365
Case 3	0.089336	0.089401	0.138806	0.238611
Case 4	0.485825	0.485768	0.485627	0.311142

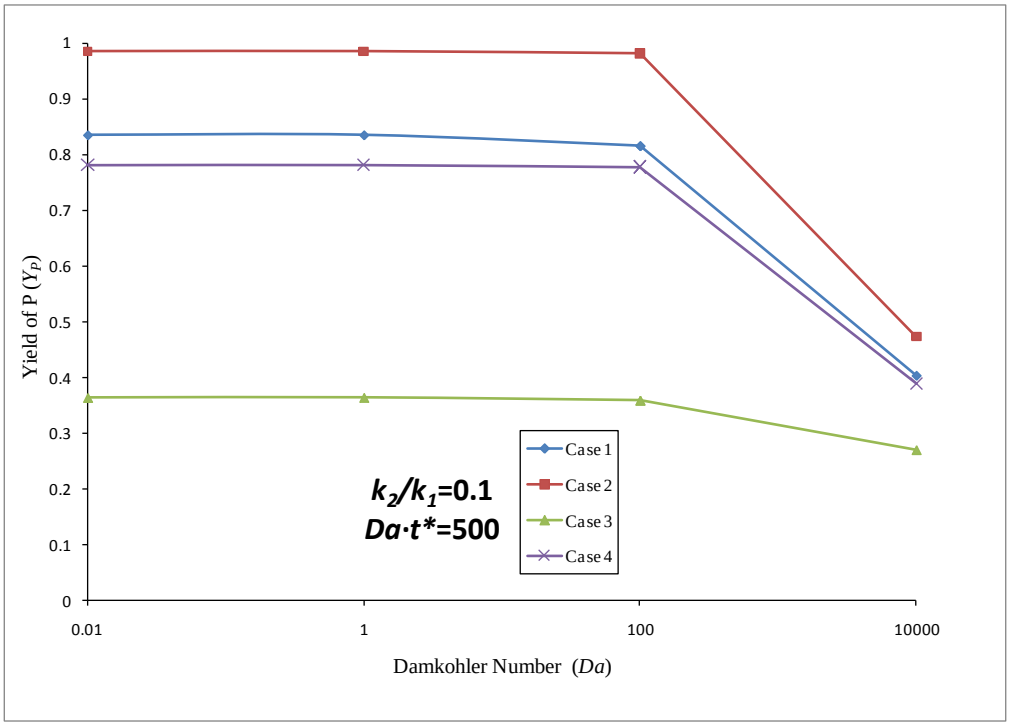

Figure A-30. Plot of Yield of *P* vs *Da* for k_2/k_1=0.1 at *Da*·*t**=500 for C-P cases

Table A-30. Data for Yield of *P* vs *Da* for k_2/k_1=0.1 at *Da*·*t**=500 for C-P cases

k_2/k_1 = 0.1 *Da*·*t** = 500

	Yield of *P*			
Da	**0.01**	**1**	**100**	**10000**
Case 1	0.835052	0.835066	0.815543	0.402615
Case 2	0.984832	0.984816	0.98098	0.473025
Case 3	0.363595	0.363809	0.358733	0.26895
Case 4	0.781719	0.781886	0.778014	0.389749

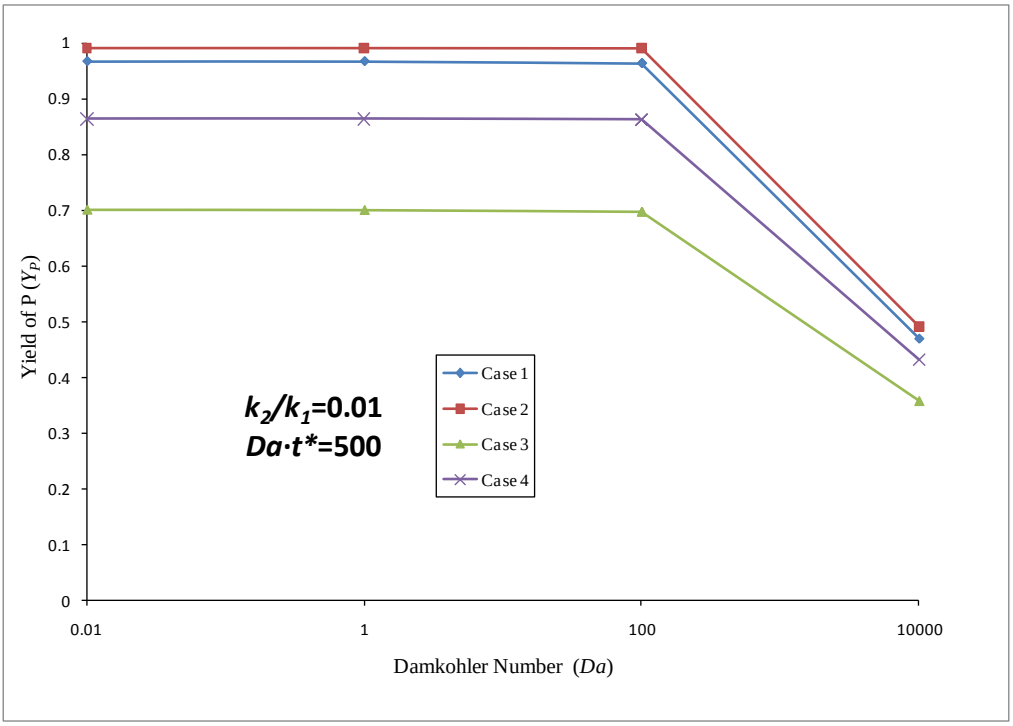

Figure A-31. Plot of Yield of *P* vs *Da* for k_2/k_1=0.01 at *Da*·*t**=500 for C-P cases

Table A-31. Data for Yield of *P* vs *Da* for k_2/k_1=0.01 at *Da*·*t**=500 for C-P cases

k_2/k_1 = 0.01 **Da·t* = 500**

Yield of *P*

Da	**0.01**	**1**	**100**	**10000**
Case 1	0.966434	0.966416	0.962859	0.468746
Case 2	0.991453	0.991441	0.990976	0.491935
Case 3	0.701398	0.700784	0.697756	0.35746
Case 4	0.863384	0.863462	0.862132	0.431838

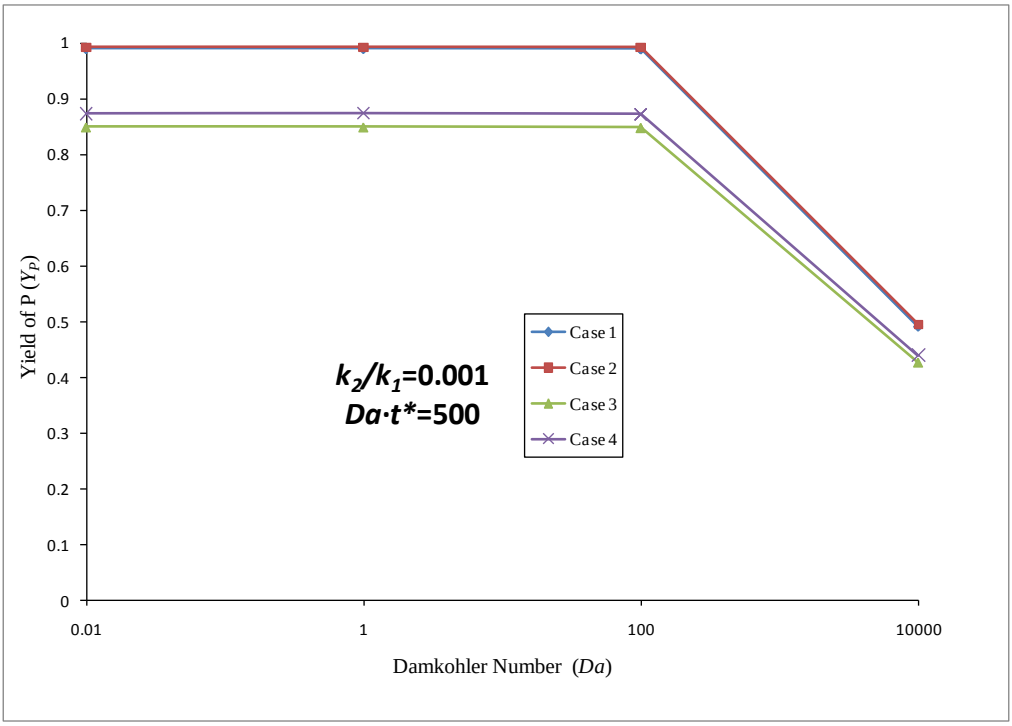

Figure A-32. Plot of Yield of *P* vs *Da* for k_2/k_1=0.001 at *Da*·*t**=500 for C-P cases

Table A-32. Data for Yield of *P* vs *Da* for k_2/k_1=0.001 at *Da*·*t**=500 for C-P cases

k_2/k_1 = 0.001 **Da·t* = 500**

Yield of *P*

Da	**0.01**	**1**	**100**	**10000**
Case 1	0.989783	0.989805	0.989356	0.491783
Case 2	0.991995	0.992007	0.991798	0.494859
Case 3	0.849533	0.849485	0.848401	0.426885
Case 4	0.873267	0.87361	0.872557	0.439871

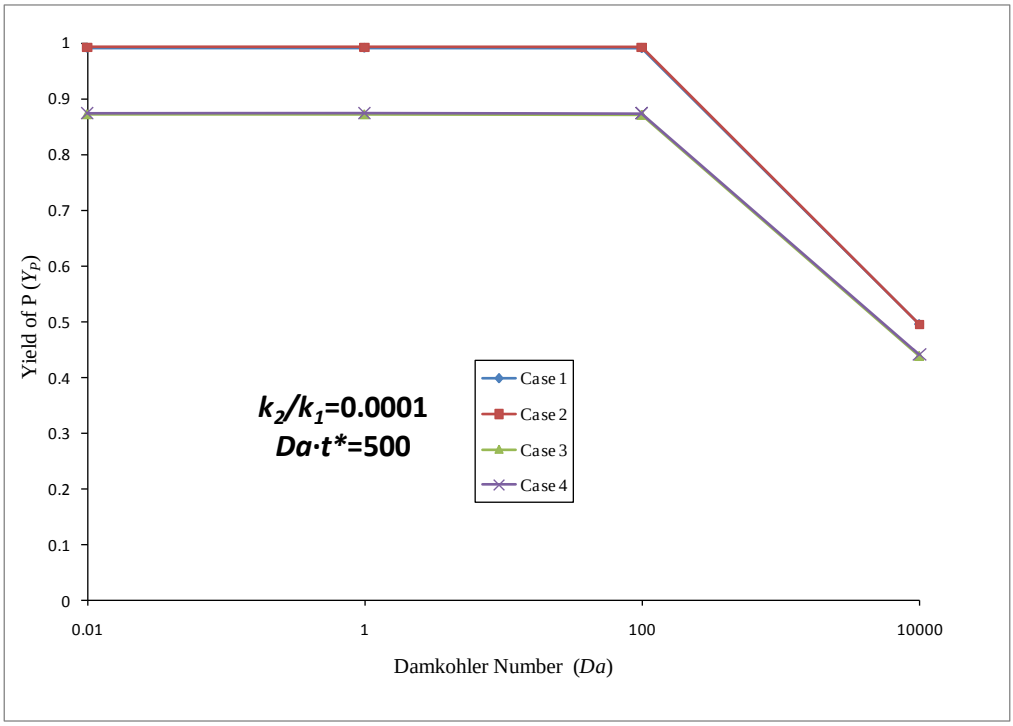

Figure A-33. Plot of Yield of *P* vs *Da* for k_2/k_1=0.0001 at *Da*·*t**=500 for C-P cases

Table A-33. Data for Yield of *P* vs *Da* for k_2/k_1=0.0001 at *Da*·*t**=500 for C-P cases

k_2/k_1 = 0.0001 *Da*·*t**= 500

Yield of *P*

Da	0.01	1	100	10000
Case 1	0.991844	0.991866	0.991657	0.494839
Case 2	0.99205	0.992062	0.991878	0.495169
Case 3	0.872145	0.872021	0.871265	0.439407
Case 4	0.874308	0.874651	0.873637	0.440767

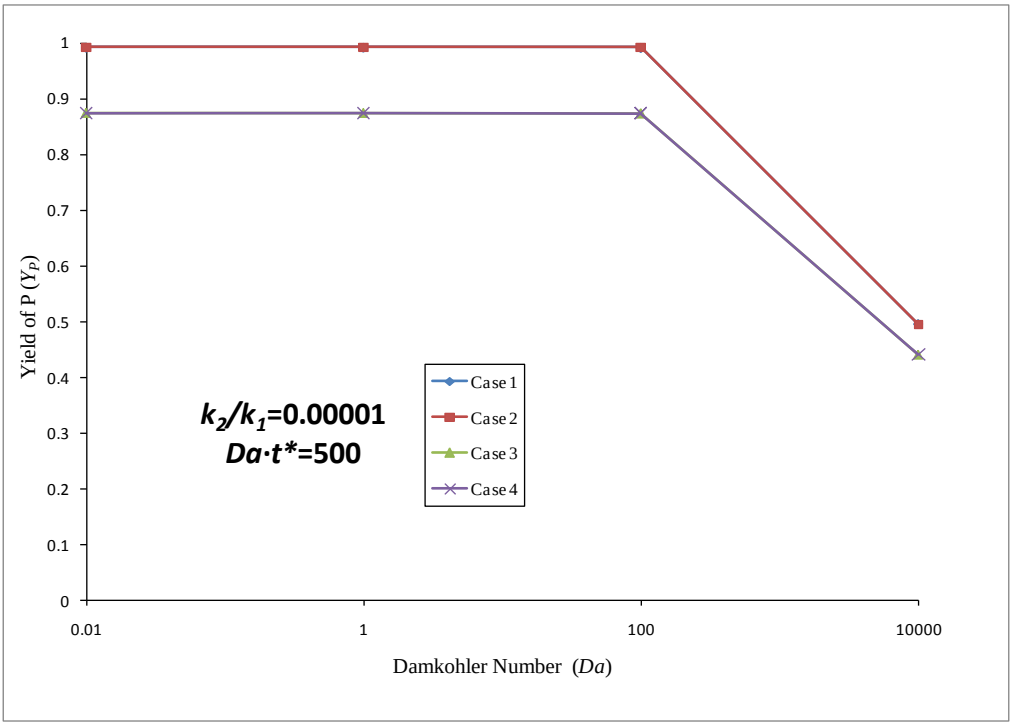

Figure A-34. Plot of Yield of *P* vs *Da* for k_2/k_1=0.00001 at *Da*·*t**=500 for C-P cases

Table A-34. Data for Yield of *P* vs *Da* for k_2/k_1=0.00001 at *Da*·*t**=500 for C-P cases

k_2/k_1 = 0.00001 *Da*·*t** = 500

	Yield of *P*			
Da	**0.01**	**1**	**100**	**10000**
Case 1	0.99204	0.992071	0.991875	0.495154
Case 2	0.992056	0.992068	0.991886	0.495201
Case 3	0.874518	0.874398	0.873662	0.440758
Case 4	0.874412	0.874756	0.873746	0.440858

A.3.2 Plots and data of Y_P versus Damkohler number with curves of non-dimensional reaction rate ratios for individual stoichiometry cases.

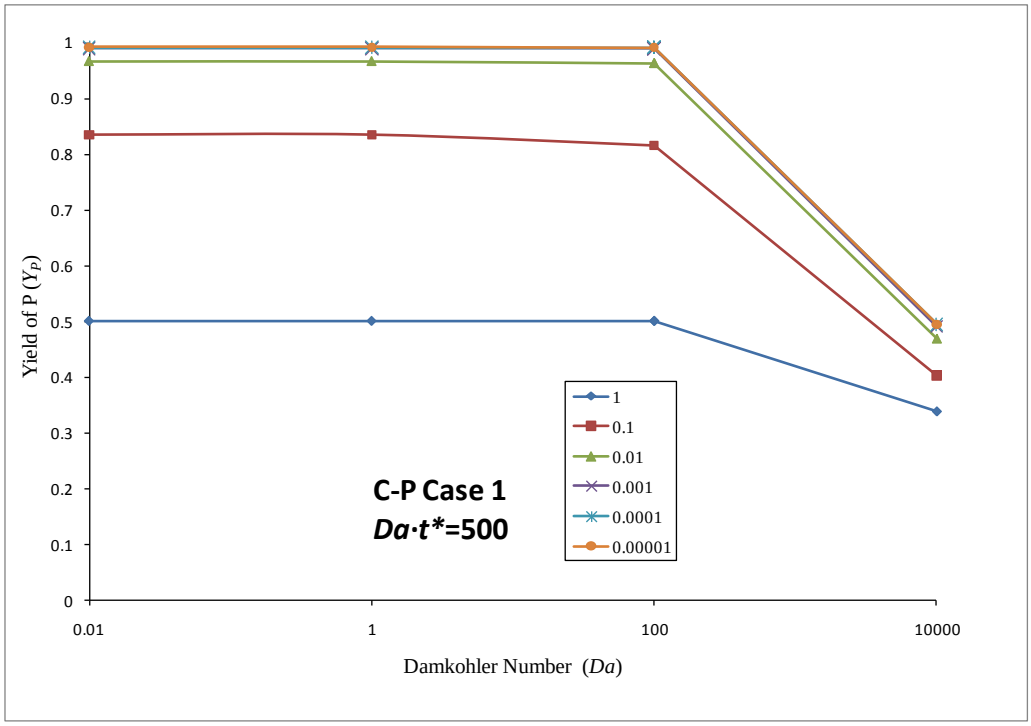

Figure A-35. Plot of Yield of *P* vs *Da* for C-P Case 1 for all k_2/k_1 at *Da*·*t**=500

Table A-35. Data for Yield of *P* vs *Da* for C-P Case 1 for all k_2/k_1 at *Da*·*t**=500

C-P Case 1 *Da*·*t = 500**

Yield of *P*

k_2/k_1	*Da*	0.01	1	100	10000
1		0.5	0.5	0.5	0.339086
0.1		0.835052	0.835066	0.815543	0.402615
0.01		0.966434	0.966416	0.962859	0.468746
0.001		0.989783	0.989805	0.989356	0.491783
0.0001		0.991844	0.991866	0.991657	0.494839
0.00001		0.99204	0.992071	0.991875	0.495154

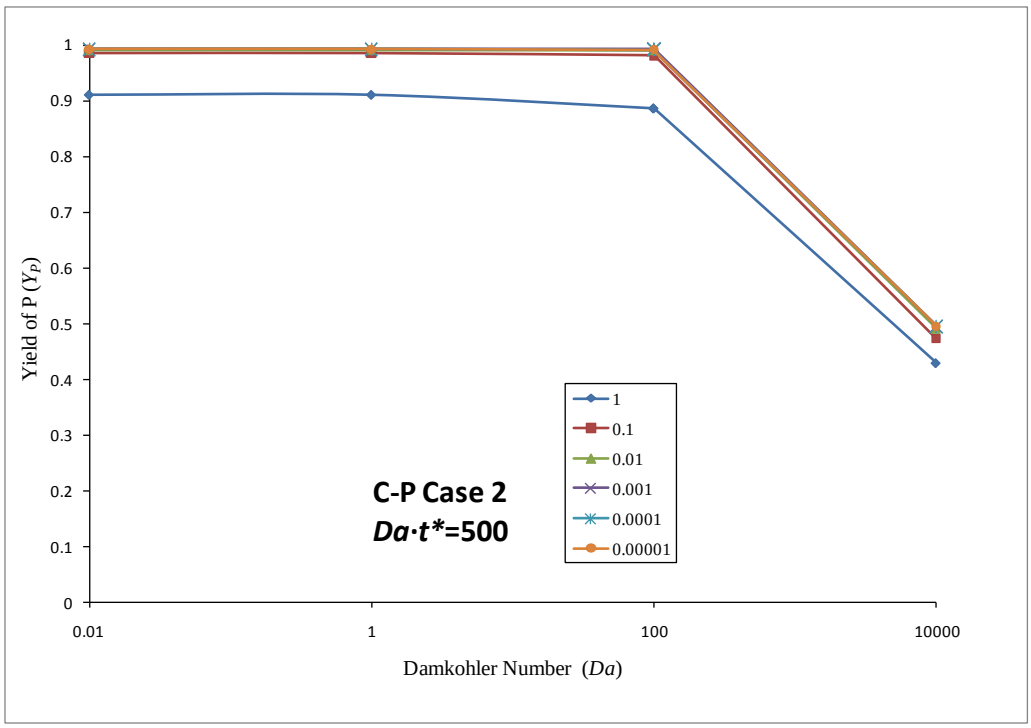

Figure A-36. Plot of Yield of *P* vs *Da* for C-P Case 2 for all k_2/k_1 at $Da \cdot t^*$=500

Table A-36. Data for Yield of *P* vs *Da* for C-P Case 2 for all k_2/k_1 at $Da \cdot t^*$=500

C-P Case 2 $Da \cdot t^* = 500$

Yield of *P*

k_2/k_1	*Da*	0.01	1	100	10000
1		0.910664	0.910649	0.886249	0.428365
0.1		0.984832	0.984816	0.98098	0.473025
0.01		0.991453	0.991441	0.990976	0.491935
0.001		0.991995	0.992007	0.991798	0.494859
0.0001		0.99205	0.992062	0.991878	0.495169
0.00001		0.992056	0.992068	0.991886	0.495201

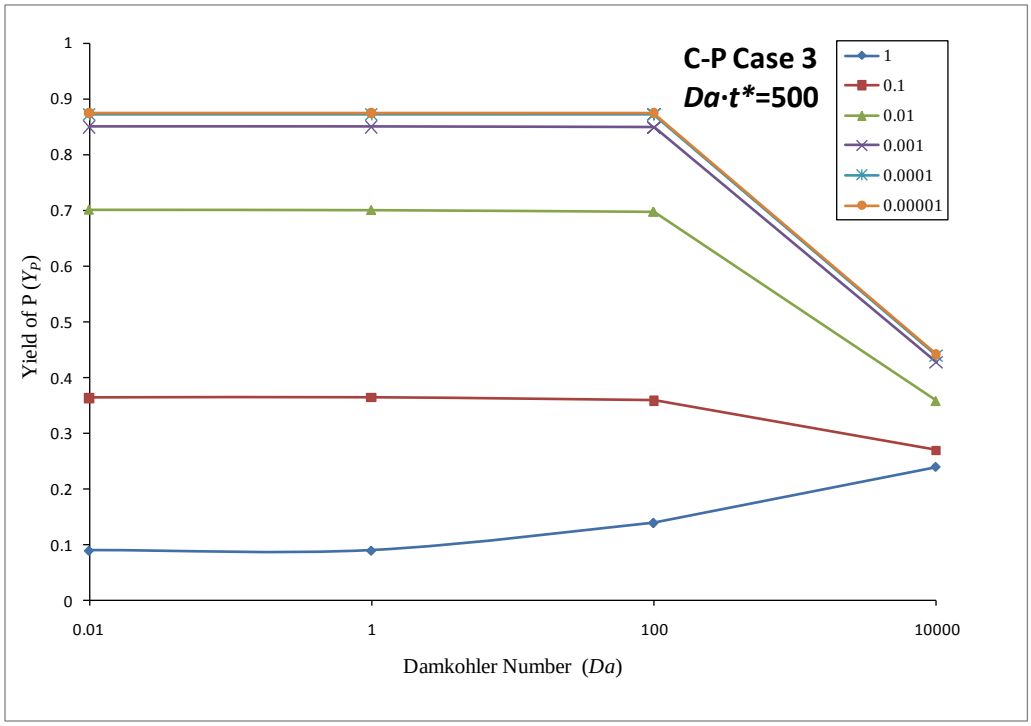

Figure A-37. Plot of Yield of *P* vs *Da* for C-P Case 3 for all k_2/k_1 at $Da \cdot t^*$=500

Table A-37. Data for Yield of *P* vs *Da* for C-P Case 3 for all k_2/k_1 at $Da \cdot t^*$=500

C-P Case 3 $Da \cdot t^* = 500$

Yield of *P*

k_2/k_1	*Da*	0.01	1	100	10000
1		0.089336	0.089401	0.138806	0.238611
0.1		0.363595	0.363809	0.358733	0.26895
0.01		0.701398	0.700784	0.697756	0.35746
0.001		0.849533	0.849485	0.848401	0.426885
0.0001		0.872145	0.872021	0.871265	0.439407
0.00001		0.874518	0.874398	0.873662	0.440758

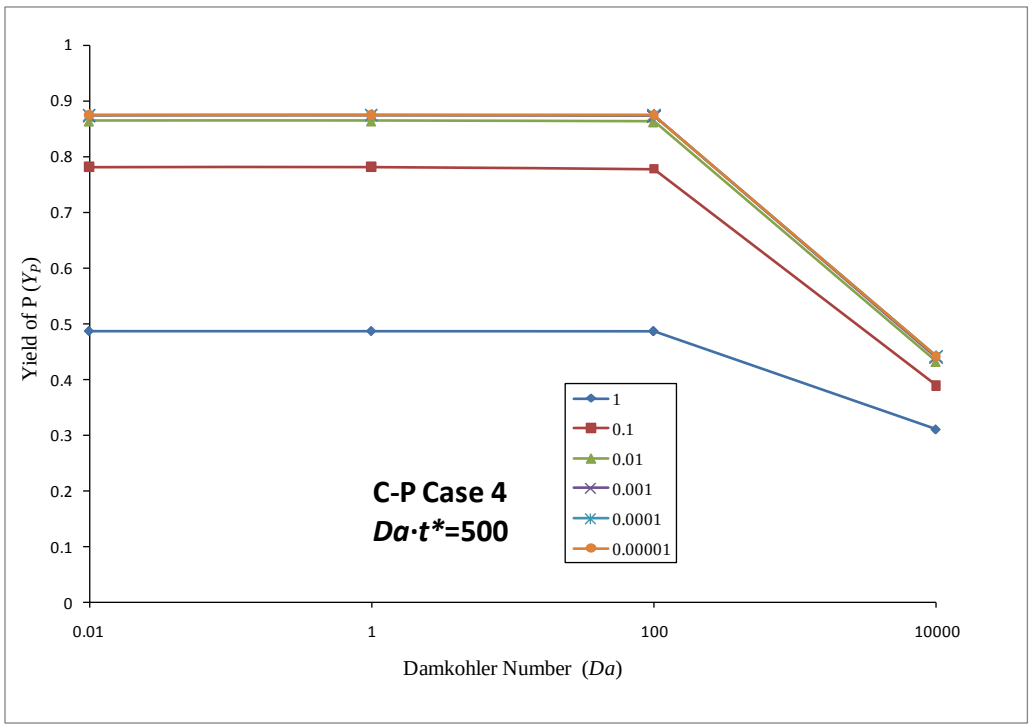

Figure A-38. Plot of Yield of *P* vs *Da* for C-P Case 4 for all k_2/k_1 at $Da \cdot t^*$=500

Table A-38. Data for Yield of *P* vs *Da* for C-P Case 4 for all k_2/k_1 at $Da \cdot t^*$=500

C-P Case 4 $Da \cdot t^* = 500$

Yield of *P*

k_2/k_1	*Da*	0.01	1	100	10000
1		0.485825	0.485768	0.485627	0.311142
0.1		0.781719	0.781886	0.778014	0.389749
0.01		0.863384	0.863462	0.862132	0.431838
0.001		0.873267	0.87361	0.872557	0.439871
0.0001		0.874308	0.874651	0.873637	0.440767
0.00001		0.874412	0.874756	0.873746	0.440858

A.3.3 Plots and data of Y_P versus non-dimensional reaction rate ratio with curves of the stoichiometry cases for different Damkohler numbers.

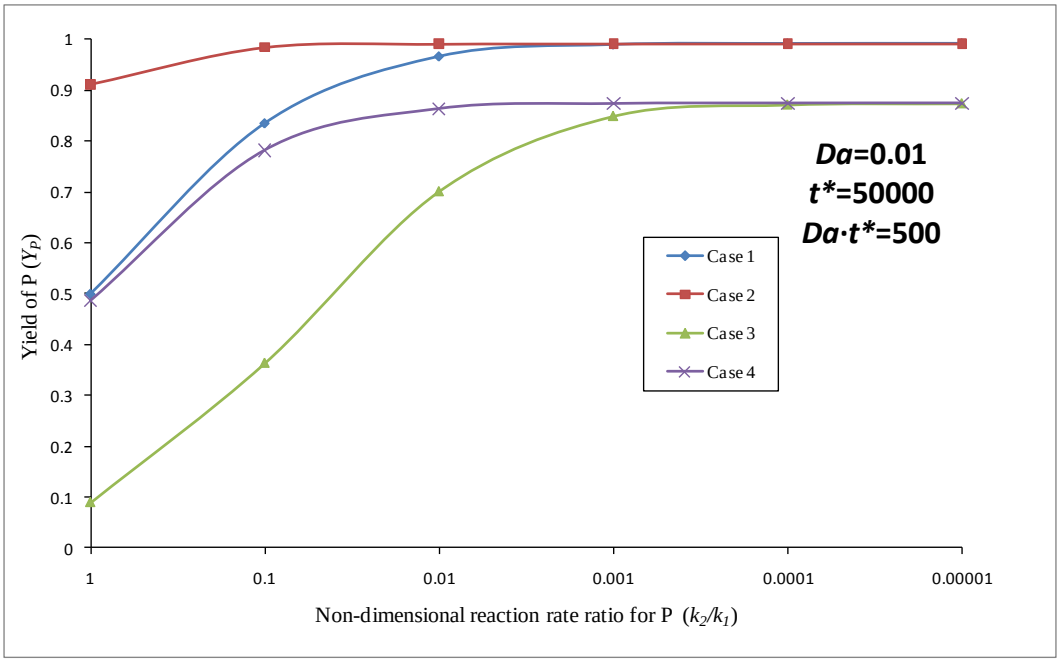

Figure A-39. Plot of Yield of *P* vs k_2/k_1 for *Da*=0.01 at *Da*·*t**=500 for C-P cases

Table A-39. Data for Yield of *P* vs k_2/k_1 for *Da*=0.01 at *Da*·*t**=500 for C-P cases

***Da* = 0.01** ***t** = 50000** ***Da*·*t** = 500**

Yield of *P*

k_2/k_1	1	0.1	0.01	0.001	0.0001	0.00001
Case 1	0.5	0.835052	0.966434	0.989783	0.991844	0.99204
Case 2	0.910664	0.984832	0.991453	0.991995	0.99205	0.992056
Case 3	0.089336	0.363595	0.701398	0.849533	0.872145	0.874518
Case 4	0.485825	0.781719	0.863384	0.873267	0.874308	0.874412

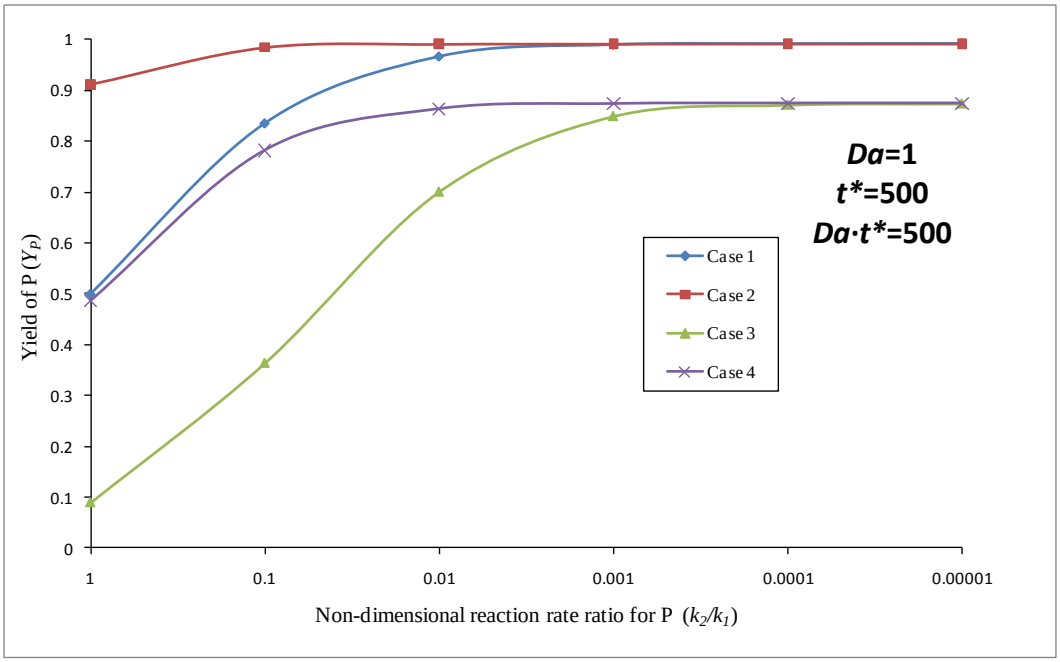

Figure A-40. Plot of Yield of *P* vs k_2/k_1 for *Da*=1 at *Da*·*t**=500 for C-P cases

Table A-40. Data for Yield of *P* vs k_2/k_1 for *Da*=1 at *Da*·*t**=500 for C-P cases

***Da* = 1** **t^* = 500** ***Da*·*t**= 500**

Yield of *P*

k_2/k_1	1	0.1	0.01	0.001	0.0001	0.00001
Case 1	0.5	0.835066	0.966416	0.989805	0.991866	0.992071
Case 2	0.910649	0.984816	0.991441	0.992007	0.992062	0.992068
Case 3	0.089401	0.363809	0.700784	0.849485	0.872021	0.874398
Case 4	0.485768	0.781886	0.863462	0.87361	0.874651	0.874756

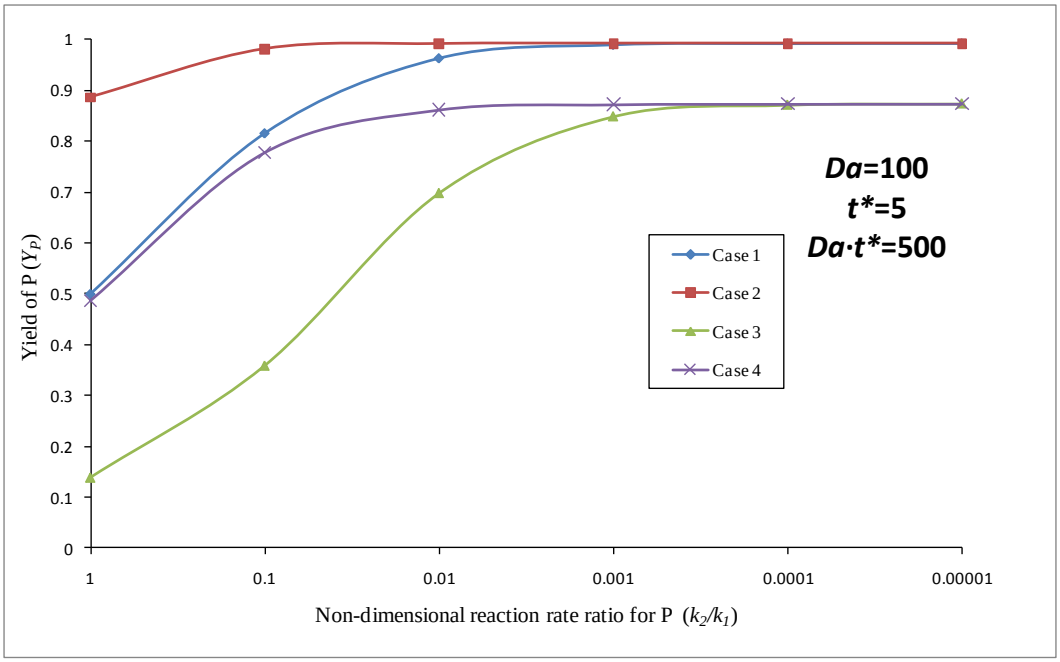

Figure A-41. Plot of Yield of *P* vs k_2/k_1 for *Da*=100 at *Da*·*t**=500 for C-P cases

Table A-41. Data for Yield of *P* vs k_2/k_1 for *Da*=100 at *Da*·*t**=500 for C-C cases

***Da* = 100** ***t**= 5** ***Da*·*t**= 500**

Yield of *P*

k_2/k_1	**1**	**0.1**	**0.01**	**0.001**	**0.0001**	**0.00001**
Case 1	0.5	0.815543	0.962859	0.989356	0.991657	0.991875
Case 2	0.886249	0.98098	0.990976	0.991798	0.991878	0.991886
Case 3	0.138806	0.358733	0.697756	0.848401	0.871265	0.873662
Case 4	0.485627	0.778014	0.862132	0.872557	0.873637	0.873746

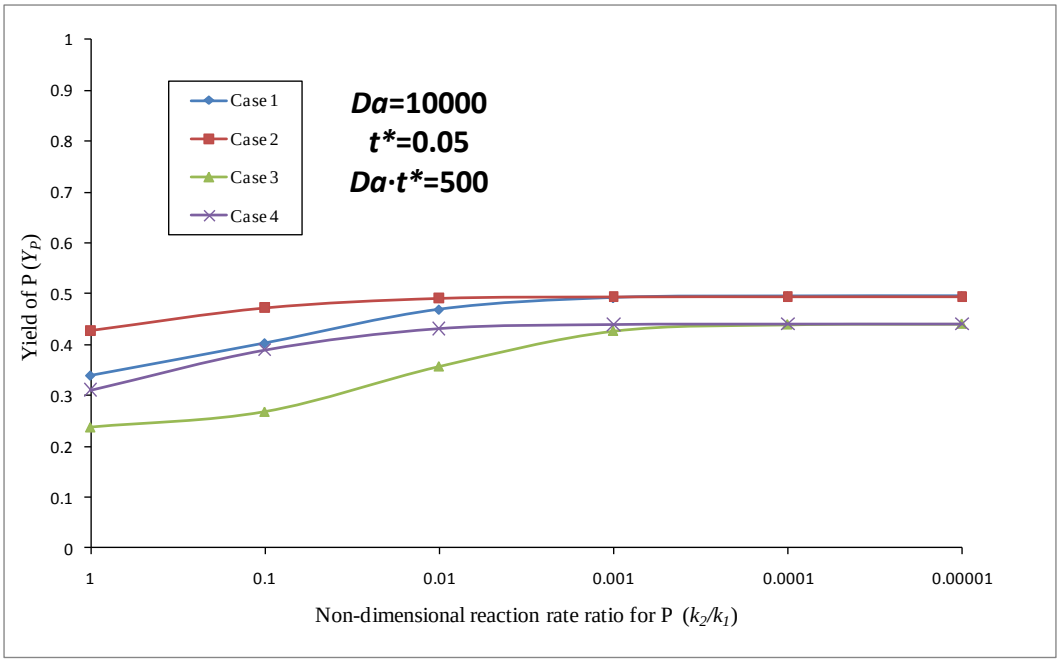

Figure A-42. Plot of Yield of *P* vs k_2/k_1 for *Da*=10000 at *Da*·*t**=500 for C-P cases

Table A-42. Data for Yield of *P* vs k_2/k_1 for *Da*=10000 at *Da*·*t**=500 for C-P cases

***Da* = 10000** ***t** = 0.05** ***Da*·*t** = 500**

Yield of *P*

k_2/k_1	1	0.1	0.01	0.001	0.0001	0.00001
Case 1	0.339086	0.402615	0.468746	0.491783	0.494839	0.495154
Case 2	0.428365	0.473025	0.491935	0.494859	0.495169	0.495201
Case 3	0.238611	0.26895	0.35746	0.426885	0.439407	0.440758
Case 4	0.311142	0.389749	0.431838	0.439871	0.440767	0.440858

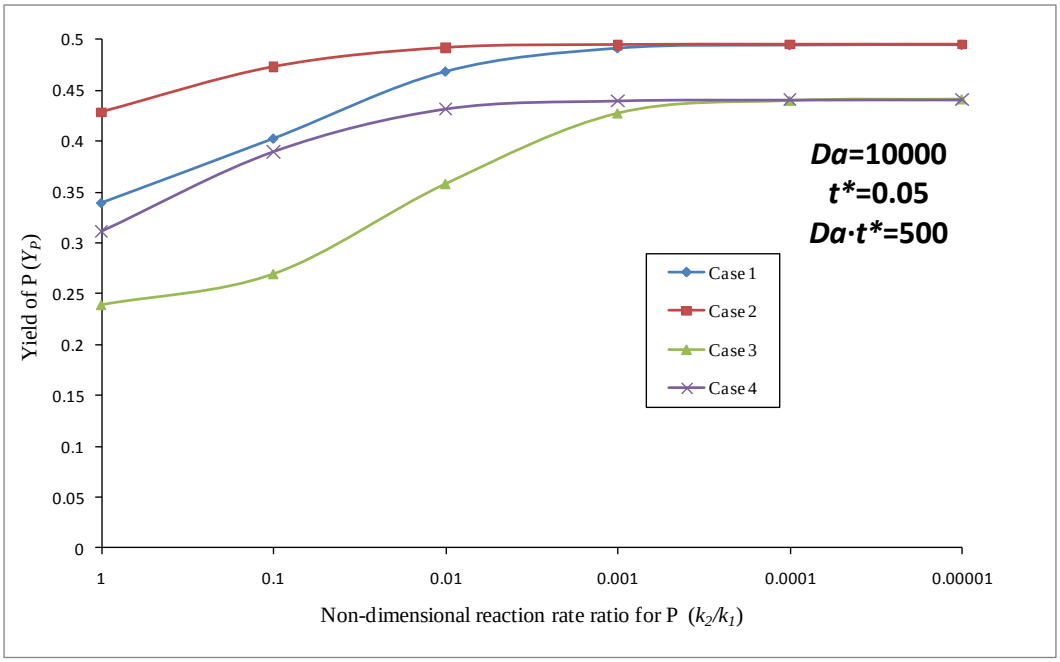

Figure A-43. Plot of Yield of *P* vs k_2/k_1 for *Da*=10000 at *Da*·*t**=500 for C-P cases with Y_P axis going only to 0.5

Table A-43. Data for Yield of *P* vs k_2/k_1 for *Da*=10000 at *Da*·*t**=500 for C-P cases with Y_P axis going only to 0.5

***Da* = 10000** **t^* = 0.05** ***Da*·t^* = 500**

Yield of *P*

k_2/k_1	1	0.1	0.01	0.001	0.0001	0.00001
Case 1	0.339086	0.402615	0.468746	0.491783	0.494839	0.495154
Case 2	0.428365	0.473025	0.491935	0.494859	0.495169	0.495201
Case 3	0.238611	0.26895	0.35746	0.426885	0.439407	0.440758
Case 4	0.311142	0.389749	0.431838	0.439871	0.440767	0.440858

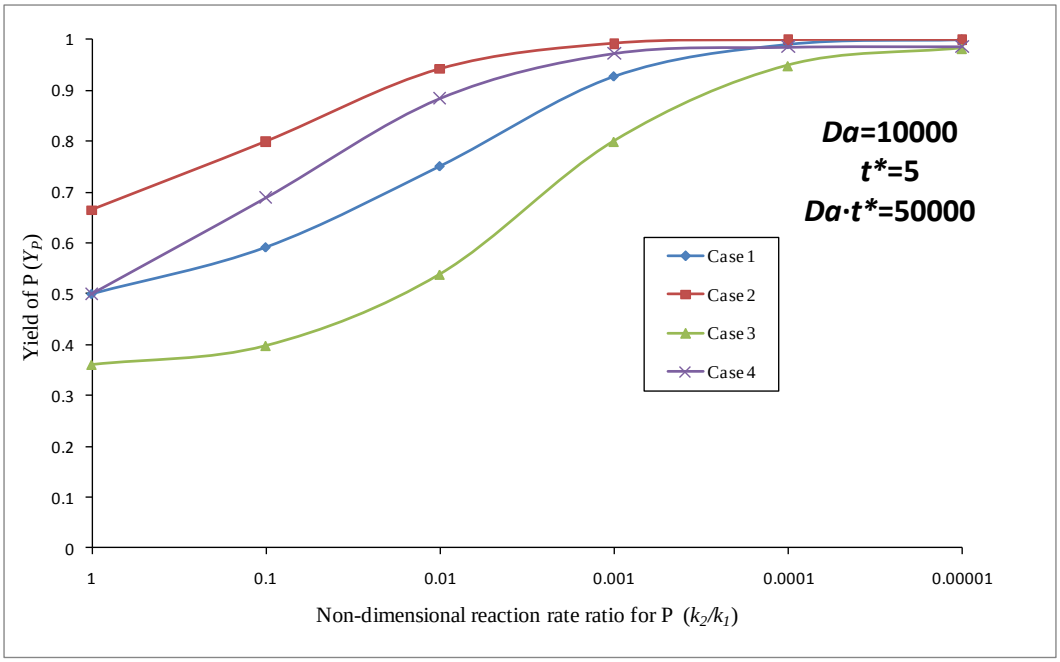

Figure A-44. Plot of Yield of *P* vs k_2/k_1 for *Da*=10000 at *Da*·*t**=50000 for C-P cases

Table A-44. Data for Yield of *P* vs k_2/k_1 for *Da*=10000 at *Da*·*t**=50000 for C-P cases

Da = 10000 **t* = 5** **Da ·t* = 50000**

Yield of *P*

k_2/k_1	1	0.1	0.01	0.001	0.0001	0.00001
Case 1	0.5	0.591513	0.750421	0.926494	0.989629	0.998884
Case 2	0.664455	0.798914	0.941894	0.992354	0.999208	0.999866
Case 3	0.360675	0.397831	0.538119	0.799616	0.948686	0.982532
Case 4	0.499834	0.688849	0.884477	0.973235	0.985677	0.986884

A.3.4 Plots and data of Y_P versus non-dimensional reaction rate ratio with curves of Damkohler numbers for individual stoichiometry cases.

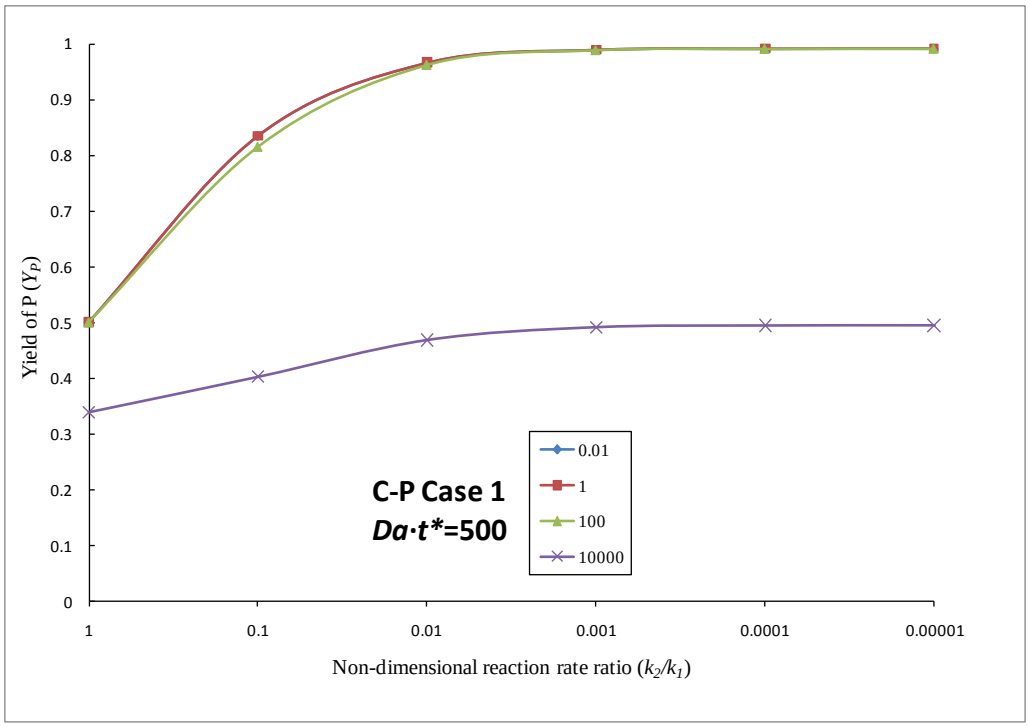

Figure A-45. Plot of Yield of *P* vs k_2/k_1 for C-C Case 1 for all *Da* at *Da*·*t**=500

Table A-45. Data for Yield of *P* vs k_2/k_1 for C-P Case 1 for all *Da* at *Da*·*t**=500

C-P Case 1 ***Da*·*t** = 500**

Yield of *P*

Da	k_2/k_1	**1**	**0.1**	**0.01**	**0.001**	**0.0001**	**0.00001**
0.01		0.5	0.835052	0.966434	0.989783	0.991844	0.99204
1		0.5	0.835066	0.966416	0.989805	0.991866	0.992071
100		0.5	0.815543	0.962859	0.989356	0.991657	0.991875
10000		0.339086	0.402615	0.468746	0.491783	0.494839	0.495154

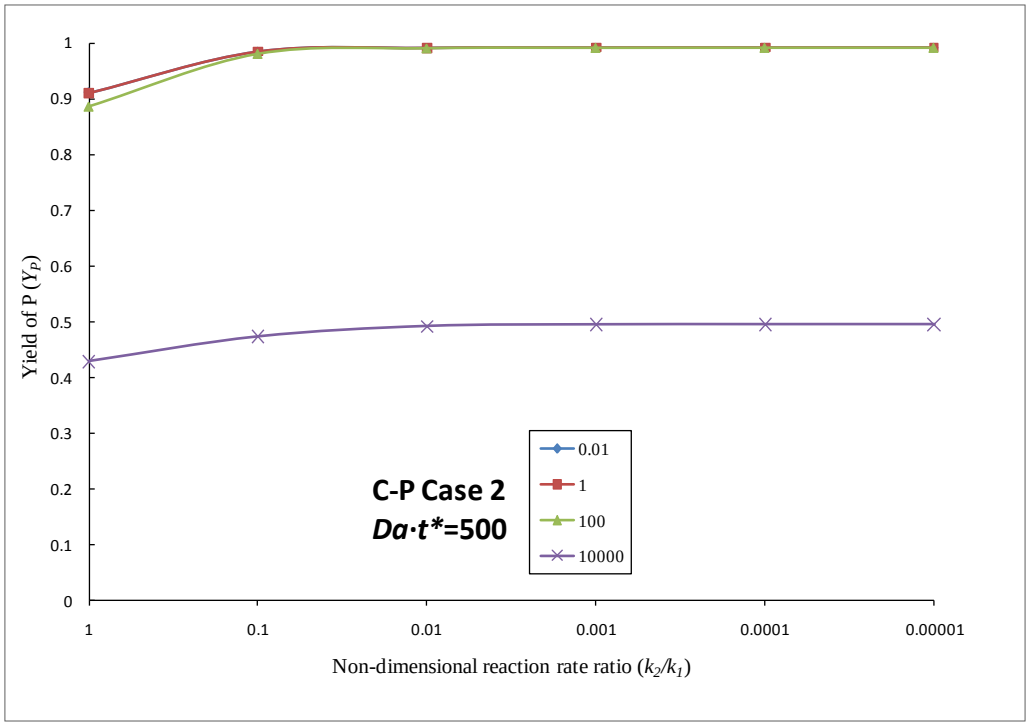

Figure A-46. Plot of Yield of *P* vs k_2/k_1 for C-C Case 2 for all *Da* at *Da*·*t**=500

Table A-46. Data for Yield of *P* vs k_2/k_1 for C-P Case 2 for all *Da* at *Da*·*t**=500

C-P Case 2 ***Da*·*t**= 500**

Yield of *P*

Da	k_2/k_1	**1**	**0.1**	**0.01**	**0.001**	**0.0001**	**0.00001**
0.01		0.910664	0.984832	0.991453	0.991995	0.99205	0.992056
1		0.910649	0.984816	0.991441	0.992007	0.992062	0.992068
100		0.886249	0.98098	0.990976	0.991798	0.991878	0.991886
10000		0.428365	0.473025	0.491935	0.494859	0.495169	0.495201

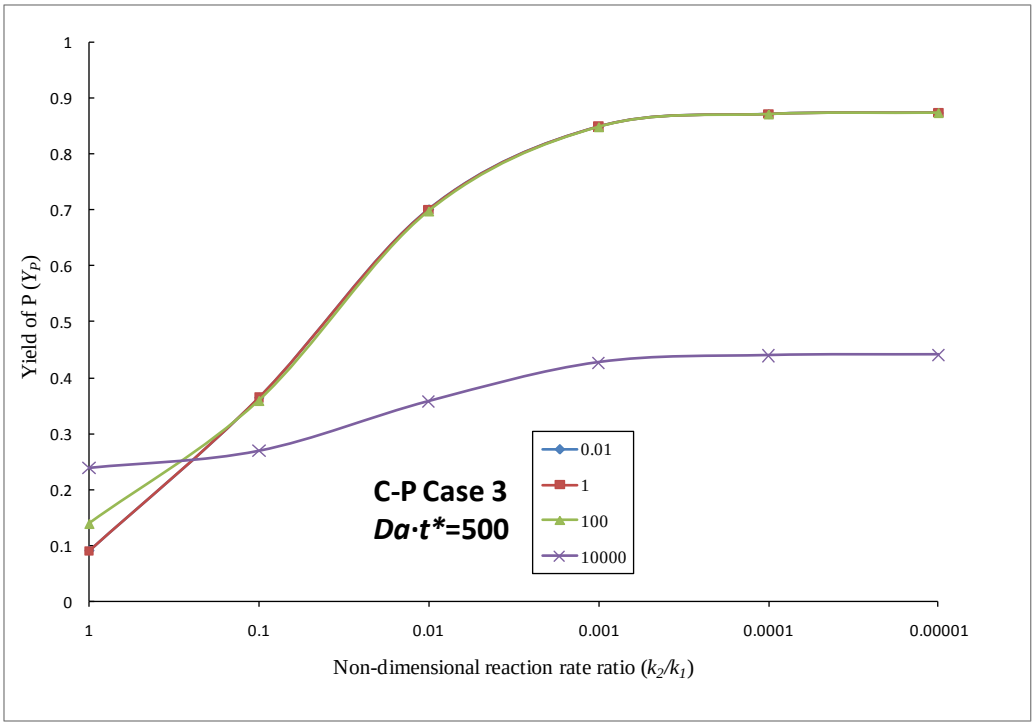

Figure A-47. Plot of Yield of *P* vs k_2/k_1 for C-C Case 3 for all *Da* at *Da*·*t**=500

Table A-47. Data for Yield of *P* vs k_2/k_1 for C-P Case 3 for all *Da* at *Da*·*t**=500

C-P Case 3 ***Da*·*t**= 500**

Yield of *P*

Da	k_2/k_1	**1**	**0.1**	**0.01**	**0.001**	**0.0001**	**0.00001**
0.01		0.089336	0.363595	0.701398	0.849533	0.872145	0.874518
1		0.089401	0.363809	0.700784	0.849485	0.872021	0.874398
100		0.138806	0.358733	0.697756	0.848401	0.871265	0.873662
10000		0.238611	0.26895	0.35746	0.426885	0.439407	0.440758

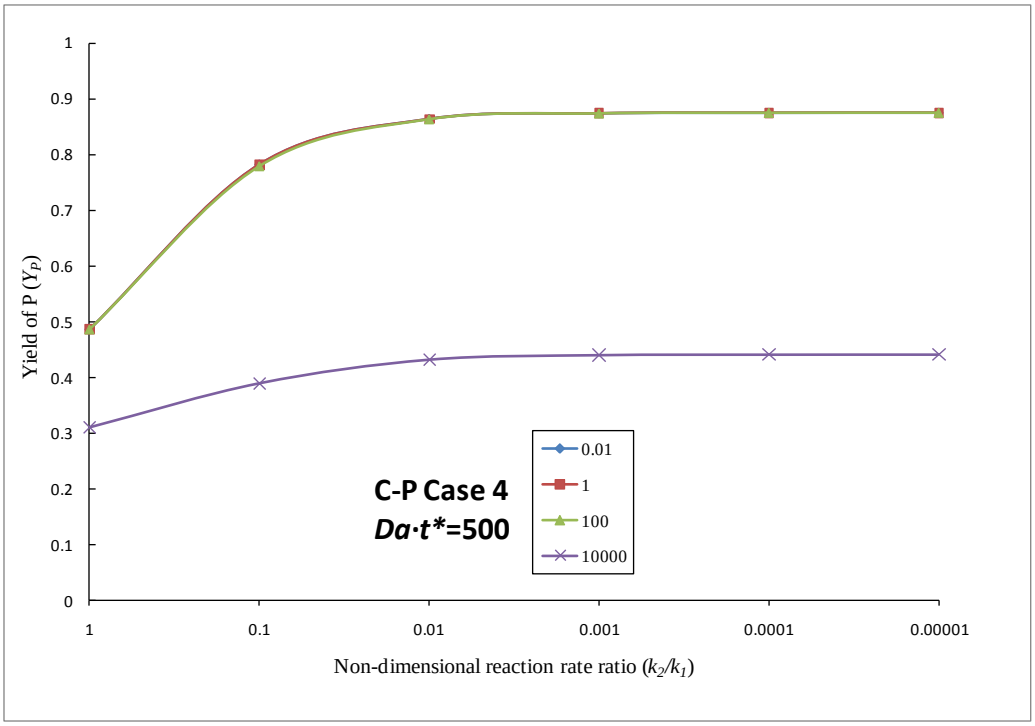

Figure A-48. Plot of Yield of *P* vs k_2/k_1 for C-C Case 4 for all *Da* at *Da*·*t**=500

Table A-48. Data for Yield of *P* vs k_2/k_1 for C-P Case 4 for all *Da* at *Da*·*t**=500

C-P Case 4 ***Da*·*t**= 500**

Yield of *P*

Da	k_2/k_1	**1**	**0.1**	**0.01**	**0.001**	**0.0001**	**0.00001**
0.01		0.485825	0.781719	0.863384	0.873267	0.874308	0.874412
1		0.485768	0.781886	0.863462	0.87361	0.874651	0.874756
100		0.485627	0.778014	0.862132	0.872557	0.873637	0.873746
10000		0.311142	0.389749	0.431838	0.439871	0.440767	0.440858